Fall 1995

Removal of VOCs from waste gas streams by a hollow fiber permeator

Varinder Pal Malik
New Jersey Institute of Technology

Copyright Warning & Restrictions

The copyright law of the United States (Title 17, United States Code) governs the making of photocopies or other reproductions of copyrighted material.

Under certain conditions specified in the law, libraries and archives are authorized to furnish a photocopy or other reproduction. One of these specified conditions is that the photocopy or reproduction is not to be "used for any purpose other than private study, scholarship, or research." If a, user makes a request for, or later uses, a photocopy or reproduction for purposes in excess of "fair use" that user may be liable for copyright infringement,

This institution reserves the right to refuse to accept a copying order if, in its judgment, fulfillment of the order would involve violation of copyright law.

Please Note: The author retains the copyright while the New Jersey Institute of Technology reserves the right to distribute this thesis or dissertation

Printing note: If you do not wish to print this page, then select "Pages from: first page # to: last page #" on the print dialog screen

ABSTRACT

REMOVAL OF VOCs FROM WASTE GAS STREAMS BY A HOLLOW FIBER PERMEATOR

by
Varinder Pal Malik

Removal of various VOCs from air/nitrogen feed streams using a novel hollow fiber membrane was studied. Hollow Fiber Module (HFM) used had composite silicone membranes wherein an ultrathin ($\sim 1\mu m$), nonporous silicone rubber membrane layer had been plasma polymerized on a porous (porosity: 0.4) polypropylene substrate. VOCs studied were toluene, methanol, acetone, methylene chloride and hexane. Primary focus was on single VOCs, although separation of VOC mixtures was also briefly studied. HFM was found to be extremely effective in removing various VOCs from feed streams. Removal of 90-99 % of various VOCs was achieved at low feed flow rates and high inlet VOC concentrations. The membrane exhibited high selectivities for VOC over nitrogen/air. The VOC permeance was found to be dependent on the VOC concentration. Tube-side feed and shell-side feed modes of operation were analyzed for methanol and toluene; it was observed that tube-side feed mode gives better VOC separations. A mathematical model was developed and numerically simulated to explain the observed VOC (toluene and methanol) separation behavior of HFM. The model was able to explain the experimental results reasonably well. Removal of VOC (acetone) from a high pressure gas was also studied. HFM was also successful in separating a mixture of VOCs (toluene, methanol, acetone) from a nitrogen feed stream.

REMOVAL OF VOCs FROM WASTE GAS STREAMS BY A HOLLOW FIBER PERMEATOR

by
Varinder Pal Malik

A Thesis
Submitted to the Faculty of
New Jersey Institute of Technology
in Partial Fulfillment of the Requirements for the Degree of
Master of Science in Chemical Engineering

Department of Chemical Engineering,
Chemistry and Environmental Science

October 1995

APPROVAL PAGE

REMOVAL OF VOCs FROM WASTE GAS STREAMS BY A HOLLOW FIBER PERMEATOR

Varinder Pal Malik

Dr. Kamalesh K. Sirkar, Thesis Advisor — Date
Professor of Chemical Engineering and Sponsored
Chair in Membrane Separations and Biotechnology
New Jersey Institute of Technology

Dr. Henry Shaw, Committee Member — Date
Professor of Chemical Engineering
New Jersey Institute of Technology

Dr. Demetri Petrides, Committee Member — Date
Professor of Chemical Engineering
New Jersey Institute of Technology

BIOGRAPHICAL SKETCH

Author: Varinder Pal Malik

Degree: Master of Science in Chemical Engineering

Date: October 1995

Undergraduate and Graduate Education:

- Master of Science in Chemical Engineering,
  New Jersey Institute of Technology,
  Newark, NJ, 1995

- Bachelor of Science in Chemical Engineering,
  Punjab University,
  Chandigarh, India, 1988

Major: Chemical Engineering

This thesis is dedicated to my parents

ACKNOWLEDGEMENT

I wish to express my sincere gratitude to my supervisor, Professor K.K. Sirkar for his guidance, encouragement and moral support through this research. I feel greatful that he gave me an opportunity to be a part of his research group. His dedicated style of teaching, constructive criticisms and thoughtful suggestions have contributed immensely to enhance my overall technical skills.

Special thanks to Dr. H.Shaw and Dr. D. Petrides for serving as the members of the committee and making helpful suggestions.

The financial support provided by Center for Waste Reduction Technology (CWRT), through the Sponsored Chair in Membrane Separation and Biotechnology is greatly acknowledged.

I am really greatful to the members of Membrane Separations group without whose help this work would not have been possible. I would like to thank especially Gordana Obuskovic, Uttam Shanbag, Dr. J. Cha, Dr. S. Majumdar and Sarma Kovvali for making useful suggestions and rendering help whenever required. I feel proud to have Gordana, Manmeet and Tejbir as my friends. I sincerely appreciate their help; I cherish the pleasant moments I have spent with them. I wish to acknowledge the help and support of my roommates, Purnendu and Abhinav: I would also like to extend my thanks to other members of the group, including Dr. D. Bhaumik, Dilip Mandal, Dr. R. Li and Dr. T. Poddar. I express my thanks to Ms. Judy Kapp for helpful advice and help. A heartful gratitude is due to members of my family for their love and support. Finally I express my sincere gratitude to almighty God.

TABLE OF CONTENTS

TABLE OF CONTENTS
(Continued)

LIST OF TABLES

LIST OF TABLES
(Continued)

LIST OF FIGURES

LIST OF FIGURES
(Continued)

Figure **Page**

LIST OF FIGURES
(Continued)

Figure **Page**

NOMENCLATURE

A	Membrane surface area in a module, $\pi.D_{lm}.l.N$, cm^2
a,b	Regression constants determined from experimental data
D_i, D_o	Inside and outside diameters of microporous hollow fibers
D_{lm}	Logarithmic mean diameter of a hollow fiber , cm
F_i, F_o,	Feed side total gas flow rate at the feed inlet end and feed outlet end of the permeator, gmol/sec
Fp	Permeate side total gas flow rate at the permeate outlet end of the permeator, gmol/sec
J_{VOC}, J_{N2}	Flux of VOC and flux of N_2, gmol/cm^2/sec
L, L_f	Feed side gas flow rate per fiber at any location and at the feed inlet end of the permeator, gmol/sec
L^*, L_f^*	Dimensionless feed side gas flow rate per fiber at any location and at the feed inlet end of the permeator, Equation (2.12)
L_{ref}	Reference flow rate per fiber, gmol/sec
l	Distance of any permeator location, starting from the feed outlet end, cm
l_f	Total length of permeation in a permeator, cm
N	Number of fibers in a module
P,P_f,Pw	Feed side pressure at any location, at the feed inlet end and at the feed outlet end of the permeator, cm Hg
P_{if}	Partial pressure of species i on the feed side, cm Hg
P_{ref}	Reference pressure, cm Hg
p	Permeate side pressure, cm Hg
p_{iP}	Partial pressure of species i on the permeate side, cm Hg

NOMENCLATURE
(Continued)

Q_i	Permeability of species i, (gmol-cm)/(cm^2-sec-cm Hg)
Q_i	Permeability of species i, (gmol-cm)/(cm^2-sec-cm Hg)
Q_{ref}	Reference permeability, (gmol-cm)/(cm^2-sec-cm Hg)
Q_i/δ_m	Permeance of species i, gmol/(cm^2-sec-cm Hg)
R	Universal gas constant, (cm^3-atm)/(gmol-°K)
S	Dimensionless area defined by Equation (2.12)
T	Absolute temperature, °K
V, V_f, V_w	Permeate side gas flow rate per fiber at any location, at the permeate outlet end, and at the permeate inlet end of the permeator, gmol/sec
V^*, V_w^*	Dimensionless permeate side gas flow rate per fiber at any location and at the permeate inlet end of the permeator, Equation(2.12)
x, x_f, x_w	Mole fraction of VOC in the feed side gas mixture at any location, at the feed inlet end, and at the feed outlet end of the permeator
y, y_f, y_w	Mole fraction of VOC in the permeate side gas mixture at any location, at the permeate outlet end, and at the permeate inlet end of the permeator
$y_{N2,p}$	Mole fraction of nitrogen in the permeate side gas mixture at the permeate outlet end of the permeator
x_{N2}, $x_{N2,i}$, $x_{N2,o}$	Mole fraction of nitrogen in the feed side gas mixture at any location, at the feed inlet end, and at the feed outlet end of the permeator

Greek Symbols

δ_m	Thickness of the rubbery silicone membrane, cm
α_i	Dimensionless permeability of species i, Equation (2.12)

NOMENCLATURE
(Continued)

μ_F	Viscosity of feed at any location of the permeator, g/cm/sec
μ_{ref}	Reference viscosity, g/cm/sec
γ_1, γ_{1f}, γ_{1w}	Dimensionless feed pressure at any location, at the feed inlet end, and at the feed outlet end of the permeator
γ_2, γ_{2w}	Dimensionless permeate pressure at any location and at the closed end of the permeator
β	Dimensionless parameter, defined in Equation (2.12)

CHAPTER 1

INTRODUCTION

1.1 Background

Volatile organic solvents commonly find application as carrier and dissolving agents in industrial processes. During these operations, these volatile organic compounds commonly identified as VOCs, escape into the atmosphere through exhaust air streams. The more common VOCs are toluene, xylene, acetone, trichloroethylene, ethanol and methanol. These organic vapors react with nitrogen oxides and other airborne chemicals to form ground-level ozone which is a major component in the formation of smog (Ruddy and Carroll, 1993). Total nationwide emissions of VOCs in 1975 from stationary sources were estimated by the EPA to be about 31 million tons (EPA, 1976). Till now, these compounds were simply discharged into the atmosphere. Nowadays stringent environmental regulations, most notably the Clean Air Act Amendments of 1990 (CAAA), have focused the attention on pollution prevention and emissions control. One of the most formidable challenges posed by CAAA is the search for efficient and economical control strategies for volatile organic compounds. As a result of CAAA, thousands of currently unregulated sources will be required to reduce or eliminate VOC emissions. In addition, sources that are currently regulated will have to seek to evaluate alternative VOC control strategies to meet stricter regulatory requirements such as Maximum Achievable Control Technology (MACT) under Title III of CAAA (Mukhopadhyay and Moretti, 1993).

A number of physical or chemical processes can be used to separate different kinds of industrially-emitted VOCs. Some common techniques for reducing emissions are incineration or thermal oxidation, condensation, absorption in a liquid and adsorption on activated carbon.

Incineration is frequently uneconomical due to the very dilute concentration of VOCs in the air and the possibility of formation of chlorinated compounds like dioxin (Armand et al., 1990). Supplemental fuel-firing is required if VOC concentration is not high enough. Incineration also has to avoid also inlet concentrations of VOC in excess of 25% of the LEL (lower explosive limit) (Ruddy and Carroll, 1993).

Condensation comes out to be a very expensive alternative when used to cool large volumes of dilute gas to condense the VOCs.

Absorption of VOCs using oil scrubbers can be uneconomical for large or small flow rates. The equipment is often bulky and suffers from flooding and loading problems. Absorbed VOCs still have to be separated from the scrubbing solvent to regenerate the solvent.

High concentrations of VOCs would require a large amount of activated carbon for adsorption thus making the whole process very expensive. Adsorption always needs two beds for a continuous operation. The process becomes less efficient if relative humidity in inlet stream exceeds 50% and if process stream contains VOCs like ketone, aldehyde, and ethers (Ruddy and Carroll, 1993). The exothermic adsorption process can lead to frequent operational problems and even fire in plants (Armand et al., 1990). Contamination of activated carbon and equipment corrosion are some of the other problems which require expensive equipment.

Biofilters may be used but they cannot handle all VOCs and also require expensive R&D effort. A simple, cheap and reliable process that can be used at any scale and that can reduce VOC levels substantially regardless of the nature of the VOC is needed.

The potential for removing VOCs from air by membrane separation processes is being explored increasingly. Membrane-based separation processes are simple and reliable. For a higher degree of separation, the membrane, which is the major component in the membrane-based separation system, should have high permeability for the vapor component, high selectivity between gas/vapor components and high chemical, thermal, and mechanical stability. The modular nature and a high surface area per unit volume are the advantages the membrane technology has over conventional technologies. The separation of one gas from a gas mixture by preferential permeation has been investigated for a long time (Sengupta and Sirkar, 1986). However, the effort to separate VOCs from air/N_2 using rubbery polymeric membranes began recently.

There are a number of membrane transport mechanisms which can be used to separate vapors from air. The transport-cum-separation mechanisms are identified as follows (Sengupta and Sirkar, 1986) :

1. Poiseuille flow
2. Knudsen flow
3. Surface diffusion
4. Pore condensation
5. Pore blockage
6. Permeation (solution-diffusion).

Membranes having transport mechanisms 1 to 5 can be either porous or microporous.

This depends on the size of pores in the matrix of membrane, gas pressure and temperature. Membranes, where permeation is the mechanism, are nonporous. This thesis explores vapor separation process using the mechanism of vapor permeation in a composite membrane. The permeation of a vapor through a nonporous polymeric membrane is usually studied by solution-diffusion model. The permeation of the vapor depends amongst others on the nature of the membrane. The membrane can be glassy or rubbery or a gel. Glassy polymers facilitate the removal of small molecules of gases like H_2 and He through the small openings between rigid polymer backbones rather than gaseous species having larger diameters like organic solvents. Therefore glassy polymeric membranes are normally not used for selective VOC permeation-based separation; instead, rubbery polymeric membranes are being employed extensively for removing VOCs from air.

1.1.1 Rubbery Membranes

The permeation of a gas/vapor through the dense polymeric membrane depends on the diffusion and solubility coefficient of the gas/vapor in the polymer. Generally the diffusion coefficient of a molecule decreases with increasing molecular size, but the solubility coefficient increases with increasing molecular size and with increasing condensibility of the gas/vapor molecules. The transport of a gas/vapor through a rubbery polymeric membrane is determined more by its solubility coefficient than by its diffusion coefficient. The high solubility of organic vapors in rubbery polymers is the reason for their high permeability.

Baker et al. (1987) conducted experiments for the separation of nitrogen and

organic vapors using various polymeric membranes and concluded that permeabilities of VOCs (toluene,acetone etc.) increase with increasing solvent vapor pressure in the gas phase. Among these membranes, silicone rubber showed the highest VOC permeability and Neoprene rubber exhibited the highest selectivity for toluene/N_2 and acetone/N_2.

Strathmann et al. (1986) developed composite membranes using poly(dimethylsiloxane) as the selective barrier both in the form of hollow fibers and flat sheets to study the permeation/separation of toluene, acetone, trichloroethane etc. .

Kimmerle et al. (1988) explored the separation of acetone from acetone/air using a thin film composite hollow fiber membrane using poly(dimethylsiloxane) laminated to the inner surface of a polysulfone hollow fiber. Although the actual coating thickness was 1.5 μm, the theoretical coating thickness was much higher (12.7 μm) due to the low porosity of the polysulfone substrate.

Wijmans and Helm (1989) used MTR (Membrane Technology & Research, Menlo Park, CA) multilayer composite membranes assembled into spiral-wound modules for the separation of organic vapors from N_2.

Although silicone {poly(dimethylsloxane)} membranes exhibit high permeabilities for various VOCs and have been used in a number of studies, yet the overall membrane configurations and membrane modules as explained above are not highly efficient. For example polysulfone substrate used by Kimmerle et al. (1988) had a low porosity; this resulted in a very low value of permeability coefficient and a high value of effective membrane thickness. These quantities adversely affect the VOC flux through the membrane, all other conditions remaining constant. MTR-based membranes are flat and have to be supported. They are packed into a module using the spiral wound

configuration (Baker et al., 1987 ; Wijmans and Helm, 1989). As a result the membrane surface packing density of these membranes is much lower than that possible in a hollow fiber module. This decreases the separation/permeation performance of spiral wound module as the area available for permeation is substantially less than in hollow fiber module.

Cha (1994) used ultrathin silicone membranes bonded to microporous polyproplyene hollow fiber substrate by plasma polymerization. Cha (1994) used hollow fiber module configuration to explore the permeation/separation of methanol and toluene from a N_2-VOC mixture. His study demonstrated that this module configuration was highly efficient and it also eliminated the shortcomings of both Kimmerle et al. (1988) and Baker et al. (1987). The silicone membrane was ultrathin and the membrane surface packing density was an order of magnitude higher than that possible in a spiral wound module. A mathematical model was used to describe the experimental permeation and separation behavior in the hollow fiber module. None of the earlier hollow fiber-based studies of VOC separation had attempted to describe the module permeation behavior via such models. However the work done by Cha (1994) needed to be carried out further for a number of reasons explained below.

The experimental results indicated by Cha (1994) had to be confirmed first before an extension of his study could be carried out. Although a mathematical model had been developed to explain VOC permeation/separation, limited attempt was made to simulate the model for checking the validity of theoretical results with the experimental observations. In order to simulate the model there was a need to experimentally determine the relationship between the VOC permeance and the feed concentration of the

VOC. The VOCs needed to be studied were toluene and methanol since Cha (1994) had studied them. It was also necessary to explore the permeation/separation behavior of other VOCs (methylene chloride, acetone, hexane etc.) using the same module configuration, to find out how general the observed behavior of toluene and methanol were. Cha (1994) had focused on separation of specific individual VOCs, but many a times, the industrial exhaust streams contain multiple VOCs; so a study of simultaneous removal of multiple VOCs present in a feed mixture was also called for.

The mode of feed introduction and the pressure of the feed entering the module can have an effect on the extent of removal of the VOC. Cha (1994) had focused only on one mode of feed introduction, feed entering from the tube side of the membrane module with vacuum being pulled from the shell side. Thus there is a need to analyze other modes of feed introduction, for example, feed entering the module from shell side and vacuum being pulled from the tube side of the membrane module. Many industrial streams contaminated with VOCs are present at pressures higher than atmospheric. Cha (1994) did not explore the effect of high pressure inlet feed on the separation of VOCs. Some other issues that needed further study were the behavior of N_2 flux and permeance under varying feed conditions and change in permeation/separation of various VOCs if feed used were VOC/air mixture instead of VOC/N_2 mixture as studied by Cha (1994).

In this thesis an attempt has been made to explain the overall VOC permeation-separation mechanism in general for individual VOC permeation and to address the above mentioned concerns in particular.

CHAPTER 2

REMOVAL OF VOCs FROM NITROGEN/AIR BY A RUBBERY MEMBRANE

2.1 Introduction

2.1.1 Transport in Nonporous Membranes

Research on vapor permeation/separation using membranes began recently even though gas separation membrane processes have been studied for more than twenty years. In vapor permeation using membranes, the feed, either a vapor mixture or a gas-vapor mixture is passed over a permselective, nonporous membrane and the component to be separated from the feed mixture permeates through the membrane. In contrast to vapor permeation, vacuum-based pervaporation is a process where the feed is a liquid and the component to be separated permeates through the membrane and appears in the gas phase on the permeate side of the membrane maintained under vacuum.

The permeation of organic vapors/gases through nonporous membranes is best explained by the solution-diffusion model. According to this model, molecules of the vapor/gas in the feed get dissolved in the high pressure side of the nonporous membrane, then diffuse through the membrane and finally they get desorbed on the low pressure side of the membrane. Usually the separation is carried out at a low pressure although in this thesis separation results from a high pressure feed have also been reported. For the component permeating preferentially through the membrane, the rate of permeation

depends on the partial pressure difference on the two sides of the membrane (Wijmans and Helm, 1989), the membrane thickness and the permeability of that specific component. Permeability is defined as the product of diffusivity of the gas/vapor through the membrane and its solubility in the membrane. Diffusivity is a kinetic property and increases with the decreasing size of the permeant molecule. Solubility is a thermodynamic property and it increases with the increasing size and condensibility of the permeant molecule.

The permeability of very small molecules like He or H_2 is high in polymeric membranes because of their high diffusivity through the polymeric membrane. On the other hand, large molecules such as CO_2 have also a high permeability due to their high solubility in the membrane. In the case of the vapors, because of their high condesibility, the permeabilities are significantly higher than simple gases in most polymers (Baker et al., 1987 & 1988; Feng et al., 1991 & 1993).

Solubility rather than diffusivity of the vapor determines its transport through a rubbery polymeric membrane. Most of the vapors have high condensibility due to their high critical temperature; so they have high solubility and thus high permeability in the rubbery membrane. Secondly, higher sorption at high organic vapor pressures leads to plasticization of the membrane which increases the diffusivity of organic vapor through the plasticized polymer matrix. Permeabilities of organic vapors are therefore a strong function of their partial vapor pressure in the gas phase and it increases with increasing vapor concentrations. The nature of the polymer membranes also effects the permeation of gas/vapor through nonporous membranes. Rubbery polymers such as silicone rubber have high chain mobility and thus they show relatively high permeabilities for most

gases/vapors, but the selectivities are generally poor. On the other hand glassy polymers such as polystyrene show lower permeabilities but higher selectivities than rubbery membranes.

For simple gases such as, O_2, N_2 etc, pemeabilities through a nonporous polymeric membrane are generally not a function of their concentration or partial pressure in the gas phase. For rubbery membranes, the permeabilities of the simple gases are taken as constant (Stern and Frisch, 1981).

Since nonporous silicone rubbery membranes have extremely high permeabilities for VOCs and lower permeabilities for nitrogen or oxygen, they are most widely used for vapor separation (Peinemann et al., 1986). The selective membrane in this study is therefore an ultrathin silicone membrane.

2.1.2 Objective of this Study

The objective of this thesis is to develop as well as study the selective permeation-recovery of volatile organic compounds (VOCs) from N_2/air emissions via highly VOC-selective hollow fiber membranes. This research explores experimentally the extent of selective removal of VOCs, e.g., acetone, methanol, methylene chloride, toluene and hexane from N_2/air at atmospheric pressure and models the separation performance of the hollow fiber permeator for toluene and methanol. The aim is to try to reduce inlet N_2/air VOC concentrations of around 5,000 - 20,000 ppmv + to the level of 200 - 800 ppmv or lower in the treated N_2/air stream exiting from the hollow fiber membrane permeator. A particular objective is to study and explain different modes of operation through the hollow fiber membrane module namely the mode where feed is going

through the lumen of the fibers with vacuum being pulled from the shell side and the reverse mode. This thesis also pursues an initial exploration of the effect on separation of VOCs for the feed entering the hollow fiber module at high pressures. Although the primary focus has been to remove individual VOCs from the streams, yet the simultaneous removal of multiple VOCs from the feed streams has also been briefly studied experimently.

2.1.3 Membrane Form, Structure and Operational Mode

In the hollow fiber module (HFM), membranes are self-supporting against any applied pressure difference needed for vapor separation, whereas flat membranes need additional mechanical support. For a high vapor permeation rate the membrane should be ultrathin, so a thin (~ 1 μm) film composite (TFC) membrane structure has been chosen here supported on a microporous hollow fiber substrate for mechanical strength. In order to reduce the mass transfer resistance through the support, the porosity of the support should be high. Celgard x-10 fiber is isotropic and has a porosity of 0.3 which is quite high. Thus hollow fibers of this study have an ultrathin silicone coating on the outside surface of a Celgard x-10 fiber and thus high substrate porosity will not reduce the flux through the coating (Matson et al., 1983; Sengupta and Sirkar, 1986). Generally the hollow fiber modules have a membrane surface packing density of 40-80 cm^{-1} as compared to 5-7 cm^{-1} as in case of spiral wound membranes. It is also important that support material be cheap and have a reasonably high solvent resistance. Polypropylene is quite suitable in this regard as it is strong, cheaper than polyetherimide (Behling et al., 1989) and also has considerable solvent resistance compared to polysulfone used by

others (Strathmann et al., 1986; Kimmerle et al., 1988). The fibers used in this study have been obtained from AMT (Applied Membrane Technology, Minnetonka, MN) . These fibers have an ultrathin plasma-polymerized silicone layer ($\sim 1\ \mu m$) strongly bonded to the substrate and can handle a pressure difference up to 200 psia (Papadopoulos, 1992). The strength of these bonds makes it possible for the silicone membrane to withstand extra stress and possible delamination when vacuum is pulled through the shell side and feed gas flows through the tube side.

Normally feed streams containing VOC are available at atmospheric pressure and a vacuum is pulled on the other side of the membrane to provide a partial pressure driving force for the VOC. With hollow fiber membranes this can be achieved in two ways. Figures 2.1 and 2.2 show the schematic diagrams of the two different modes of operation. Vacuum can be pulled through the porous substrate but this would result in considerable pressure drop not only through the substrate but also through the fiber lumen (figure 2.2). There is also a possibility of reduced separation due to shell-side bypassing of the feed if feed gas were to flow through the shell-side. Therefore it is advantageous to pull the vacuum through the shell side and have the feed gas flow through the tube side (figure 2.1). However this operational mode subjects the silicone coating on the fiber outside diameter to extra stress and possible delamination from the substrate, but in this case since the silicone rubber coating has been plasma polymerized on the substrate, the bond is strong enough to bear the induced stress. As high removal of VOC is desirable, the gas flow rate through the fiber bore would have to be low and this will reduce the flow pressure drop in feed gas substantially. Thus the membrane form, structure and operational mode chosen for this study are likely to be optimal.

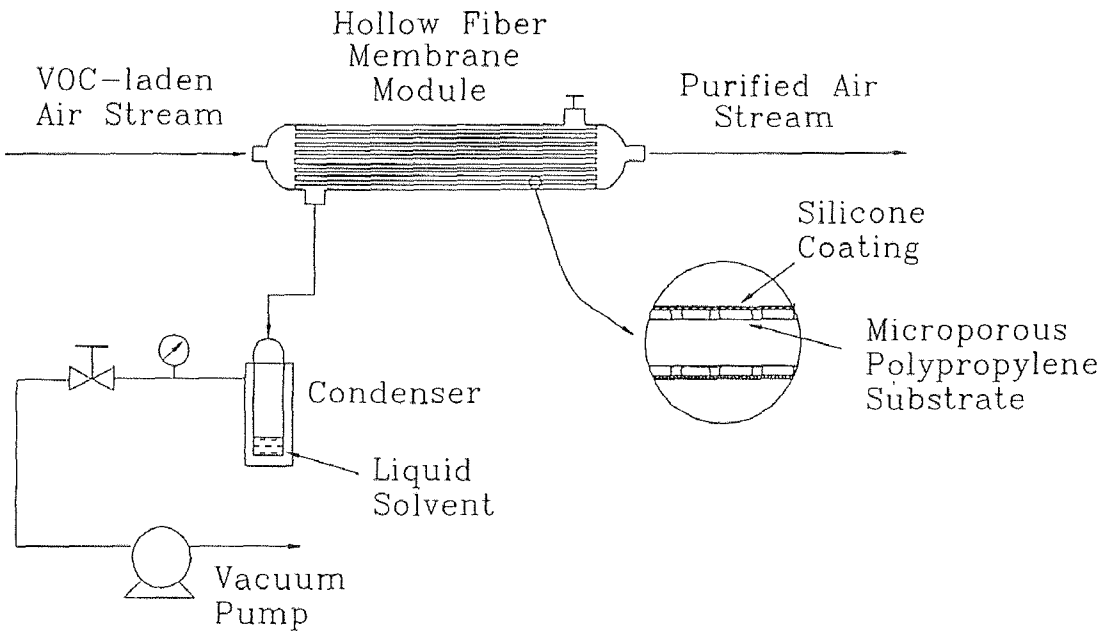

Figure 2.1 Schematic of VOC Separation from Air/ Nitrogen at Atmospheric Pressure by Permeation through a Hollow Fiber Module

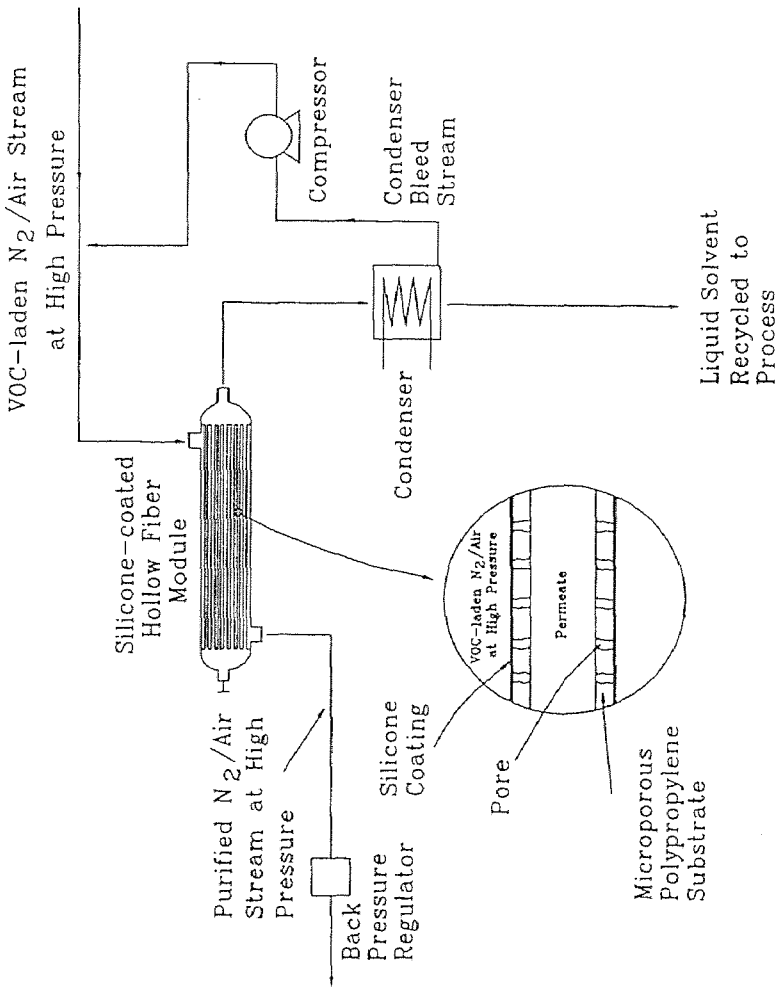

Figure 2.2 Schematic Diagram of VOC Separation-Recycle from Air/Nitrogen at High Pressure

Hollow fibers provide high membrane surface packing density. Celgard x-10 substrate is cheap, strong, chemically resistant and has a high porosity. The actual silicone membrane is ultrathin, has a low permeation resistance but is strongly bonded to the substrate to handle high pressure drops.

2.2 Experimental

2.2.1 Materials, Chemicals and Equipment

The materials, chemicals, and equipment used for experiments were as follows :

Multiple Flow Controller (Model 8249, Matheson,East Rutherford, NJ)

Mass Flow Transducer (Model 8141, Matheson, East Rutherford, NJ)

Mass Flow Controller (Model 8251, Matheson, East Rutherford, NJ)

Silicone-Coated Hollow Fibers (AMT, Minnetonka, MN)

Gas Chromatograph (GC, Hewlett Packard Model 5890A)

Automatic 10-port Gas Sampler (Hewlett Packard Model 18900F)

Integrator (Hewlett Packard Model 3392A)

Vacuum Pump (Model 1410, Welch Scientific Inc., Skokie, IL)

Vacuum Gauge (Heise, Newtown, CT)

Cold Trap (Model 8640, Pope Scientific Inc., Menomonee Falls, WI)

Insta-Ice Dry Ice Machine (No.475, Polyfoam Packers Corp, Wheeling, IL)

Constant Temperature Bath Heater (Haake, Germany)

Bubble Flow Meter (Varian, CA)

Nitrogen Dry, Air Dry, Air Zero, Hydrogen Zero, Helium Zero, Methylene Chloride: 1000,6000ppmv, Acetone; 1000,3000ppmv, Hexane: 1062ppmv (Matheson, East Rutherford, NJ)

Toluene, Methanol, Methylene chloride, Acetone (ACS grade, Fisher Scientific, Springfield, NJ)

In HP 5890A gas chromatograph, a new 10-port automatic gas sample valve (HP 18900F) which has 0.25 c.c. sampling loop inside the valve was installed for automatic sample analysis.

2.2.2 Hollow Fiber Module Preparation

The hollow fibers used for making the module were supplied by Applied Membrane Technology (AMT, Minnetonka, MN). As a first step fibers were taken from the roll and were cut. Two different modules were prepared. Fifty and fifteen fibers of specified length (25 cm and 6 cm respectively) were taken and spread on a vinyl sheet on a table. Then the spread out fibers were collected and one end was tied with a string. This end was then pulled through the bore of a stainless-steel tubing (I.D.: 0.62 cm) used as the shell for the module.

A three-layer potting was done to prepare a leak-free tube sheet for the module. Figure 2.3 shows the cross section of one fiber and three layers of potting and figure 2.4 gives the schematic diagram of a hollow fiber module. For the first layer a two component RTV118 translucent silicone rubber adhesive sealant (GE Silicones, General Electric Co.,Waterford, NY) was applied. This adhesive was used because it was very viscous and had high compatibility (or sealing) with the silicone fibers. After a curing

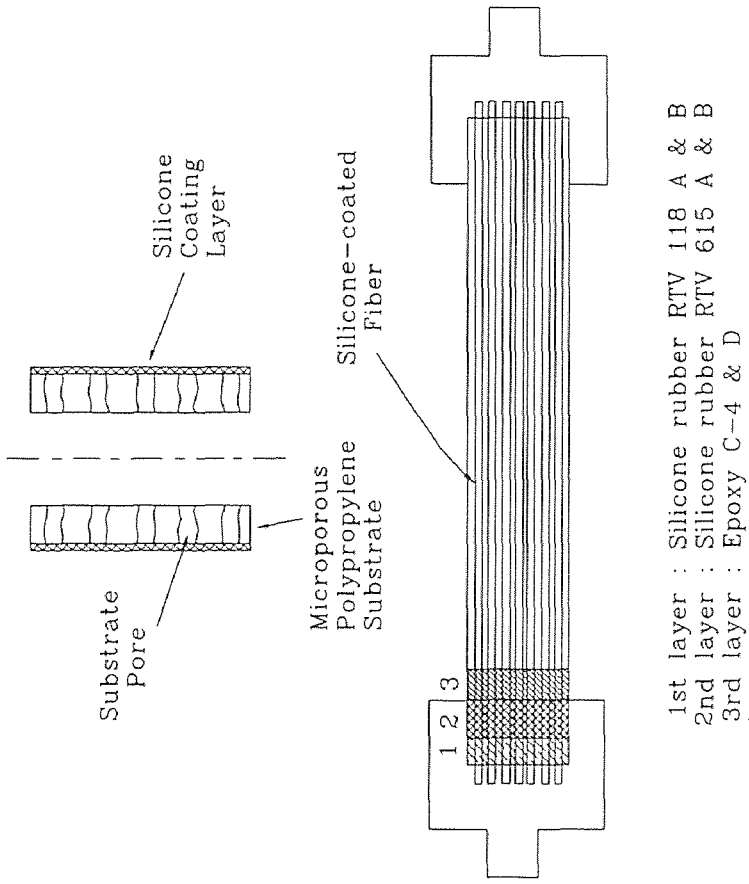

Figure 2.3 Schematic of Silicone-Coated Fiber and Potting

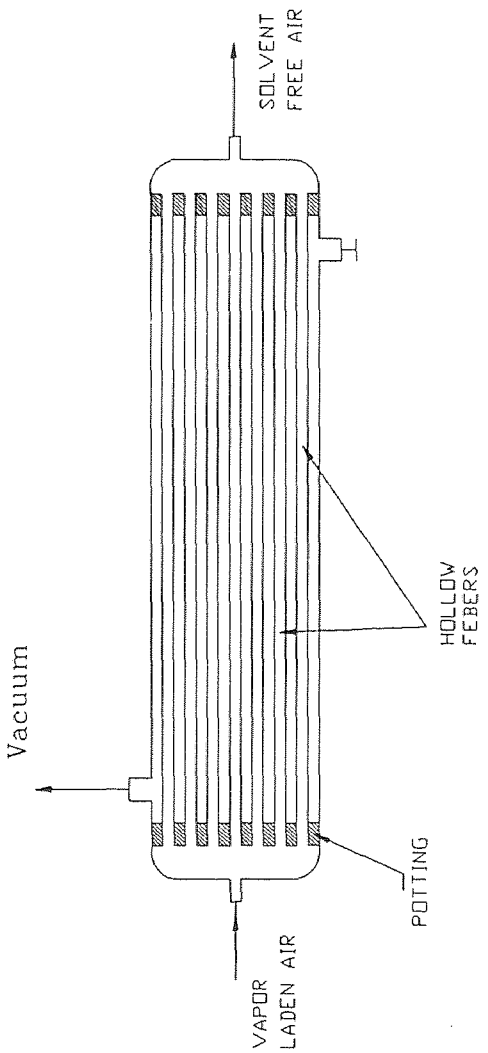

Figure 2.4 Schematic of a Hollow Fiber Module

period of one day, another two-component silicone rubber, RTV 615 (GE Silicones, General Electric Co., Waterford, NY), mixed thoroughly using 10 % by weight of the B curing agent with the A silicone compound (entrapped air removed in a desiccator using vacuum pump for approximately 5 min.), was applied as a second layer through the shell side. This compound undergoes an addition hydrosililation reaction and develops crosslinking.

The curing time for this silicone rubber is longer and it depends on the temperature. At slightly higher temperature condition (40-50 °C) the curing time will reduce a little bit, but usually it takes over 72 hours (Cha, 1994). The second layer of silicone rubber was cured for four days and then epoxy was applied as the third layer through the shell side opening. The epoxy comprised of two components, C4 and "D" activator (Beacon Chemicals, Mt.Vernon, NY) mixed in an epoxy/activator weight ratio of 4/1. Epoxy was used as the third layer because it has good sealing properties with the metal parts. This epoxy was used because it made a leakproof seal with module metal parts and was also resistant to VOCs used in experiments.

The effective surface area of the module 2 was 103.78 cm^2 (# of fibers : 50, length : 25 cm) and this module was used throughout the separation experiments. The much smaller module 4 had an effective surface area of 7.47 cm^2 (# of fibers : 15, length : 6 cm) and was used for the measurement of permeance of VOCs. The specifications of the modules prepared are shown in table 2.1 and figure 2.5 shows the photographs of the two membrane modules used in this study. Module 2 was the same as used by Cha (1994) for his experimental study. Module 4 was specially made as a part of this research effort.

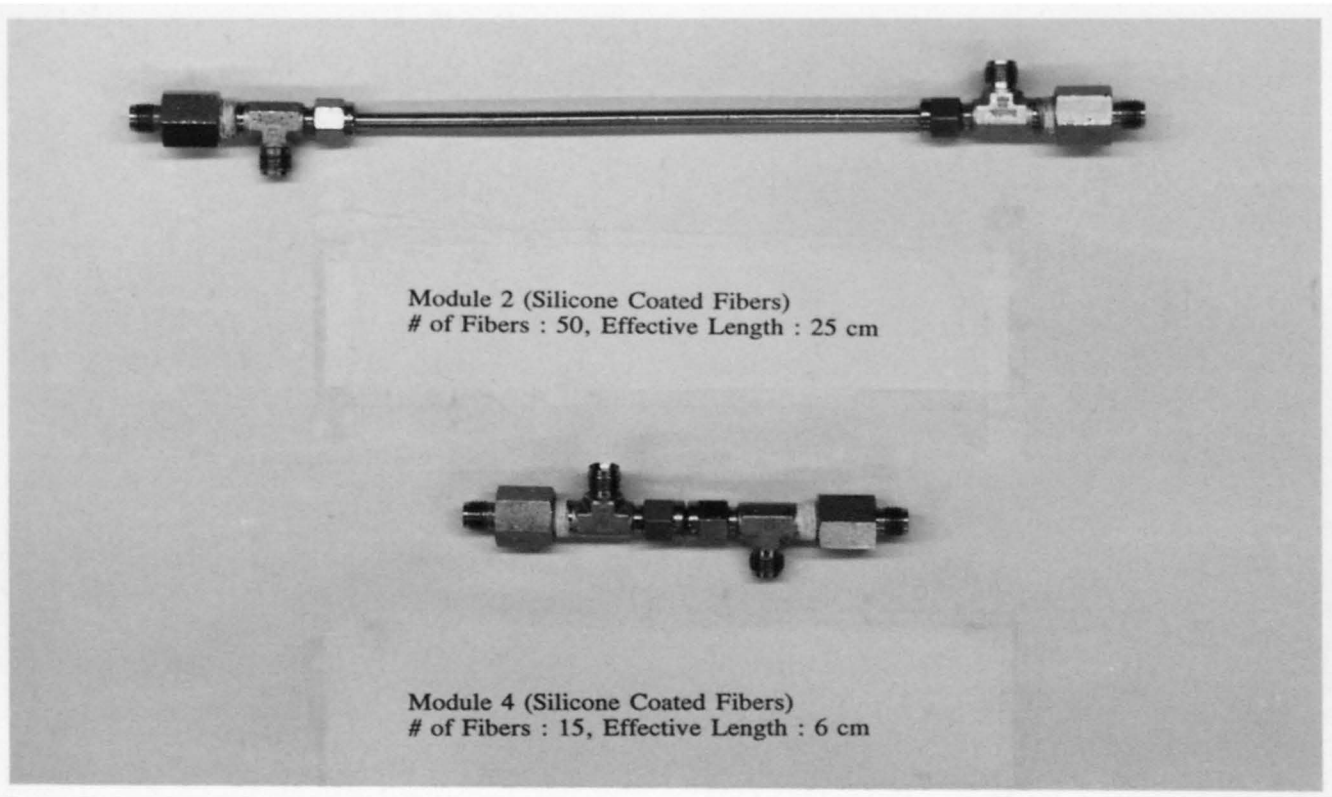

Figure 2.5 Photograph of the Membrane Modules used

Table 2.1 Specifications of the Modules Prepared

#	# of Fibers	Effective Fiber Length (cm)	Surface Area of Module (cm^2)	I.D./O.D. of the Fibers (μm)	Coated Layer Thickness (μm)	Average Support Porosity	Avg. Pore Size (μm)
4	15	6	7.47	240/290	~1	0.4	0.03
2	50	25	103.8	240/290	~1	0.4	0.03

For testing the module for any possible leaks, distilled water was filled into the shell side of the module. Water pressure was raised to 10-20 psig for about 10 minutes. No water was seen coming through the tube side and this confirmed that there was no leakage in the module. Pure nitrogen was passed through the tube and shell side of the module for two hours to completely dry the fibers prior to experiments.

2.2.3 Experimental Apparatus

The experimental setup is shown schematically in figure 2.6. A stream of nitrogen was introduced from a cylinder to a stainless steel bubbler filled with the VOC. An air diffuser was used to make fine nitrogen bubbles in the VOC bubbler so as to enhance the contact of nitrogen with the VOC. The VOCs used were methanol, acetone and toluene. This stream was then blended with a second stream of pure nitrogen to produce a stream

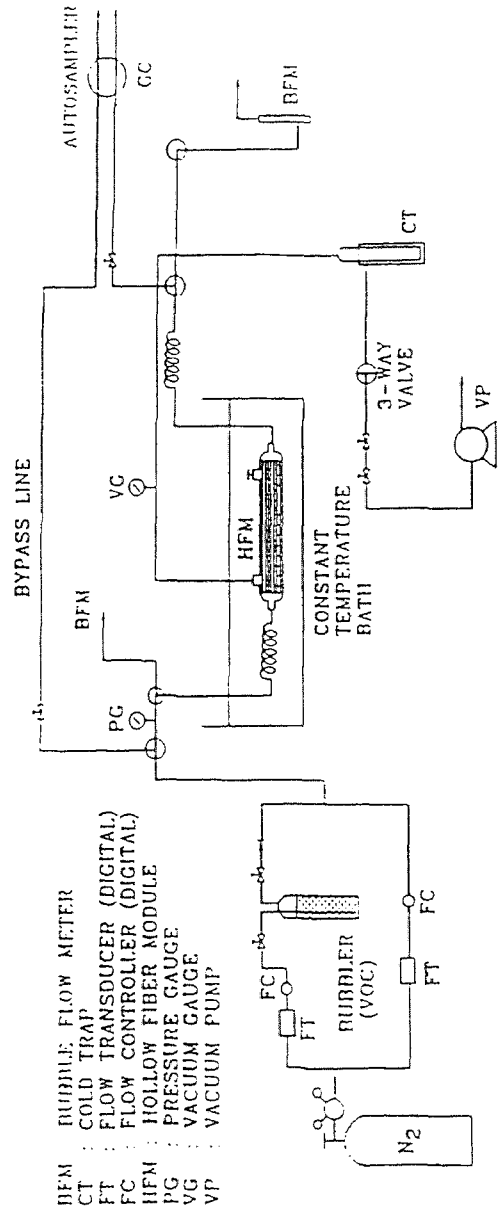

Figure 2.6 Schematic of Experimental Setup for Permeation of VOC from Nitrogen using Rubbery Membrane

of desired VOC concentration and flow rate. The flow rates of the two streams were monitored by a Matheson digital readout and control module (Model 8249). The same module was used to set and control the flow rates. Check valves (1/3 psi) were placed at appropriate places to check any backflow into the bubbler. The VOC/N_2 stream of desired concentration was then split into two streams. One stream which had a small flow rate (1 cc/min) was directed to sample loop 1 of the automatic gas sampler of the gas chromatograph (GC) to measure the concentration of the VOC prior to separation. The other stream was introduced to the tube side of the HFM as vacuum was applied countercurrently in the module shell-side. In all experiments vacuum was kept at 1.0 torr. Pressure gages were placed at the inlet and outlet of the HFM to measure any pressure drop through the module. The outlet stream from the HFM was also split into two streams. The smaller stream, whose flow rate was carefully controlled by using two valves to be about 1 cc/min, was sent to sample loop 2 of the automatic gas sampler of the GC to measure the VOC concentration after the separation. The other stream was vented to the laboratory hood. In this way feed inlet as well feed outlet samples were simultaneously analyzed during the experiments. Two two-way valves were placed in the VOC/N_2 lines at the inlet and outlet of HFM. This was done to measure the inlet and outlet flow rates through the HFM with bubble flow meter. A vacuum pump (Model 1410, Welch Scientific Inc., Skokie, IL) was used to pull vacuum in the shell side. A cold trap was connected between the vacuum pump and the HFM. A mixture of dry ice and acetone was used in the cold trap to condense the VOC in the permeated gas stream.

In some experimental runs, VOC-containing N_2 feed gas was obtained from a primary standard mixture cylinder (Matheson, E. Rutherford, NJ). A high pressure

primary standard acetone-N_2 mixture cylinder containing 3000 ppmv acetone was used for high pressure runs (upto 60 psig, i.e., about 4 atmospheres gauge) where feed was on the shell-side with vacuum on the tube-side. A back pressure regulator was used at the outlet of the module to maintain the required high pressure. The runs with methylene chloride as VOC were carried out using two primary standard methylene chloride-N_2 mixture cylinders of 998 and 6000 ppmv. The run for multiple VOCs employed a primary standard mixture cylinder containing 1010, 780 and 900 ppmv of acetone, methanol and methylene chloride respectively; experiments for hexane separation were carried out using a cylinder containing 1062 ppmv of hexane in N_2. These cylinders were obtained from Matheson, E. Rutherford, NJ. Feed gas flowed, in this case, through the fiber bores.

The membrane module was immersed in a water bath. The temperature of the bath was maintained at 30°C by a constant temperature immersion circulator (Hakke, Germany).

The concentration of VOC in the gas stream was measured in a GC (Hewlett Packard Model 5890A) via a flame ionization detector (FID). The two streams from the inlet and the outlet of the HFM were connected to a 10-port automatic gas sample valve (HP 18900F) which had two 0.25 cc sampling loops. The inlet and outlet streams were connected to loops 1 and 2, respectively. There were two injections in each run; injection of sample loop 2 was implemented 2 minutes after the injection of loop 1. The column used was a stainless steel Carbograph column (length: 8 feet, mesh size: 60/80, Alltech, Deerfield, IL). The temperature of the injector, oven, and detector were set at 200, 230, and 250°C, respectively. The retention times for methanol, toluene, acetone,

methylene chloride and hexane were 0.89, 13, 1.34, 1.38 and 5.01 minutes, respectively. After all experiments, approximately 30 cc/min. of nitrogen was passed through the fiber bores to purge out any residual contaminants.

2.2.4 GC Calibrations for Toluene, Methanol, Acetone, Hexane and Methylene Chloride

The calibration curves of toluene and methanol were available from Cha's (1994) work (Figures A.1, A.2 and A.3). Similar method was employed for the calibration of other VOCs. For the preparation of the GC calibration curves, different volumes of various combinations of toluene, methanol, methylene chloride and acetone were mixed with a diluent. For example, methanol and toluene were mixed together with isopropyl alcohol as the diluent in 7 different concentrations for detection and analysis at low concentration range (range = 8) and in 14 different concentrations for high concentration range (range = 13). Acetone (Figures A.4 and A.5) was mixed with toluene in 8 different concentrations and methylene chloride (Figures A.6, A.7 and A.8) was also mixed with toluene in 7 different concentrations. For acetone and methylene chloride, range = 8 was used for detection. The GC used for calibration was HP 5890. The following GC settings were used throughout the calibration process: oven temp.= 200°C, injector temp.=230°C, detector temp.= 250°C.

A new Carbograph column (8 feet long, s.s., mesh size : 60/80, Alltech, Deerfield, IL.) was used to separate the VOCs from the diluent. This new column was baked at 200°C with a carrier gas flow rate of 30 cc/min. overnight before using in the experiments. From each sample solution exactly 1.0 μl of sample was taken by a syringe and injected to the GC. GC peak areas corresponding to the known number of moles of

toluene, methanol, acetone and methylene chloride in 1.0 μl of sample were noted down. In the cases of acetone and methylene chloride, primary standard mixture cylinders from Matheson (acetone = 3000 ppmv, methylene chloride = 1000 ppmv) were used in addition to the manual injections. The total number of moles in the 0.25 cc sample loops of the automatic sampler were calculated. In this case, temperature was taken to be the same as the injector temperature. By comparing the number of moles the VOC in 1.0 μl sample with the moles/mole fraction of the same VOC in the sample loop corresponding to the same GC area, ppmv of the VOC was calculated and plotted against the GC peak area to obtain the calibration curve for each VOC. The calibration of hexane (Figure A.9) was carried out by using the standard mixture (1100 ppmv) from Matheson. These calibrations curves are provided in the Figures A.1 to A.9.

2.2.5 Types of Experiments

1: For the determination of the permeance, (Q_i/δ_m), of toluene and methanol, feed gas was introduced at a high flow rate into the small module 4 so that gas composition changed by less than ten percent. The feed was introduced through the tube side of the HFM.

2: The extent of removal of VOCs (toluene, methanol, methylene chloride, acetone and hexane) was studied at various feed flow rates using module 2; feed VOC concentrations, feed inlet pressures were varied for different experiments. The experiments were carried out using two different modes of operation for feed (viz. tube-side and shell-side) entering the hollow fiber module.

2.2.5.1 Permeance of VOC as a Function of Concentration The permeability of a VOC through silicone rubber is strongly dependent on the partial pressure of the VOC in the gas stream (Baker et al., 1987). To predict the VOC removal performance of silicone coated HFM, it is necessary to know the permeance (Q_i/δ_m) of the VOC in the silicone membrane at a constant partial pressure of VOC. It is difficult to maintain a constant partial pressure of a VOC in a HFM. Experiments were therefore carried out such that the VOC partial pressure changed by a limited amount (less than 10 %) between the inlet and the outlet streams of the module. Thus, the partial pressure of VOC throughout the length of the module was maintained in a small range. These experiments were carried out in module 4 which has a much smaller active area. Experiments were carried out with toluene (inlet concentration varying from 780-12500 ppmv) and with methanol (inlet concentration varying from 500-35000 ppmv) to determine the relation between (Q_i/δ_m) and the partial pressure of toluene and methanol respectively. High feed gas flow rates were used to achieve small changes in the VOC partial pressure along the module. When the inlet VOC concentration was increased the inlet feed flow rate was also increased to achieve the desired minimal removal.

2.2.5.2 VOC Removal in the Hollow Fiber Module In these experiments Module 2 was used to analyze the performance of the HFM under varying feed conditions. In the first set of experiments N_2/air containing VOC/VOCs was passed through the tube side of the HFM and high vacuum (1 torr; 0.1 cm Hg) was applied to the shell side. The flow rate of the gas stream varied between 10 and 150 cc/min. For each flow rate different VOC concentrations were used. The feed concentrations used ranged in

volume % from 0.4 to 1.4% for toluene, 0.4 to 7.10% for methanol, 0.1 to 0.6% for methylene chloride, 0.8 to 2.2% for acetone and 0.01% for hexane. A feed containing multiple VOCs (0.1% acetone, 0.078% methanol and 0.09% toluene) was also used in one of the experiments.

In the second set of experiments N_2 containing a single VOC was passed through the shell side of the HFM and high vacuum (1 torr; 0.1 cm Hg) was applied through the tube side. The flow rate of the gas stream was varied between 60 and 150 cc/min. For each flow rate, different VOC concentrations were used. The feed concentrations used ranged in volume % from 0.4 to 0.95% for toluene and 0.55% to 7.55% for methanol. In another experiment N_2/acetone feed (55 cc/min, 0.3%) was passed through the shell-side at three different inlet pressures (159, 231, and 376 cm Hg) with 0.1 cm Hg of vacuum being applied on the tube side.

The mathematical model described in the next section was used to model the results of toluene and methanol from the first set of experiments using (Q_i/δ_m) as a function of the VOC partial pressure.

2.3 Gas Permeation Model in a Silicone Coated Hollow Fiber Module

The mathematical model for binary gas mixture separation by conventional permeation modes in a hollow fiber module having a significant pressure drop is available in Pan and Habgood (1978). The mathematical analysis of binary gas mixture separation in a HFCLM (hollow fiber contained liquid membrane) permeator under various modes of operation was discussed by Majumdar (1986) and Guha (1989). Majumdar proposed a

three component permeation model with pressure drop in both feed and permeate sides for the sweep gas mode of operation. Guha (1989) extended Majumdar's work to various modes of operations such as vacuum, sweep water, conventional permeation. Using appropriate assumptions these analyses may be adopted to the present situation. A key difference between such modeling analyses and the present work is the strong dependence of the specific permeability or permeance (i.e. Q_i/δ) of a VOC on the partial pressure of VOC. A schematic of the silicone membrane permeator under vacuum mode of operation is presented in the figure 2.1. A mixture of nitrogen and organic vapor (toluene or methanol) was used as a feed gas/vapor mixture. The feed gas/vapor mixture was passed through the bore of the fibers and at one end of the shell side, vacuum was applied so that the shell side flow is countercurrent to the feed side flow.

The following assumptions were employed in developing a model for permeation-separation of a VOC/N_2 feed gas mixture in a coated hollow fiber permeator.

1. The permeability coefficient of a VOC through the silicone coating depends on the VOC partial pressures on two sides of the silicone coating.
2. Axial diffusion is insignificant compared to bulk gas convection.
3. The pressure in the permeate side is constant along the module.
4. There is no mass-transfer resistance in the bulk gas phases and in the pores of the hollow fiber substrate.
5. Hagen-Poiseuille law governs the pressure drop through the fiber lumen.
6. The end effects inside the permeator are negligible.
7. The deformation of the hollow fiber under external pressure is negligible.

A schematic diagram where a VOC/N_2 feed and the permeate stream flow

countercurrently is shown in Figure 2.7. An overall material balance between the feed inlet end and any location at a distance l from the closed end of the permeate side leads to

$$L - V = L_f - V_f \tag{2.1}$$

The mass balances for VOC and N_2 can be written as

VOC:
$$Lx - Vy = L_f x_f - V_f y_f \tag{2.2}$$

N_2:
$$L(1-x) - V(1-y) = L_f (1-x_f) - V_f (1-y_f) \tag{2.3}$$

If the axial coordinate l is positive in the direction of permeate gas flow, the governing differential equations for permeation of two species are:

VOC:
$$\frac{d(Lx)}{dl} = \pi D_o \left(\frac{Q_a(Px,\ py)}{\delta_m}\right)(Px - py) = \frac{d(Vy)}{dl} \tag{2.4}$$

N_2:
$$\frac{d[L(1-x)]}{dl} = \pi D_o \left(\frac{Q_b\ (Px,\ py)}{\delta_m}\right)[P(1-x) - p(1-y)] = \frac{d[V(1-y)]}{dl} \tag{2.5}$$

Note that the permeability coefficients of VOC and N_2, Q_a and Q_b, respectively are functions of partial pressures of VOC in both feed ($Px = P_{iF}$) and permeate ($py = p_{iP}$) streams. The equation governing the pressure drop in the bore of the fiber is

$$\frac{dP}{dl} = \frac{128RTL\mu_F}{\pi P D_i^4} \tag{2.6}$$

Rearranging the above equations and writing them in dimensionless form, one can get

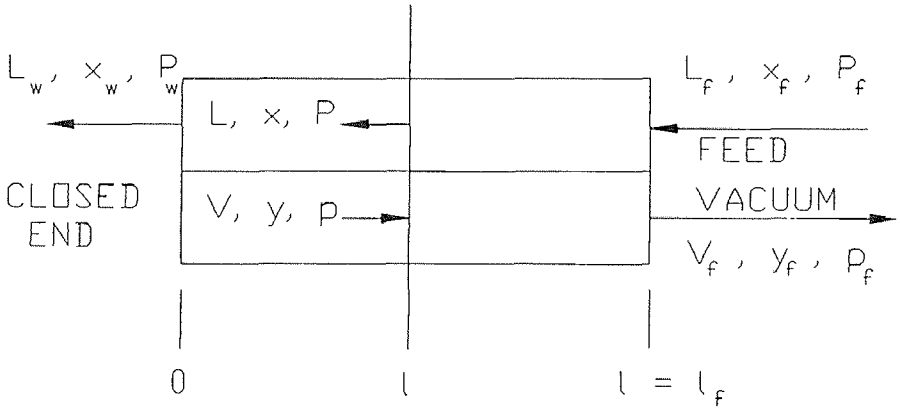

Figure 2.7 Schematic of a Hollow Fiber Permeator for Modelling Vacuum Mode of Operation

$$\frac{dL^*}{dS} = \alpha_a(\gamma_1 x - \gamma_2 y) + \alpha_b[\gamma_1(1 - x) - \gamma_2(1 - y) \tag{2.7}$$

$$\frac{dV^*}{dS} = \alpha_a(\gamma_1 x - \gamma_2 y) + \alpha_b[\gamma_1(1 - x) - \gamma_2(1 - y)] \tag{2.8}$$

$$\frac{dx}{dS} = [\alpha_a(1 - x)(\gamma_1 x - \gamma_2 y) - \alpha_b x(\gamma_1(1 - x) - \gamma_2(1 - y)]/L^* \tag{2.9}$$

$$\frac{d\gamma_1}{dS} = \beta \mu_F^* L^*/\gamma_1 \tag{2.10}$$

$$\frac{dy}{dS} = [\alpha_a(1 - y)(\gamma_1 x - \gamma_2 y) - \alpha_b y(\gamma_1(1 - x) - \gamma_2(1 - y))]/V^* \tag{2.11}$$

where

$$L^* = L/L_{ref} \; ; \qquad V^* = V/L_{ref}$$

$$\alpha_a = Q_a/Q_{ref} \; ; \qquad \alpha_b = Q_b/Q_{ref}$$

$$\gamma_1 = P/P_{ref} \; ; \qquad \gamma_2 = p/P_{ref}$$

$$\mu_F^* = \mu_F/\mu_{ref} \; ; \qquad S = \pi D_o(Q_{ref}/\delta_m)(P_{ref}/L_{ref})l$$

$$\beta = 128RTL_{ref}^2\mu_{ref}/[\pi^2 D_o(Q_{ref}/\delta_m)P_{ref}^3 D_i^4] \tag{2.12}$$

Generally, it is convenient to specify the domain of the independent variable between 0 and 1. In this case the total dimensionless area (for $l = l_f$) can be made equal to unity with proper choice of reference parameters (i.e., Q_{ref}, P_{ref}, and, L_{ref}) in definition (2.12) (Majumdar, 1986). Equations (2.7)-(2.11) have to be solved simultaneously using the boundary conditions

at $l = 0$, $y = y_w$; $V^* = V_w^*$

at $l = l_f$, $L^* = L_f^*$; $x = x_f$; $\gamma_1 = \gamma_{1f}$ (2.13)

V_w^* is zero when vacuum is applied to the permeate side in countercurrent flow. The permeate VOC mole fraction, y_w, can not be specified explicitly in the vacuum mode; it has to be determined from Equations (2.4) and (2.5) by using the boundary conditions at $l = 0$; y_w in the vacuum mode is shown to be (Guha et al., 1992):

$$y_w = \frac{A - (A^2 - B)^{1/2}}{C} \tag{2.14}$$

where $A = \alpha_b\gamma_{1w} + (\alpha_a-\alpha_b)(\gamma_{1w}+\gamma_{2w})$

$B = 4\alpha_a\gamma_{1w}\gamma_{2w}x_w(\alpha_a-\alpha_b)$

$C = 2\gamma_{2w}(\alpha_a-\alpha_b)$

Equation (2.10) is also indeterminate at $l = 0$ when vacuum is applied to the permeate side. By applying the L'Hospital rule, this equation is changed to

$$\frac{dy}{dS}\Big|_{S=o} = \frac{D}{E} \tag{2.15}$$

where D and E are

$$D = \frac{d\alpha_a}{dS}(1-y)(\gamma_1 x - \gamma_2 y) + \alpha_a(1 - y)(\frac{d\gamma_1}{dS}x + \frac{dx}{dS}\gamma_1) - \frac{d\alpha_b}{dS}y[\gamma_1(1 - x) - \gamma_2(1 - y)] - \alpha_b y[\frac{d\gamma_1}{dS}(1 - x) - \gamma_1\frac{dx}{dS}] \tag{2.16a}$$

$$E = \frac{dV^*}{dS} + \alpha_a(\gamma_1 x - \gamma_2 y) + \alpha_a\gamma_2(1 - y) + \alpha_b[\gamma_1(1 - x) - \gamma_2(1 - y)] + \alpha_b y\gamma_2 \tag{2.16b}$$

Note that

$$\frac{d\alpha_a}{dS} = \frac{dx}{dS}\frac{d\alpha_a}{dx} + \frac{d\gamma_1}{dS}\frac{d\alpha_a}{d\gamma_1} + \frac{dy}{dS}\frac{d\alpha_a}{dy} \qquad (2.17a)$$

$$\frac{d\alpha_b}{dS} = \frac{dx}{dS}\frac{d\alpha_b}{dx} + \frac{d\gamma_1}{dS}\frac{d\alpha_b}{d\gamma_1} + \frac{dy}{dS}\frac{d\alpha_b}{dy} \qquad (2.17b)$$

The IMSL subroutine BVPFD was used to solve numerically the set of nonlinear ordinary differential equations (2.7), (2.8), (2.9), (2.10), and (2.11) using the boundary conditions (2.13), (2.14), and (2.15). Initial estimate for each dependent variable at the selected grid point were generated by solving the system of differential equations as an initial value problem, assuming cocurrent flow. The initial value problem was solved by the IMSL subroutine IVPRK (Majumdar, 1986; Guha, 1989). This mathematical model (Sirkar, 1994) was used to simulate the permeator behavior for separation of toluene and methanol.

2.4 Results and Discussion

To analyze the performance of the hollow fiber module, experimental data were used to calculate the percent VOC removal, VOC permeate flux, VOC permeance and separation factor for various VOCs and nitrogen. The equations given below were used; detailed sample calculations are given in Appendix B.

Flux of VOC (J_{voc}, gmol/min.cm^2)

$= (F_p . y_f) / A$

where $F_p = F_i - F_o$ and $y_f = (F_i . x_f - F_o . x_w) / F_p$

Flux of N_2 (gmol/min.cm^2)

$= (F_p.x_{N2,p}) / A$

where $x_{N2,p} = 1 - y_f$

Percent Removal of VOC (%)

$= (F_p.y_f / F_i.x_f) \times 100$

Module-Averaged Permeance of VOC

Q_{voc} / δ_m, (gmol/sec.cm^2.cm Hg)

$= (J_{VOC}) / \{ 60 \times (P_{voc} - p_{voc}) \}$

where $p_{voc} = p.y_f$ and $P_{voc} = (P_f . x_f + P_w . x_w) / 2$

Separation Factor(α)

$= Q_{voc} / Q_{N2} = \{(Q_{voc}/\delta_m) / (Q_{N2}/\delta_m)\}$

Experimental data were also used to compare the results obtained by numerically simulating the mathematical model. Table 2.2 gives the description and values of various parameters used in the simulation of VOC separation.

Table 2.2 Description and Values of Parameters used in Numerical Simulation of VOC Permeation with Coated Fiber Module (Module # 2)

Item No.	Description of the Parameter, unit	Value
1	Feed: Toluene/N_2 Or MeOH/N_2	
2	Length of the fiber, cm	25.0
3	Experimental temperature, °C	30.0
4*	a, constant of Q(voc) = a * exp(b* P_{voc}), gmol/(sec.cm^2 .cm Hg)	185.6E-10 (Toluene) 267.70E-10 (MeOH)

Table 2.2 Continued

Item No.	Description of the Parameter, unit	Value
5*	b, second constant of above equation; 1/atm.	78.81 (Toluene) 27.52 (MeOH)
6**	$a(N_2)$, constant of $Q(N_2) = a(N_2)*\exp\{b(N_2) *P_{voc}\}$, gmol/(sec.cm^2. cm Hg)	3.803E-10
7	$b(N_2)$, second constant of above equation; 1/atm.	0.0
8	ID of the fiber, cm	240.0E-04
9	OD of the fiber, cm	292.0E-04
10	Pressure of the feed inlet, cm Hg	(Exptl. value)
11	Pressure on the vacuum side, cm Hg	0.1
12	Viscosity of N_2 at 30 °C, poise (g/cm s)	1800.0E-07
13	Flow rate of the feed gas, cc/min	(Exptl. value)
14	No. of fibers	50
15	Mole fraction of VOC at the feed inlet	(Exptl. value)

* Constants a and b for respective VOCs were obtained by fitting their permeance data, given later.

** Constants a and b for N_2 were obtained by fitting the N_2 permeance data derived from flux data, given later.

The result of single VOC-Nitrogen runs will be provided first; the observed behavior of various VOCs will be illustrated as well as explained.

Experiments to determine the permeance of toluene vapor as a function of its concentration were carried out in module 4 having a surface area of 7.47 cm^2. To maintain the toluene vapor concentration as constant (maximum 10% change) as possible along the length of the module, very high flow (upto 500 cc/min.) rates were used. The calculated permeances are plotted against the averaged feed concentrations in figure A.10, a semi-logarithmic plot. The relationship between (Q_i/δ_m) and toluene partial pressure on feed side, P_{if} (=Px), is best explained by an exponential relation, $(Q_i/\delta_m) = a * \exp(b*Px)$. The regression results for a and b were found to be $185.6*10^{-10}$ (gmol/sec/cm^2/cm Hg) and 78.81 (1/atm) respectively. This relation was introduced into the mathematical model to obtain numerical values for the solution. These theoretical results are plotted along with the experimental values in figures A.11 and A.12. The results from the model are shown as solid lines in figures A.11 and A.12. It is clear that the experimental results have been described reasonably by the mathematical model.

Table 2.3 shows the flux and percent removal of toluene vapor for changing feed flow rates as well as changing toluene concentrations in module 2 with feed entering through the tube side and vacuum being pulled from the shell side. Three different flow rates (from 60 to 150 cc/min.) were employed and at a given feed flow rate, inlet toluene concentration was varied between 4,435 ppmv to 13,570 ppmv. Permeate side vacuum was kept constant at 1.0 torr throughout these experiments. As the flow rate was increased there was a slight increase in the pressure drop through the tube side flow.

Percent removal of toluene with changing feed concentration is plotted for different flow rates in figure A.11. For feed flow rates of upto 100 cc/min., 92-98% removal was achieved for the whole feed concentration range. The percent removal of

Table 2.3 Flux and Percent Removal of Toluene from Nitrogen (Tube-Side Feed) at Different Flow Rates (60-150 cc/min.) and Toluene Concentrations (Module # 2)

Feed Inlet			Feed Outlet			Toluene Flux (x 10^8, gmol/min.cm^2)	Percent Removal of Toluene (%)
Flow Rate (cc/min.)	Pressure (cm Hg)	Toluene Mole Fraction	Flow Rate (cc/min.)	Pressure (cm Hg)	Toluene Mole Fraction		
58.69	76.26	0.004435	53.0	76	0.000111	9.84	97.34
60.03	76.30	0.008664	54.28	76	0.000171	19.80	98.21
59.91	76.40	0.009946	54.10	76	0.000212	22.68	98.07
60.36	76.40	0.012350	54.66	76	0.000270	28.32	98.02
100.77	76.80	0.003615	94.70	76	0.000350	12.60	90.90
99.90	76.80	0.005531	93.90	76	0.000465	19.74	92.10
100.10	76.80	0.008236	93.95	76	0.000646	29.58	92.64
101.08	77.03	0.010436	93.92	76	0.000888	37.60	92.08
148.50	79.05	0.006090	144.50	76	0.001150	28.56	81.62
155.78	79.29	0.007495	150.00	76	0.001241	37.86	84.06
149.00	79.10	0.013570	144.00	76	0.002500	64.20	82.40

toluene was reduced at higher gas flow rates; however the percent removal was still considerable. For example around 80% of toluene in the feed stream was removed at a feed flow rate of 150 cc/min. The percent removal of toluene at a given feed flow rate increased with increase in feed inlet concentration. This phenomenon was also observed in all other VOCs explored. The reason is as follows: VOC permeance increases with VOC inlet concentration. It was also observed that at a given concentration of toluene, percent removal of toluene decreased with increase in feed flow rate and this behavior was also observed for all other VOCs.

Feed outlet toluene concentration is plotted in figure A.12 as a function of feed inlet concentration at different flow rates. Although feed outlet toluene concentration increased with an increase in feed inlet toluene concentration at a given flow rate, yet this did not have any adverse effect on toluene removal because percent removal of toluene also increased accordingly.

Table 2.4 shows the flux and percent removal of toluene vapor for changing feed flow rates as well as changing toluene concentrations in module 2 with feed entering through the shell side and vacuum being pulled from the tube side. Two different flow rates (60 and 100 cc/min.) were employed and at a given feed flow rate inlet toluene concentration was varied between 4,229 ppmv to 9,526 ppmv. Permeate side vacuum was kept constant at 1.0 torr throughout these experiments. Essentially no pressure drop was observed through the shell-side feed flow.

In figures A.13 and A.14, the results of shell-side feed have been compared with tube-side feed in terms of percent removal of toluene and the feed outlet toluene concentration for inlet gas flow rates of 60 and 100 cc/min. It is observed that for the

Table 2.4 Flux and Percent Removal of Toluene from Nitrogen (Shell-Side Feed) at Different Flow Rates (60-100 cc/min.) and Toluene Concentrations (Module # 2)

Feed Inlet			Feed Outlet			Toluene Flux (x 10^8, gmol/min.cm^2)	Percent Removal of Toluene (%)
Flow Rate (cc/min.)	Pressure (cm Hg)	Toluene Mole Fraction	Flow Rate (cc/min.)	Pressure (cm Hg)	Toluene Mole Fraction		
58.69	76.00	0.004229	52.54	76	0.000996	7.60	79.00
60.15	76.00	0.005184	54.20	76	0.001331	9.29	74.00
60.61	76.00	0.007003	54.86	76	0.001778	12.66	75.00
61.84	76.00	0.009526	55.80	76	0.002186	18.11	77.00
100.10	76.00	0.003800	94.57	76	0.001775	8.24	56.00
99.80	76.00	0.006116	94.60	76	0.002804	13.38	57.00
101.70	76.00	0.009301	96.17	76	0.003806	22.48	59.00

same flow rate and inlet toluene feed concentrations, percent removal of toluene is less and outlet toluene concentration is more in shell-side feed as compared to tube-side feed. The considerably reduced separation in the case of shell-side feed may be due to feed by-passing and considerable pressure drop through the microporous fiber substrate and fiber lumen; the latter two would reduce the partial pressure permeation driving force for toluene.

Figure A.15 shows the effect of feed toluene vapor concentration on the toluene vapor permeate flux at different feed flow rates (60, 100, 150 cc/min). Toluene vapor permeate flux increased with an increase in feed toluene concentration at a given flow rate. The toluene flux, also increased as the gas flow rate increased. This is due to a rapid increase in toluene permeance at higher concentrations; the latter conditions are created by the high incoming gas flow rate.

The variation of nitrogen flux with feed inlet toluene concentration has been plotted in figure A.16. The nitrogen flux did not appear to be a function of toluene concentration; at most, it decreased a bit with increasing toluene concentration. This also leads to the conclusion that the silicone membrane was not greatly swollen by toluene, otherwise nitrogen flux would have increased with increasing toluene concentration. Alternatively, if the silicone membrane were swollen, there are some other effects at play.

The separation factor, which is defined as the ratio of permeance of toluene vapor to permeance of nitrogen, has been plotted as a function of inlet toluene concentration in figure A.17. Separation factor increased slightly with increasing feed toluene concentration at a given flow rate. The permeance of toluene and nitrogen used to

calculate separation factor was based on the whole permeator (module averaged). Since the toluene vapor concentration change along the length of the module is very large, the calculated permeance does not have any significance. At higher inlet feed flow rates, the calculated permeance of toluene accordingly increased, leading to higher separation factors.

Experiments to determine the permeance of methanol vapor as a function of its concentration were carried out in module 4 having a surface area of 7.47 cm^2. To maintain the methanol vapor concentration as constant (maximum 10% change) as possible along the length of the module, very high flow rates (upto 550 cc/min.) were used. The calculated permeances are plotted against the averaged feed concentrations in figure A.18, a semi-logarithmic plot. The relationship between (Q_i/δ_m) and methanol partial pressure on feed side, P_{if} (=Px), is best explained by an exponential relation, $(Q_i/\delta_m) = a * \exp(b*Px)$. The regression results for a and b were found to be $267.7*10^{-10}$ (gmol/sec/cm^2/cm Hg) and 27.52 (1/atm) respectively. This relation was introduced into the mathematical model to obtain numerical values of the solution. These theoretical results are plotted along with the experimental values in the figures A.19 and A.20. The results from the model are shown as solid lines in figures A.19 and A.20. It is clear that the experimental results have been described reasonably by the mathematical model.

Table 2.5 shows the flux and percent removal of methanol vapor for changing feed flow rates as well as changing methanol concentrations in module 2 with feed entering through the tube side and vacuum being pulled from the shell side. Three different flow rates (from 58 to 155 cc/min) were employed and at a given feed flow rate, inlet methanol concentration was varied between 4,558 ppmv to 70,875 ppmv.

Table 2.5 Flux and Percent Removal of Methanol from Nitrogen (Tube-Side Feed) at Different Flow Rates (58-150 cc/min.) and Methanol Concentrations (Module # 2)

Feed Inlet			Feed Outlet			Methanol Flux (x 10^8, gmol/min.cm^2)	Percent Removal of Methanol (%)
Flow Rate (cc/min.)	Pressure (cm Hg)	Methanol Mole Fraction	Flow Rate (cc/min.)	Pressure (cm Hg)	Methanol Mole Fraction		
58.08	76.00	0.004558	52.40	76.00	0.000133	10.00	97.37
59.74	76.00	0.016727	52.45	76.00	0.000159	38.4	99.16
59.22	76.00	0.018368	52.77	76.00	0.000167	41.82	99.20
59.50	76.00	0.036378	52.44	76.00	0.000181	83.40	99.56
58.63	76.00	0.051713	52.04	76.00	0.000221	117.00	99.62
59.41	76.00	0.070875	51.70	76.00	0.000247	160.80	99.69
102.63	77.67	0.003710	97.64	76.00	0.000259	13.78	93.36
101.27	77.67	0.013950	95.14	76.00	0.000635	52.43	95.72
101.69	77.67	0.018745	95.52	76.00	0.000827	70.80	95.80
102.05	77.67	0.029400	96.52	76.00	0.001304	112.00	95.82

Table 2.5 Continued

Feed Inlet			Feed Outlet			Methanol Flux (x 10^8, gmol/min.cm^2)	Percent Removal of Methanol (%)
Flow Rate (cc/min.)	Pressure (cm Hg)	Methanol Mole Fraction	Flow Rate (cc/min.)	Pressure (cm Hg)	Methanol Mole Fraction		
102.48	77.67	0.038288	95.52	76.00	0.001304	147.00	96.70
100.82	77.67	0.039203	93.97	76.00	0.001623	147.60	96.14
150.80	78.85	0.005176	144.66	76.00	0.000684	26.42	87.32
154.00	78.85	0.011015	148.15	76.00	0.001376	57.84	88.00
152.14	78.85	0.021832	145.63	76.00	0.002592	114.00	88.64
154.70	78.85	0.027692	146.60	76.00	0.003295	145.80	88.65
154.72	78.85	0.036199	146.60	76.99	0.003395	192.00	91.32

Permeate side vacuum was kept constant at 1.0 torr throughout these experiments. As the flow rate was increased there was a slight increase in the pressure drop through the tube side flow.

Percent removal of methanol with changing feed concentration is plotted for different flow rates in figure A.19. For feed flow rates of upto 100 cc/min, 93-97% removal was achieved for the whole feed concentration range. The percent removal of methanol was reduced at higher gas flow rates; however the percent removal was still considerable. For example around 87% of methanol in the feed stream was removed at 152 cc/min. The percent removal of methanol at a given feed flow rate increased with an increase in feed inlet concentration. The reason is that methanol permeance increases with methanol inlet concentration. It was also observed that at a given concentration of methanol, percent removal of methanol decreased with increase in feed flow rate and this phenomenon was also observed for all other VOCs.

Feed outlet methanol concentration is plotted in figure A.20 as a function of feed inlet concentration at different flow rates. Although feed outlet methanol concentration increased with an increase in feed inlet methanol concentration at a given flow rate, yet this did not have any adverse effect on methanol separation because percent removal of methanol also increased accordingly.

Table 2.6 illustrates the flux and percent removal of methanol vapor for changing feed flow rates as well as changing feed methanol concentrations in module 2 when feed gas was introduced through the shell side and vacuum was pulled from the tube side. A gas flow rate of 60 cc/min was employed and inlet methanol concentration was varied between 5,893 ppmv to 75,063 ppmv. Permeate side vacuum was kept constant at 1.0

Table 2.6 Flux and Percent Removal of Methanol from Nitrogen (Shell-Side Feed) at a Flow Rate of 60 cc/min. and Different Methanol Concentrations (Module # 2)

Feed Inlet			Feed Outlet			Methanol Flux (x 10^8, gmol/min.cm^2)	Percent Removal of Methanol (%)
Flow Rate (cc/min.)	Pressure (cm Hg)	Methanol Mole Fraction	Flow Rate (cc/min.)	Pressure (cm Hg)	Methanol Mole Fraction		
60.07	76.00	0.005893	54.45	76.00	0.000760	12.12	88.30
60.62	76.00	0.020794	54.86	76.00	0.002565	43.44	88.80
59.65	76.00	0.039466	53.73	76.00	0.006895	76.80	84.30
60.94	76.00	0.051034	54.20	76.00	0.008237	103.20	85.60
58.43	76.00	0.057690	52.24	76.00	0.008590	113.40	86.70
64.44	76.00	0.075063	57.82	76.00	0.012015	160.80	85.60

torr throughout these experiments. No pressure drop was observed through the shell-side feed flow.

In figure A.21 the results of shell-side methanol feed have been compared with tube-side feed in terms of percent removal of methanol and the feed outlet methanol concentration for inlet gas flow rate of 60 cc/min. It is observed that for the same feed flow rate and inlet methanol feed concentrations, percent removal of methanol is less and outlet methanol concentration is more in shell-side feed as compared to tube side feed. The reduced separation in the case of shell-side feed may again be due to feed bypassing and a considerable increase in pressure drop through the microporous substrate and fiber lumen.

Figure A.22 shows the effect of feed methanol vapor concentration on the methanol vapor permeate flux at different flow rates (60, 100, 150 cc/min). Methanol vapor permeate flux increased considerably with an increase in feed methanol concentration at a given flow rate. The methanol flux also increased as the gas flow rate increased. This is due to a rapid increase in methanol permeance at higher concentrations; the latter conditions are created by the high incoming gas flow rate.

The variation of nitrogen flux with feed inlet methanol concentration has been plotted in figure A.23. The nitrogen flux decreased considerably as the feed methanol concentration increased at a given flow rate . This decrease in nitrogen flux can hardly be ascribed to a decrease in nitrogen partial pressure (maximum 6%); the decrease must be due to a decrease in nitrogen permeance.

The VOC-nitrogen separation factor has been plotted as a function of inlet methanol concentration in figure A.24. Separation factor increased significantly with

increasing feed methanol concentration at a given flow rate. Highest value of 125 and lowest value of 18 was observed. The same phenomenon was observed in case of toluene; but the extent of increase was much less.

The experimental results for acetone and methylene chloride will be presented and discussed now. For both VOCs, tube-side feed mode was employed with vacuum applied on the shell side. Tables 2.7 and 2.8 provide the flux and percent removal values for acetone and methylene chloride vapors from nitrogen respectively. For each set of experiment using module 2, feed flow rates and individual VOC concentrations were varied. For acetone, three different flow rates (from 29 to 100 cc/min) were employed and at a given feed flow rate, inlet acetone concentration was varied between 8,700 ppmv to 21,600 ppmv. For methylene chloride four different flow rates (from 60 to 242 cc/min) were employed and at a given feed flow rate, inlet methylene chloride concentration was varied between 998 ppmv to 6,000 ppmv. Permeate side vacuum was kept constant at 1.0 torr throughout these experiments. As the flow rate was increased, there was a slight increase in the pressure drop through the tube-side flow.

Percent removal of acetone with changing feed concentration is plotted at different flow rates in figure A.25. It can be seen that at a low feed flow rate (29 cc/min), 99% removal was achieved. The percent removal of acetone was reduced at higher gas flow rates. The percent removal of acetone at a given feed flow rate was relatively unaffected by an increase in feed inlet concentration. It was also observed that at a given feed concentration of acetone, percent removal of acetone decreased with an increase in feed flow rate.

Table 2.7 Flux and Percent Removal of Acetone from Nitrogen (Tube-Side Feed) at Different Flow Rates (29-100 cc/min.) and Acetone Concentrations (Module # 2)

Feed Inlet			Feed Outlet			Acetone Flux (x 10^8, gmol/min.cm^2)	Percent Removal of Acetone (%)
Flow Rate (cc/min.)	Pressure (cm Hg)	Acetone Mole Fraction	Flow Rate (cc/min.)	Pressure (cm Hg)	Acetone Mole Fraction		
29.00	76	0.013101	21.90	76	0.000119	14.63	99.30
29.10	76	0.022434	21.80	76	0.000167	25.14	99.40
58.90	76.80	0.008736	50.90	76	0.001151	17.62	88.60
59.70	76.80	0.014608	53.10	76	0.001976	29.70	87.90
59.90	76.80	0.021304	53.10	76	0.002841	43.62	88.20
100.30	77.66	0.010729	93.70	76	0.003306	29.70	71.20
101.20	77.67	0.013633	94.10	76	0.004287	37.77	70.70
101.10	77.67	0.017284	94.40	76	0.005355	48.12	71.10
100.50	77.67	0.021626	93.60	76	0.006616	60.00	71.50

Table 2.8 Flux and Percent Removal of Methylene Chloride from Nitrogen (Tube-Side Feed) at Different Flow Rates (60-242 cc/min.) and Methylene Chloride Concentrations (Module # 2)

Feed Inlet			Feed Outlet			Methylene Chloride Flux (x 10^8, gmol/min.cm^2)	Percent Removal of Methylene Chloride (%)
Flow Rate (cc/min.)	Pressure (cm Hg)	Methylene Chloride Mole Fraction	Flow Rate (cc/min.)	Pressure (cm Hg)	Methylene Chloride Mole Fraction		
61.60	76.00	0.000998	56.70	76.00	0.000017	2.35	98.43
59.22	76.00	0.003074	54.19	76.00	0.000037	6.96	98.90
57.20	76.00	0.006000	52.00	76.00	0.000050	13.14	99.24
97.20	77.80	0.000998	91.90	76.00	0.000079	3.47	92.52
101.62	78.00	0.003023	96.50	76.00	0.000196	11.16	93.84
97.51	77.80	0.006000	92.00	76.00	0.000371	21.60	94.17
155.30	79.15	0.006000	150.00	76.00	0.001005	30.24	83.82
241.70	81.17	0.006000	235.56	76.00	0.001762	40.20	71.37

Feed outlet acetone concentration is plotted in figure A.26 as a function of feed inlet concentration at different flow rates. The feed outlet acetone concentration increased almost linearly with an increase in feed inlet acetone concentration at a given flow rate and the rate of increase was sharper at higher flow rates.

Figure A.27 shows the effect of feed acetone vapor concentration on the acetone vapor permeate flux at different feed flow rates (29, 59, 100 cc/min). As expected, acetone vapor permeate flux also increased with an increase in feed acetone concentration at a given flow rate. The acetone flux was also increased as the gas flow rate was increased. The acetone-nitrogen separation factor (figure A.28) also increased with increasing feed acetone concentration at a given flow rate but the increase was not as much as was observed in the case of methanol.

The variation of nitrogen flux with feed inlet acetone concentration has been plotted in figure A.29. The nitrogen flux decreased considerably with an increase in acetone feed concentration, as in the case of methanol.

Percent removal of methylene chloride with changing feed concentration is plotted for different flow rates in figure A.30. For feed flow rates of upto 100 cc/min, 93-99% removal was achieved for the whole feed concentration range. The percent removal of methylene chloride was reduced at higher gas flow rates, however the percent removal was still considerable. For example around 83% of methylene chloride in the feed stream was removed at 155 cc/min. As in the case of all other VOCs, the percent removal of methylene chloride at a given feed flow rate increased with an increase in feed inlet concentration. The feed outlet methylene chloride concentration and methylene chloride vapor permeate flux also increased with an increase in feed inlet

methylene chloride concentration at the given flow rates (figures A.31 and A.32). The methylene chloride flux (figure A.32), also increased as the gas flow rate was increased. The methylene chloride-nitrogen separation factor (figure A.33) also increased with increasing feed methylene chloride concentration at a given flow rate (values between 23 and 50) but the increase was not as much as was observed in the case of methanol.

The variation of nitrogen flux with feed inlet methylene chloride concentration has been plotted in figure A.34. The nitrogen flux decreased a bit with an increase in methylene chloride feed concentration; as in the case of methanol and acetone. The decrease is much less here; further the variation of concentration of methylene chloride is very limited here.

As observed in the experiments on removal of acetone, methylene chloride and methanol, nitrogen flux decreased significantly with an increase in VOC concentration. This implies that at higher VOC concentrations nitrogen permeance decreases; this seems to be in conflict with analyses of Baker (1987) which indicates that at higher VOC concentration, membrane swelling would increase nitrogen permeance considerably. One hypothesis that can be pointed out in support of the present findings, is that size of the pores of microporous substrate gradually decreases at the points where the substrate has been plasma polymerized to a dense silicone membrane. This leads to a pore closure like the condition at the top surface of the pores (figure 2.8) and at higher VOC concentrations there will be pore condensation of the VOC. This will facilitate the permeation of VOC through the pores filled with pure liquid VOC whereas nitrogen will face an additional resistance of VOC liquid layer before it reaches silicone membrane. However more systematic experiments need to be carried out with other VOCs to confirm this hypothesis.

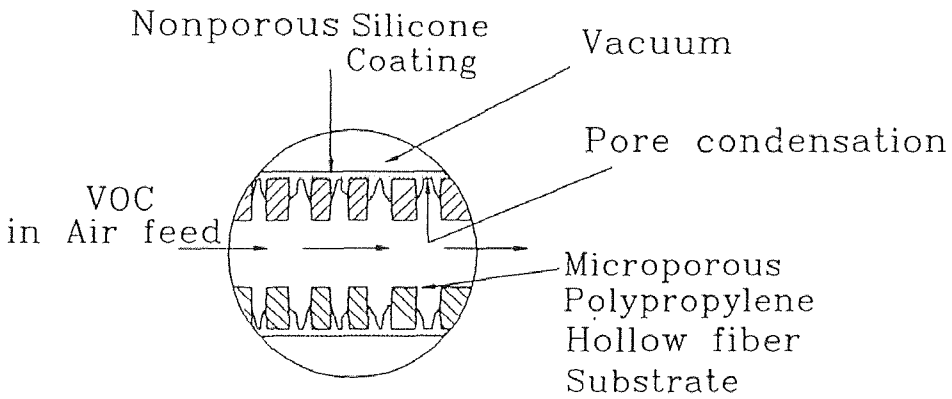

Figure 2.8 Cross Section of the Hollow Fiber Pores and Location of Possible Pore Condensation of the VOC

Table 2.9 shows the flux and percent removal of toluene vapor for changing feed flow rates as well as changing toluene concentrations in module 2 with feed air (instead of nitrogen) entering through the tube side and vacuum being pulled from the shell side. When results of air-feed are compared with those of nitrogen-feed, the only difference is that outlet gas flow rates are somewhat lower than those in nitrogen-VOC system. This is an expected result since the permeance of oxygen through the silicone rubber is higher than that of nitrogen.

Table 2.10 shows the experimental results of separation of acetone from an acetone-nitrogen mixture flowing on the shell-side at a high pressure and vacuum being pulled from the tube side. Acetone concentration was 3000 ppmv and the feed gas pressure was varied from 158.8 to 376 cm Hg. As the pressure increases, the percent recovery increases. Low inlet concentration and polar nature of acetone make this separation difficult. Moreover the VOC-nitrogen selectivity is also greatly reduced because of the high pressure feed. However membrane performance was reasonable, but higher selectivity membrane and tube-side feed configuration would give even better separations.

Table 2.11 illustrates the experimental results of simultaneous separation of multiple VOCs present in nitrogen. The feed was sent through the tube side and vacuum (1 torr) was pulled from the shell side. The mixture contained acetone (1010 ppmv), methanol (780 ppmv), toluene (900 ppmv) and nitrogen (balance). This mixture was very dilute and feed gas flow rates used were quite high (100 and 160 cc/min.). Yet the silicone membrane was able to separate the mixture to a reasonable extent. A lower gas flow rate would have achieved even better results.

Table 2.9 Flux and Percent Removal of Toluene from Air (Tube-Side Feed) at Different Flow Rates (60-153 cc/min.) and Toluene Concentrations (Module # 2)

Feed Inlet			Feed Outlet			Toluene Flux (x 10^7, gmol/min.cm^2)	Percent Removal of Toluene (%)
Flow Rate (cc/min.)	Pressure (cm Hg)	Toluene Mole Fraction	Flow Rate (cc/min.)	Pressure (cm Hg)	Toluene Mole Fraction		
59.50	76.83	0.003532	51.60	76.00	0.000100	11.04	97.50
59.50	76.83	0.006020	51.40	76.00	0.000127	18.90	98.20
60.30	76.83	0.007942	52.20	76.00	0.000145	25.30	98.40
60.20	76.83	0.012055	51.90	76.00	0.000189	38.46	98.60
98.90	77.96	0.003404	91.30	76.00	0.000303	16.62	91.80
100.30	77.96	0.006162	91.60	76.00	0.000438	31.08	93.50
100.00	77.96	0.008532	91.50	76.00	0.000587	43.02	93.70
100.50	77.96	0.010592	91.90	76.00	0.000838	53.16	92.80
153.10	77.96	0.007603	143.30	76.00	0.001268	52.86	84.40

Table 2.10 Flux and Percent Removal of Acetone from Nitrogen (Shell-Side Feed) at Different High Inlet Pressures (158-376 cm Hg) (Module # 2)

Feed Inlet			Feed Outlet			Acetone Flux (x 10^8, gmol/min.cm^2)	Percent Removal of Acetone (%)
Flow Rate (cc/min.)	Pressure (cm Hg)	Acetone Mole Fraction	Flow Rate (cc/min.)	Pressure (cm Hg)	Acetone Mole Fraction		
56.30	158.80	0.003000	7.10	158.80	0.000435	5.80	88.30
55.70	231.20	0.003000	22.80	231.20	0.000231	6.11	94.40
56.10	376.00	0.003000	51.60	376.00	0.000500	6.47	99.10

Table 2.11 Percent Removal of Acetone, Methanol and Toluene in Simultaneous Separation from Nitrogen (Tube-Side Feed) at Different Flow Rates (96-157 cc/min.) (Module # 2)

Feed Inlet Flow Rate 96.90 cc/min.			
Feed Outlet Flow Rate 91.70 cc/min.			
	Acetone	Methanol	Toluene
Inlet Mole Fraction	0.001010	0.000780	0.000900
Out let Mole Fraction	0.000302	0.000146	0.000129
Percent Removal	71.70	82.30	86.40
Feed Inlet Flow Rate 157.00 cc/min.			
Feed Outlet Flow Rate 151.50 cc/min.			
	Acetone	Methanol	Toluene
Inlet Mole Fraction	0.001010	0.000780	0.000900
Out let Mole Fraction	0.000474	0.000207	0.000226
Percent Removal	54.70	74.40	75.80

The separation results of hexane from a hexane-nitrogen feed mixture (1062 ppmv) at three different flow rates (12, 28 and 57 cc/min) are shown in Table 2.12. Reasonable separation was achieved even though the inlet concentration of hexane was low.

2.4.1 Conclusions

The efforts to separate and remove various VOCs from nitrogen/air feed streams using hollow fiber module (HFM) under different operating parameters and modes met with significant success.

HFM having ultrathin nonporous silicone membrane, plasma polymerized to porous polypropylene substrate had some innate advantages over other silicone based membranes. The selective layer (silicone membrane) was ultra thin (1μm); polypropylene substrate was highly porous (0.4) and very strongly bonded to the silicone coating. These factors considerably reduced permeation resistance and as a result HFM was very effective in removing toluene, methanol, acetone, methylene chloride, hexane and multiple VOCs from nitrogen/air gas streams.

A small HFM having a length of 25 cm and 50 fibers was enough to remove 97-99 % of the VOC from the feed stream at 60 cc/min. except in the case of acetone where a lower gas flow rate had to be applied. The feed concentration of hexane was too low to achieve high percent removal. The HFM was also very effective in separating a mixture of VOCs (toluene, methanol and acetone) from nitrogen feed stream. The percent removal of VOC was higher when inlet VOC concentration was high. The outlet concentration of methanol for a feed stream of 51,713 ppmv methanol and 60 cc/min.

Table 2.12 Flux and Percent Removal of Hexane from Nitrogen (Tube-Side Feed) at Different Flow Rates (12-57 cc/min.) (Module # 2)

Feed Inlet			Feed Outlet			Hexane Flux (x 10^8, gmol/min.cm^2)	Percent Removal of Hexane (%)
Flow Rate (cc/min.)	Pressure (cm Hg)	Hexane Mole Fraction	Flow Rate (cc/min.)	Pressure (cm Hg)	Hexane Mole Fraction		
12.50	76.00	0.001062	7.10	76.00	0.000049	0.50	97.40
28.10	76.00	0.001062	22.80	76.00	0.000280	0.90	78.50
57.10	76.00	0.001062	51.60	76.00	0.000547	1.26	55.50

flow rate was reduced to only 117 ppmv which amounts to about 99.5 % removal. Thus this process is especially suitable for treating waste streams having a low flow rate and high VOC concentration.

In the case of methanol, acetone and methylene chloride vapor, decreasing nitrogen flux was observed at high respective VOC concentrations; this may be explained in terms of substrate pore reduction/blocking and pore condensation phenomenon.

Replacing air as feed instead of nitrogen merely reduces the selectivity by a little amount because oxygen is more permeable than nitrogen through the membrane. Passing the feed through the bores of fibers and pulling vacuum through the shell-side (permeate) gives a much better separation than passing the feed through the shell-side of HFM. This may be due to pore condensation of VOC and/or reduction of permeate side pressure drop. The HFM can also be effectively utilized to remove VOCs from high pressure streams by an appropriate mode of operation.

A numerical model of HFM for VOC separation with feed flowing through the tube-side and vacuum being pulled from the shell side explained the observed toluene and methanol removal satisfactorily; experimentally-determined-VOC permeance versus VOC concentration relations were employed in model simulations. This suggests that scale up of the module in this flow configuration may be an easy effort since each fiber acts as a separate permeator.

Thus considering all aspects, this process using a novel silicone-coated, plasma polymerized hollow fiber membrane appears to have a great potential for removing VOCs from waste streams.

APPENDIX A

GRAPHS FROM CHAPTER 2

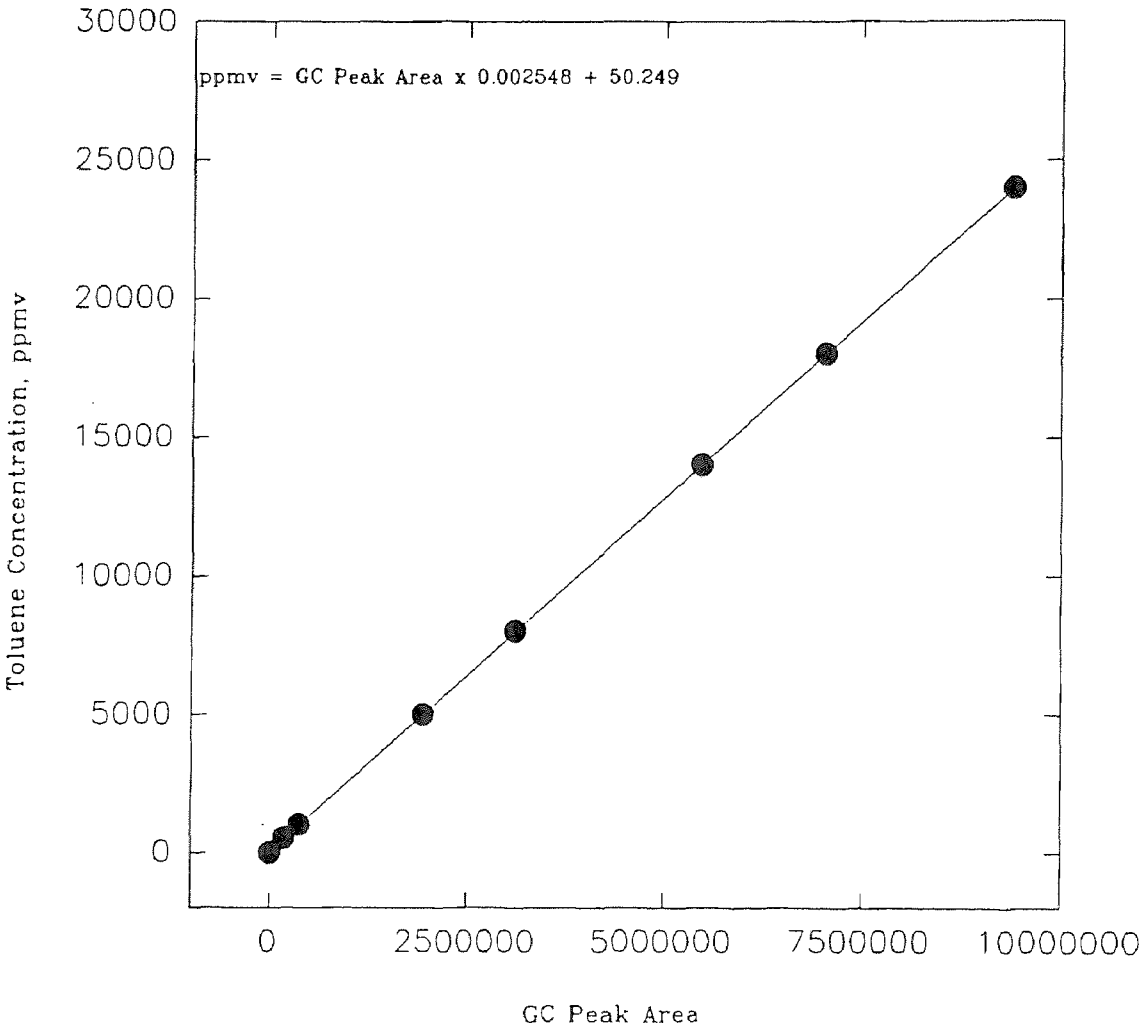

Figure A.1 Calibration Curve for Toluene (Range 8)

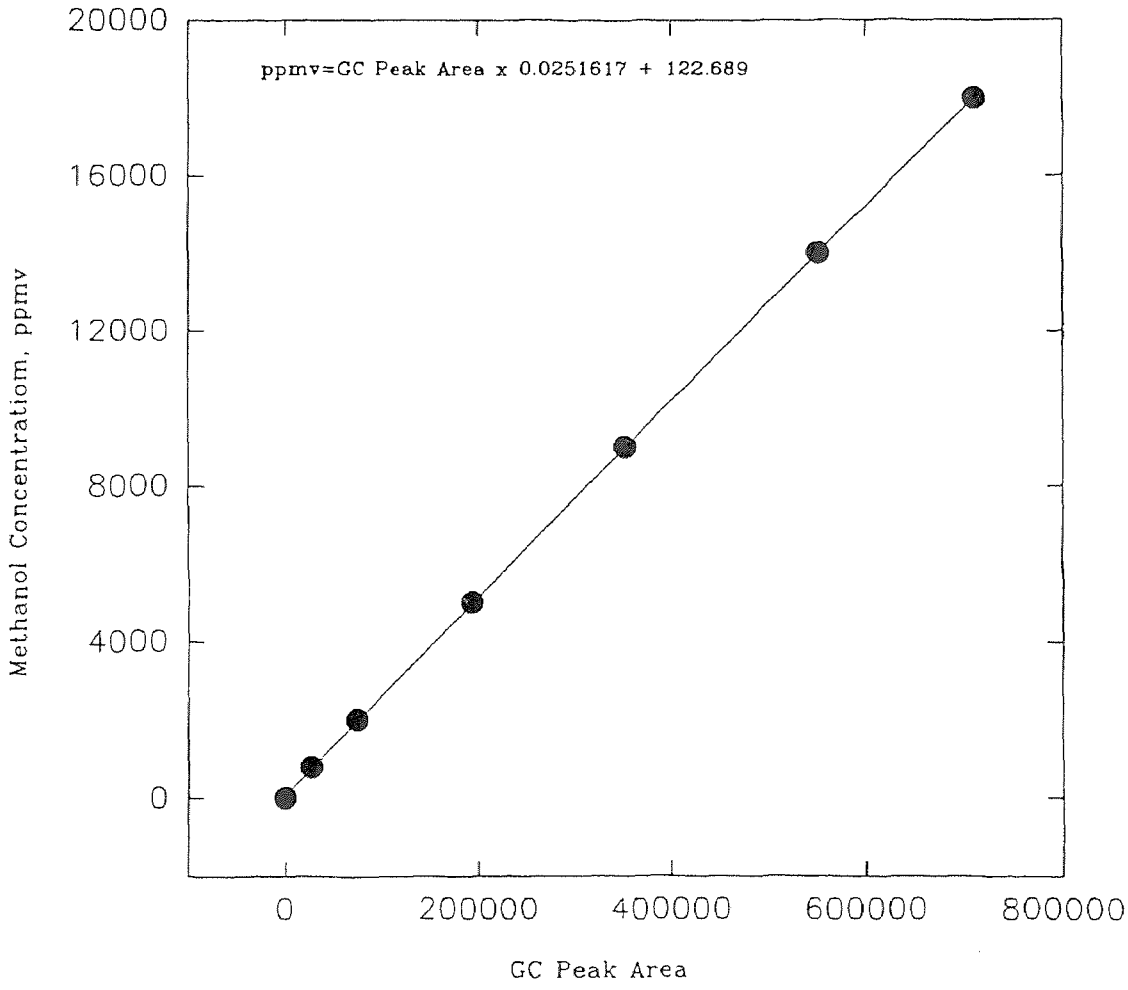

Figure A.2 Calibration Curve for Methanol (Range 8)

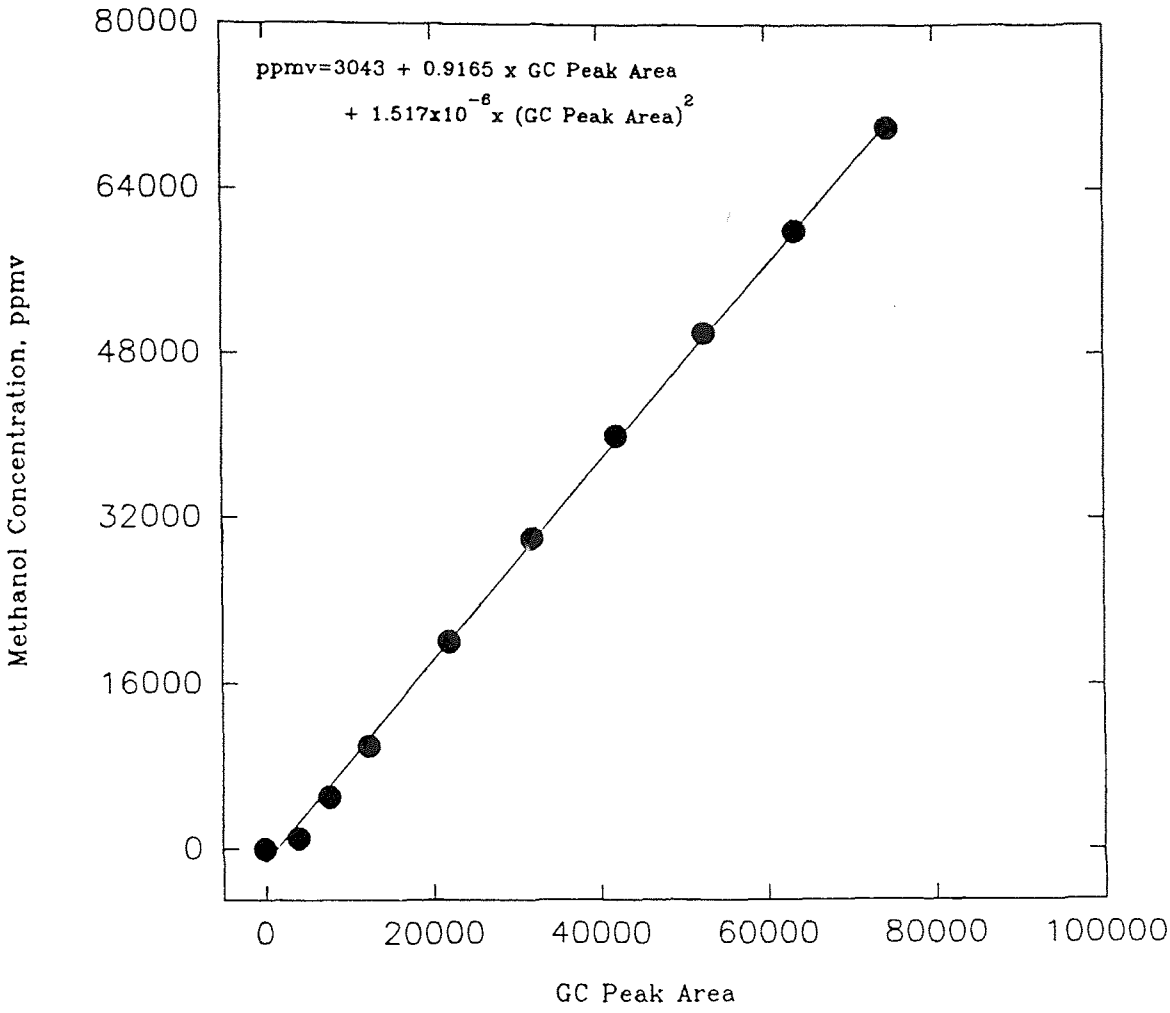

Figure A.3 Calibration Curve for Methanol (Range 13)

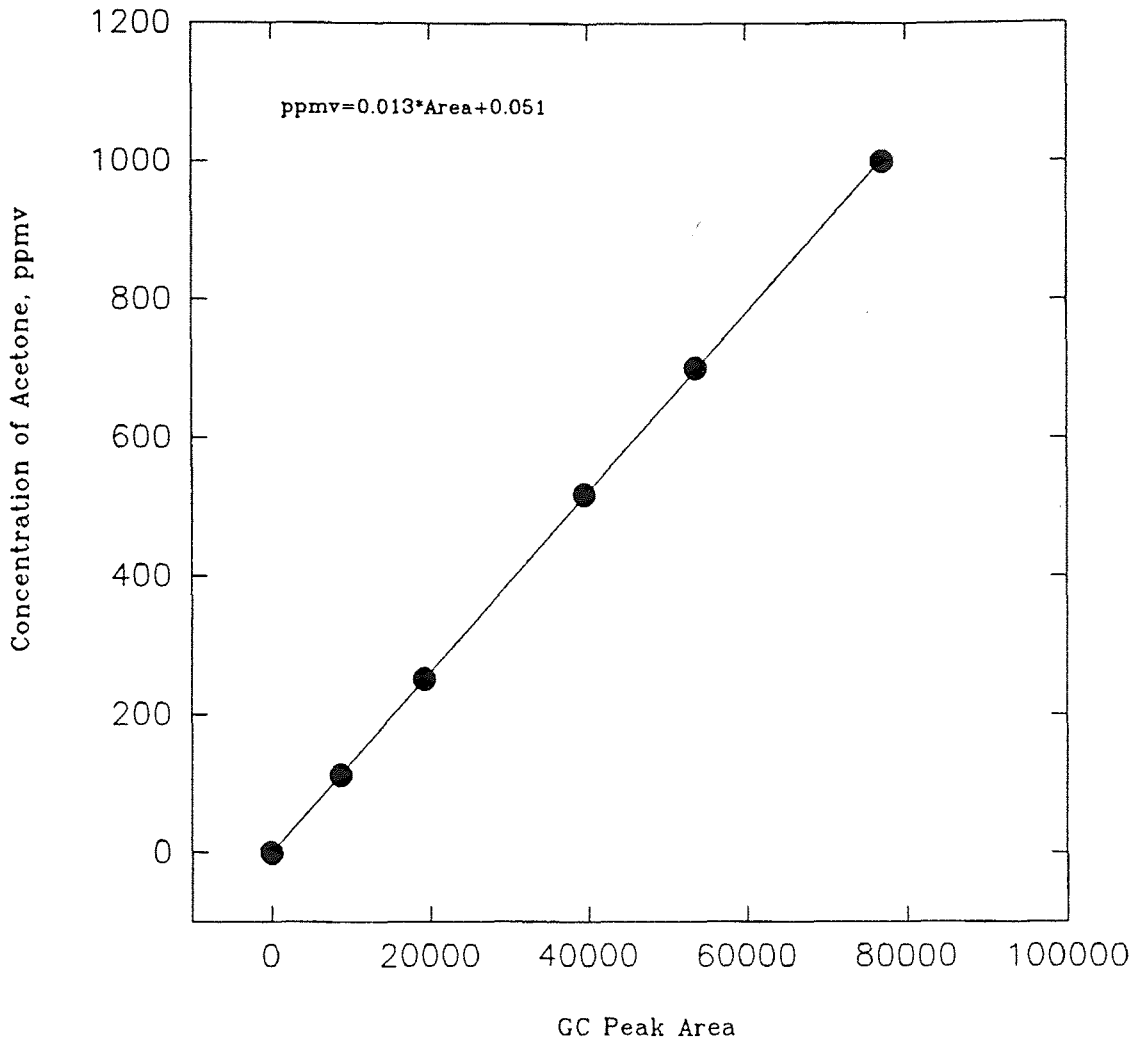

Figure A.4 Calibration Curve 1 for Acetone (Range 8)

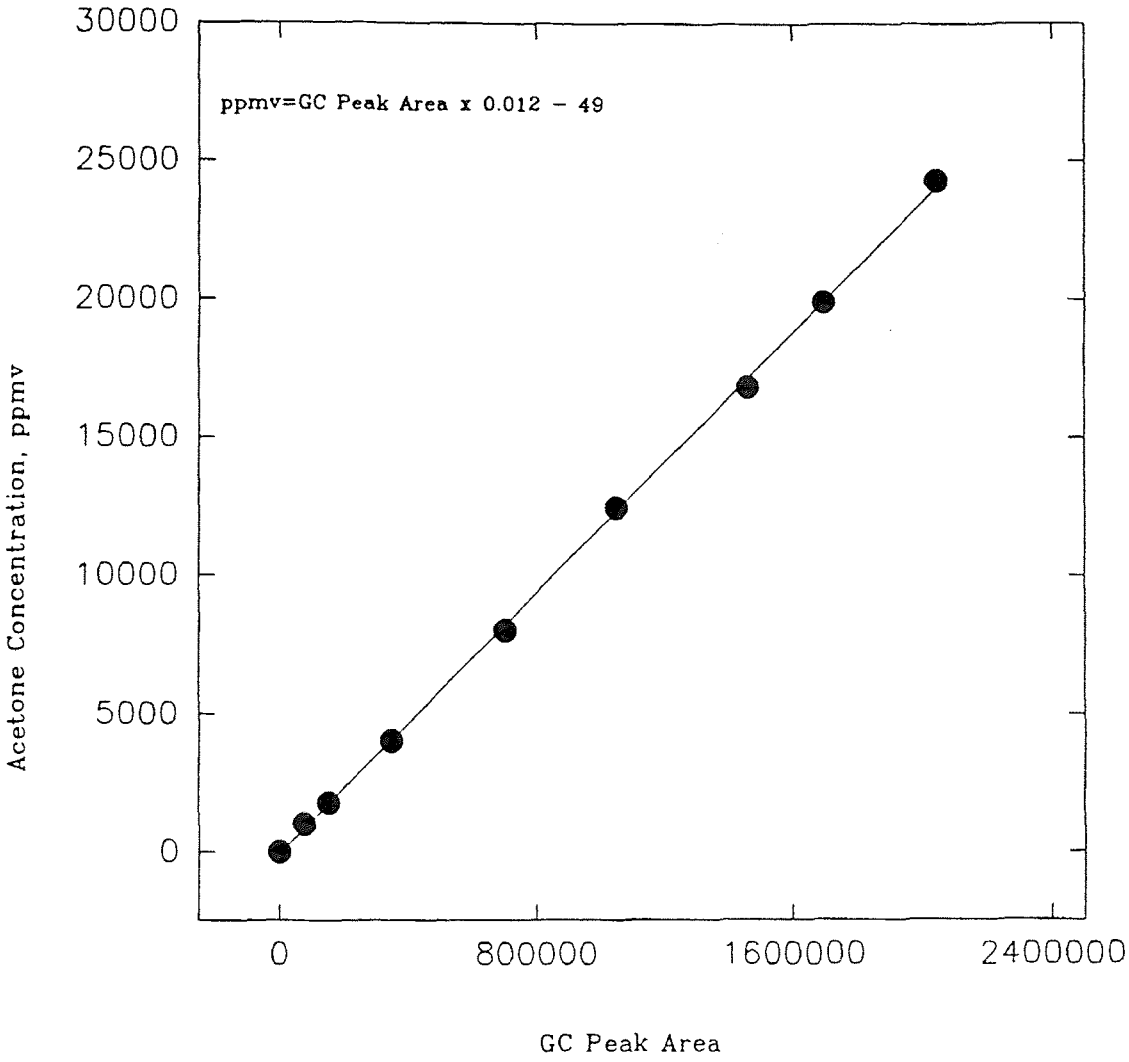

Figure A.5 Calibration Curve 2 for Acetone (Range 8)

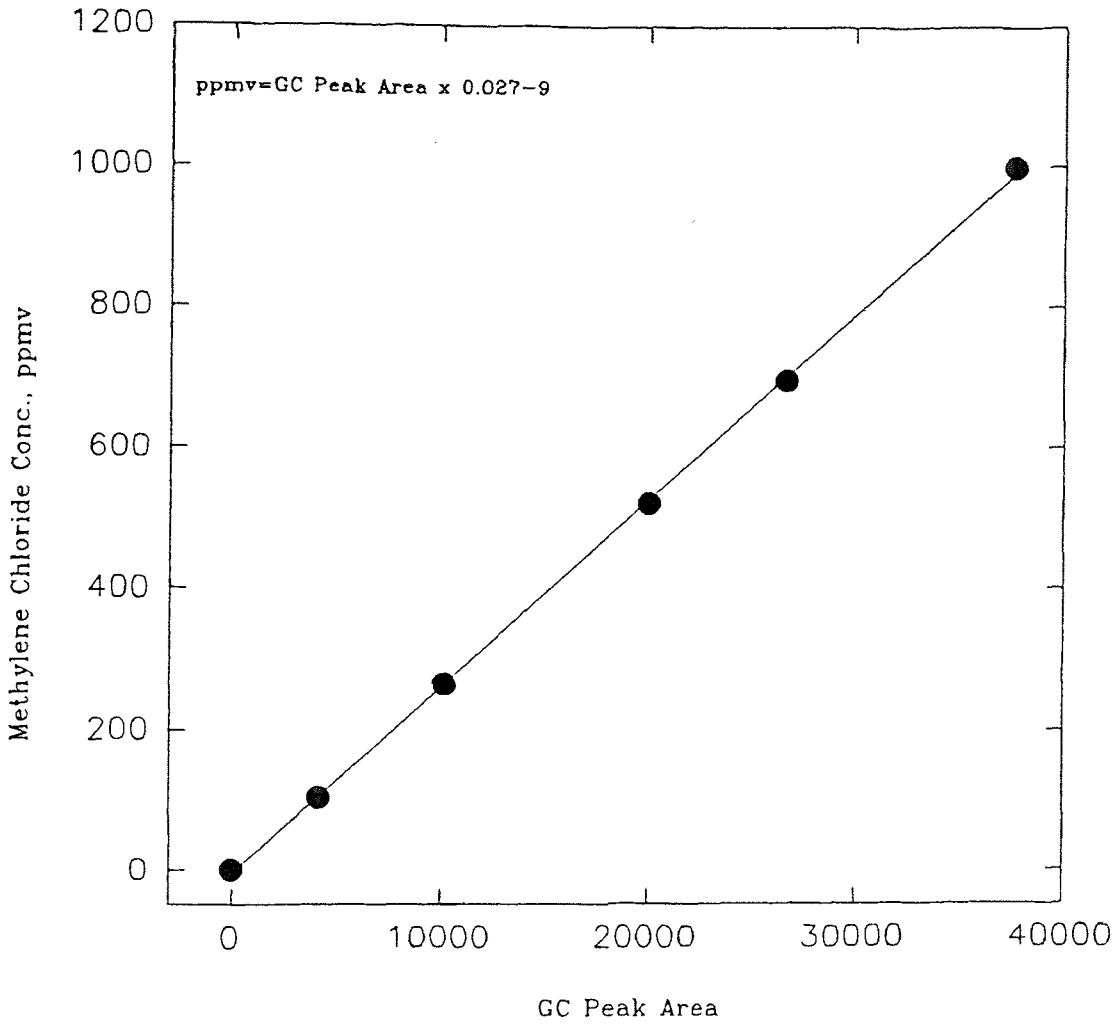

Figure A.6 Calibration Curve 1 for Methylene Chloride (Range 8)

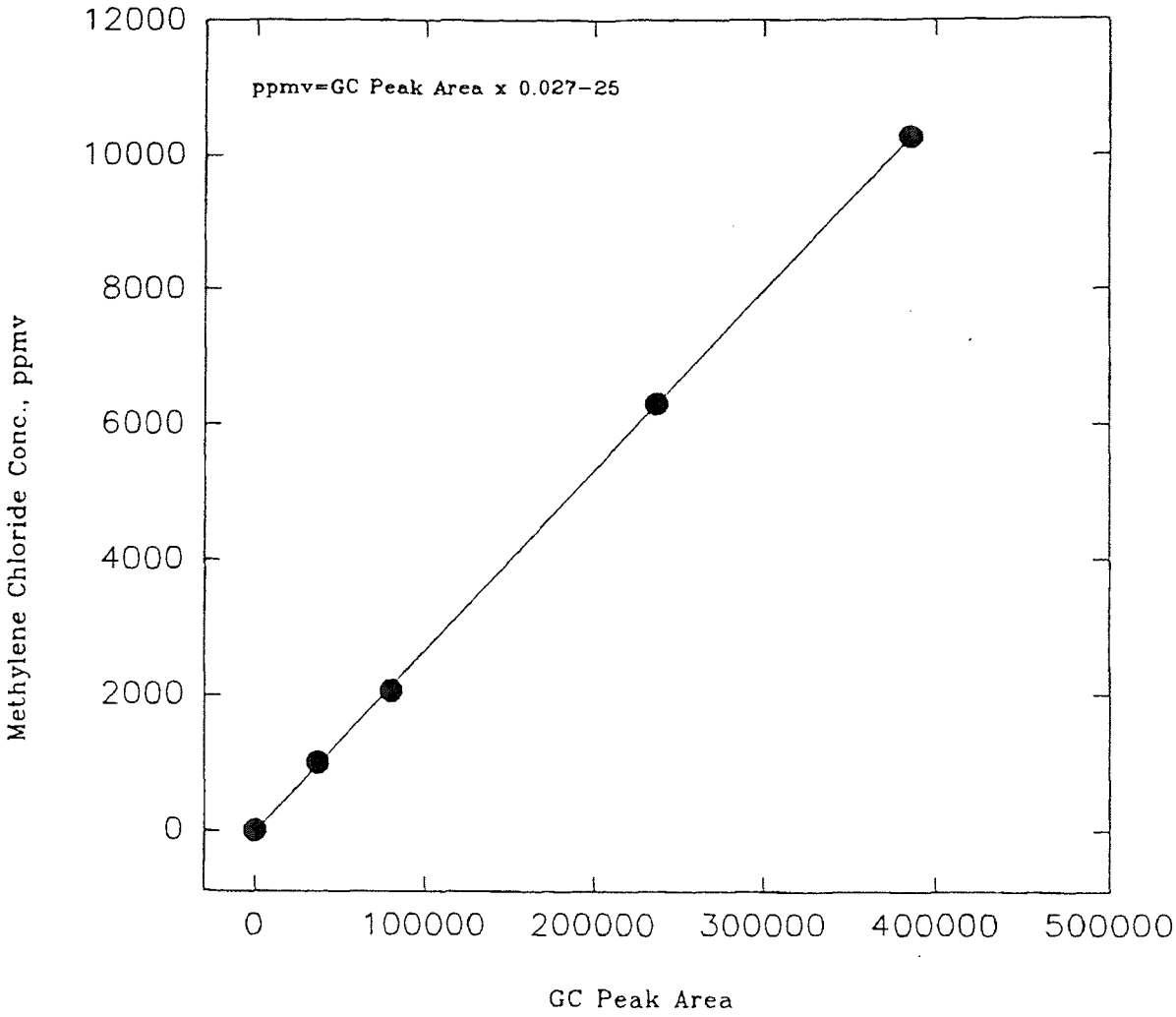

Figure A.7 Calibration Curve 2 for Methylene Chloride (Range 8)

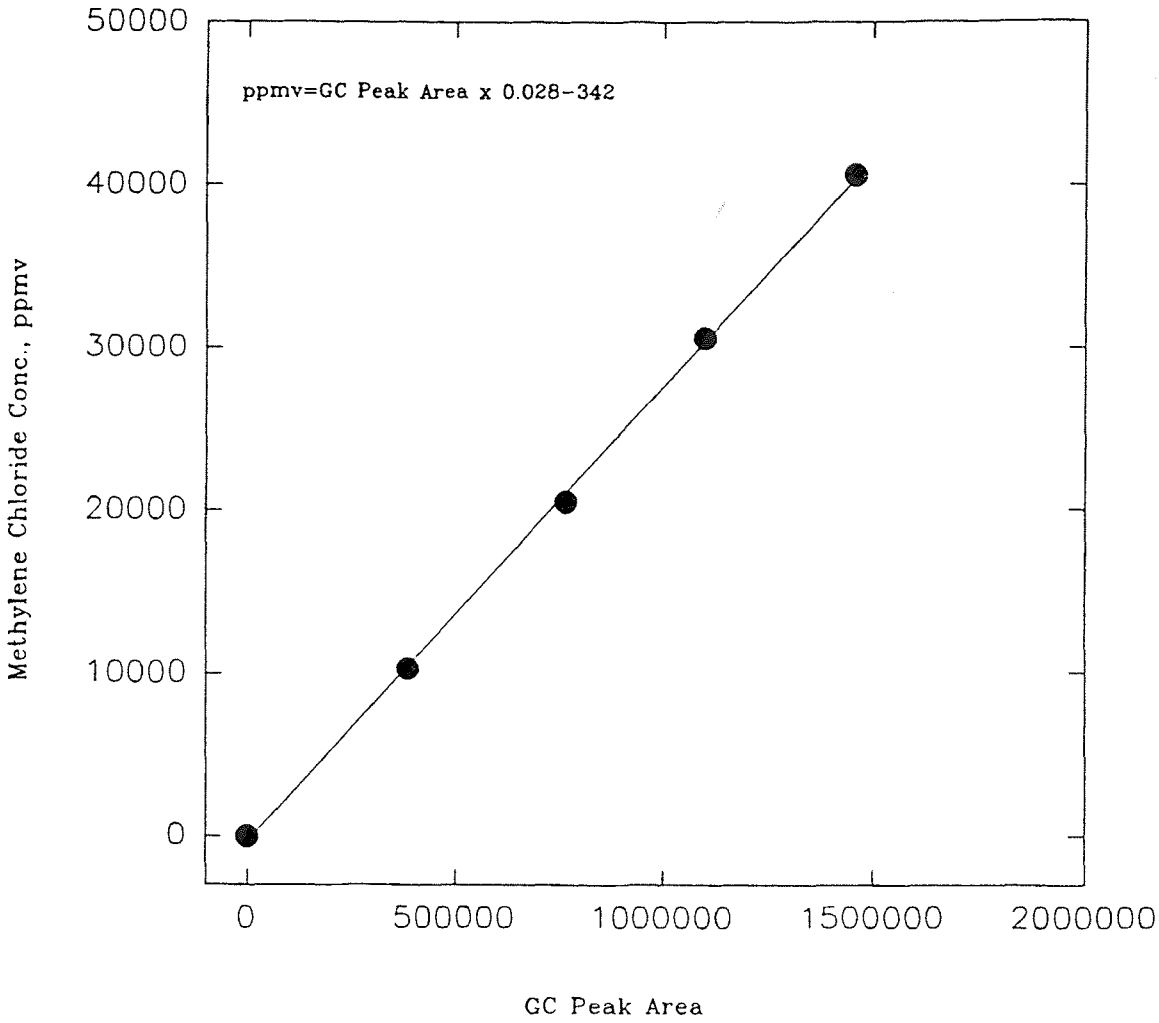

Figure A.8 Calibration Curve 3 for Methylene Chloride (Range 8)

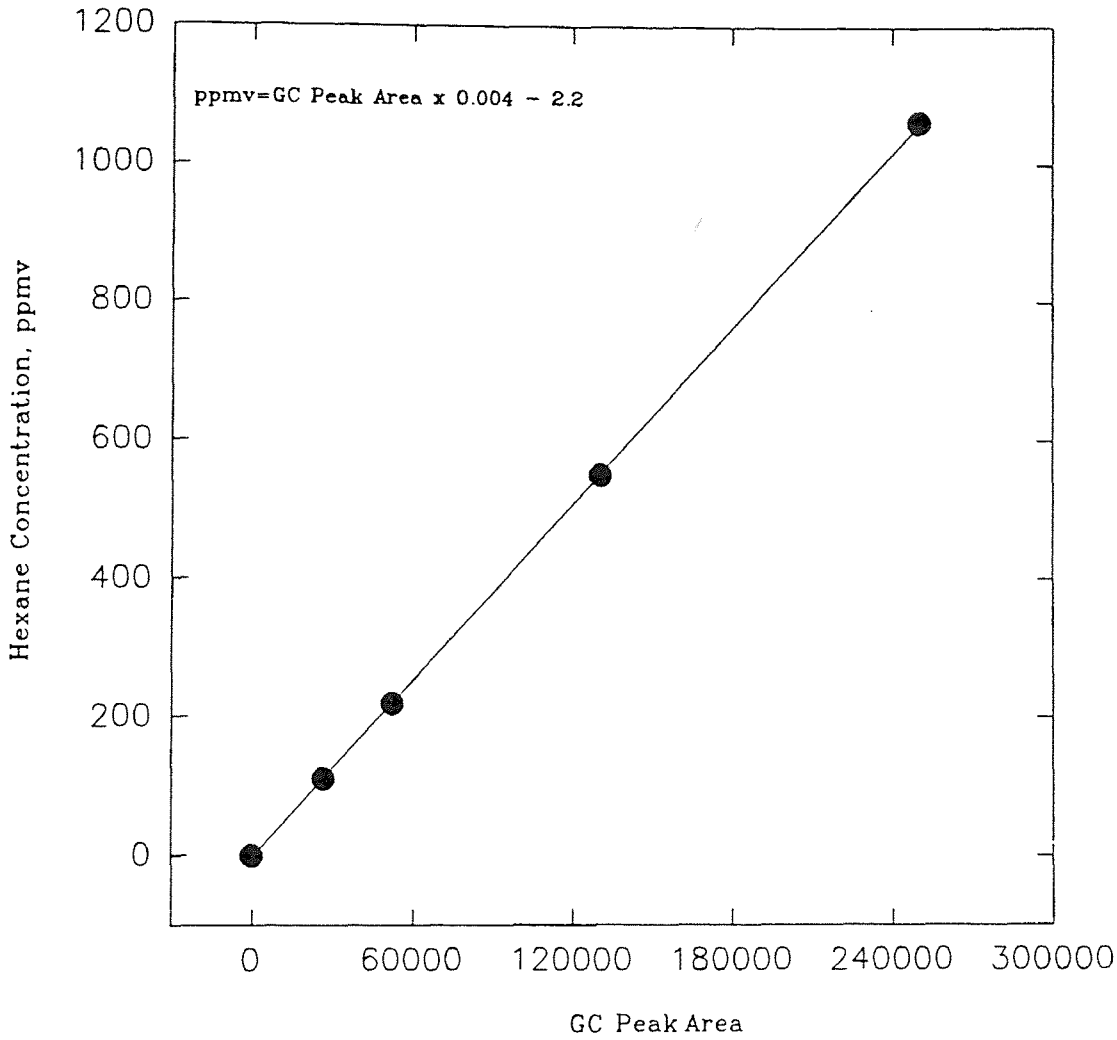

Figure A.9 Calibration Curve for Hexane (Range 8)

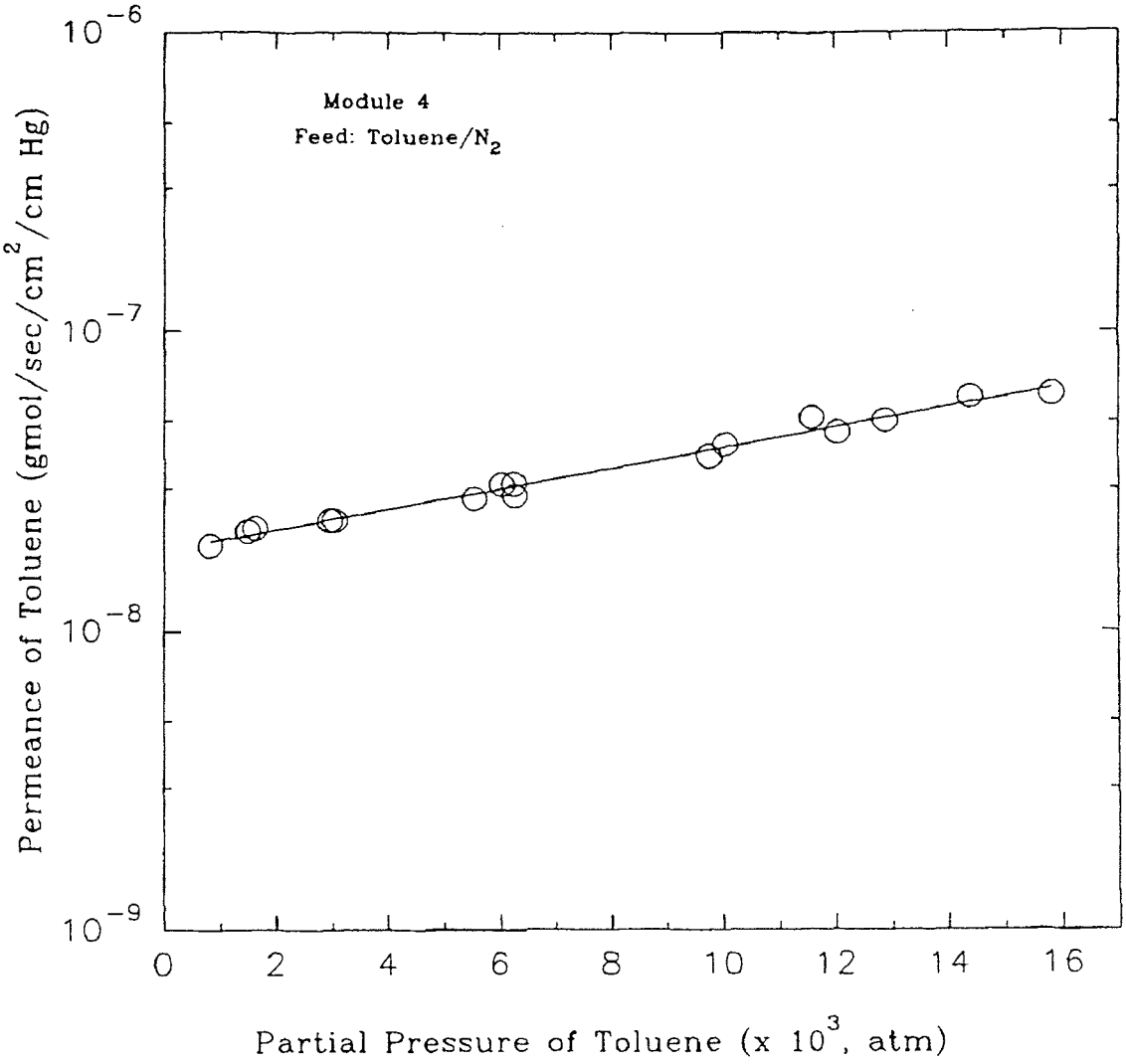

Figure A.10 Variation of Toluene Permeance with Toluene Concentration

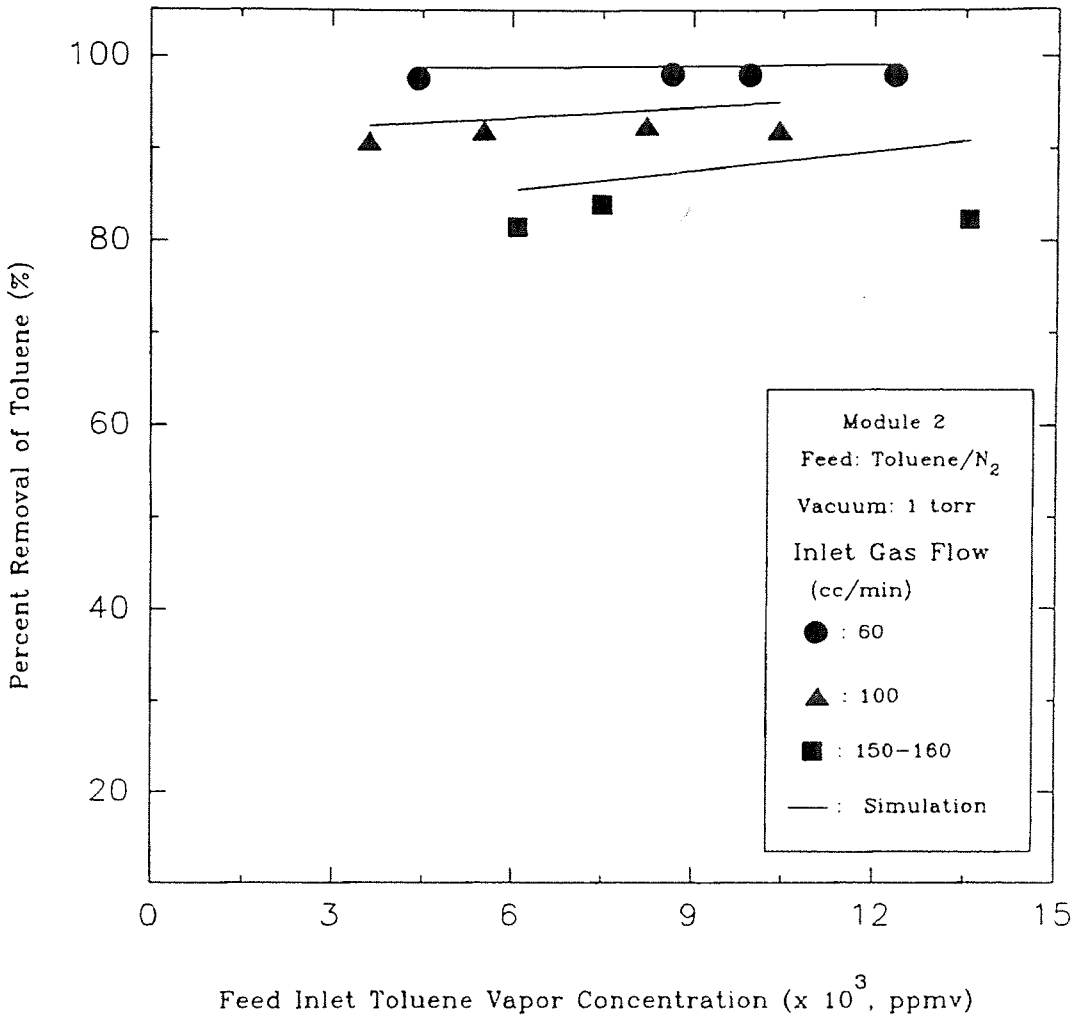

Figure A.11 Variation of Percent Removal of Toluene with Feed Inlet Toluene Vapor Concentration at Different Flow Rates

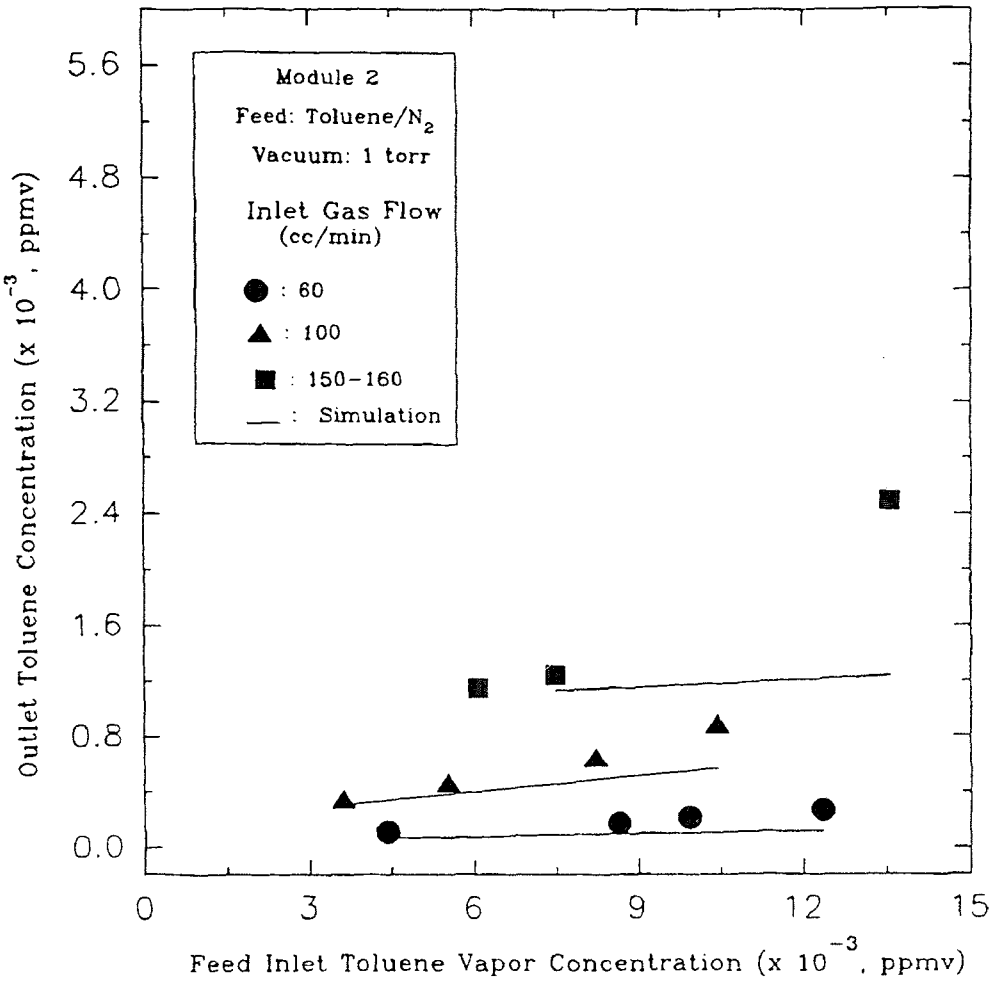

Figure A.12 Variation of Outlet Toluene Concentration with Feed Inlet Toluene Vapor Concentration at Different Flow Rates

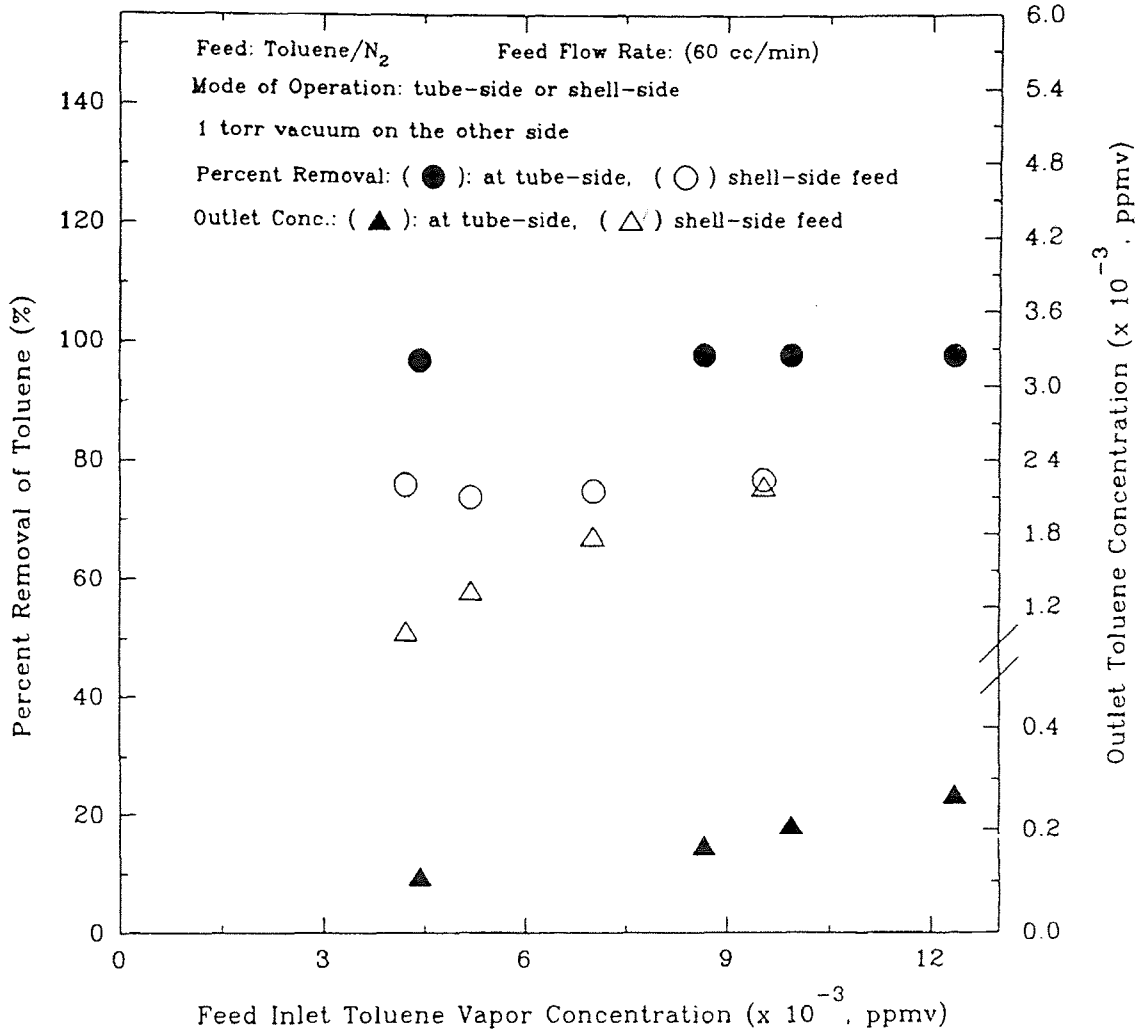

Figure A.13 Variation of Percent Removal and Outlet Concentration of Toluene with Feed Inlet Toluene Vapor Concentration for Shell-Side and Tube-Side Modes of Operation at 60 cc/min.

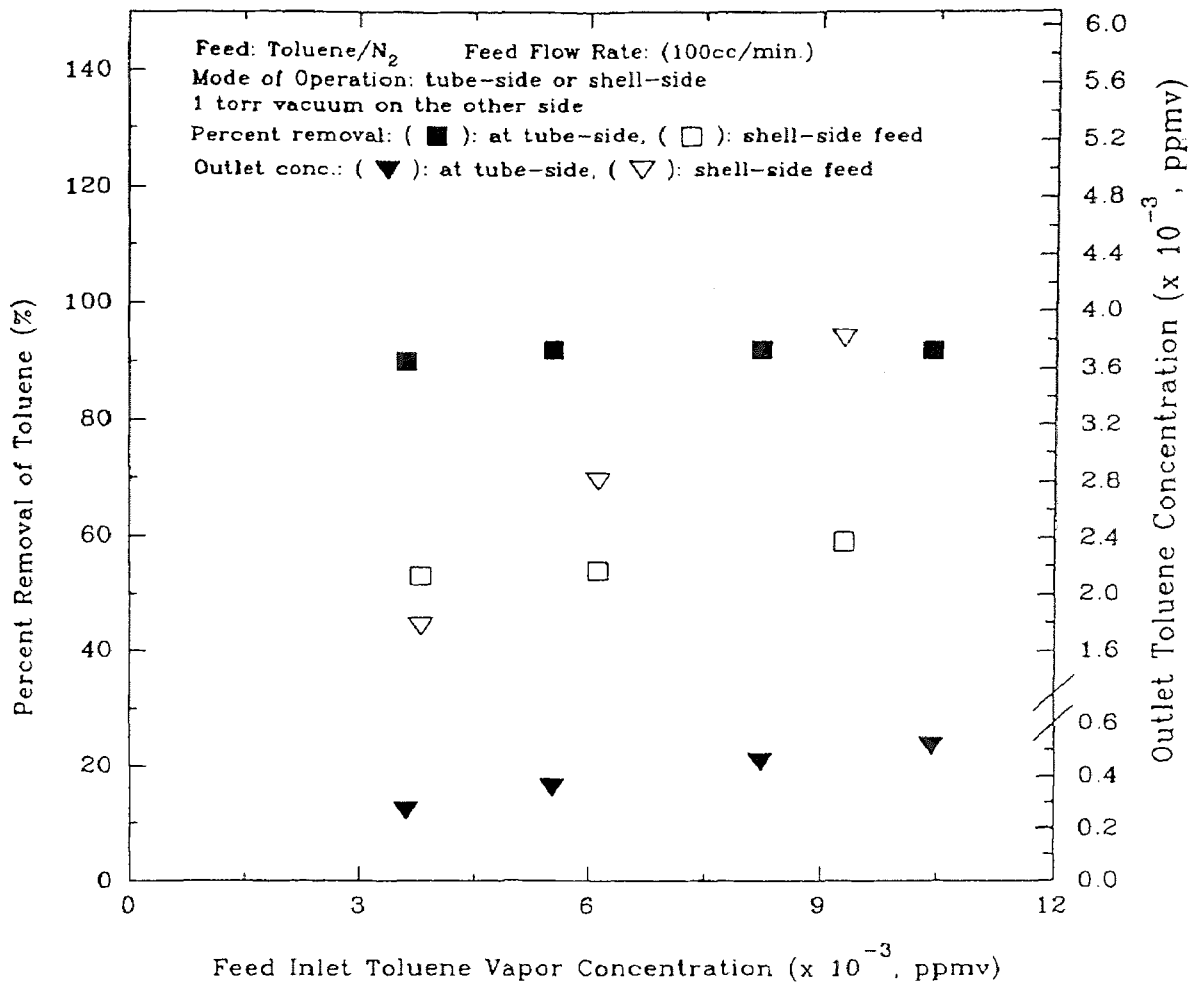

Figure A.14 Variation of Percent Removal and Outlet Concentration of Toluene with Feed Inlet Toluene Vapor Concentration for Shell-Side and Tube-Side Modes of Operation at 100 cc/min.

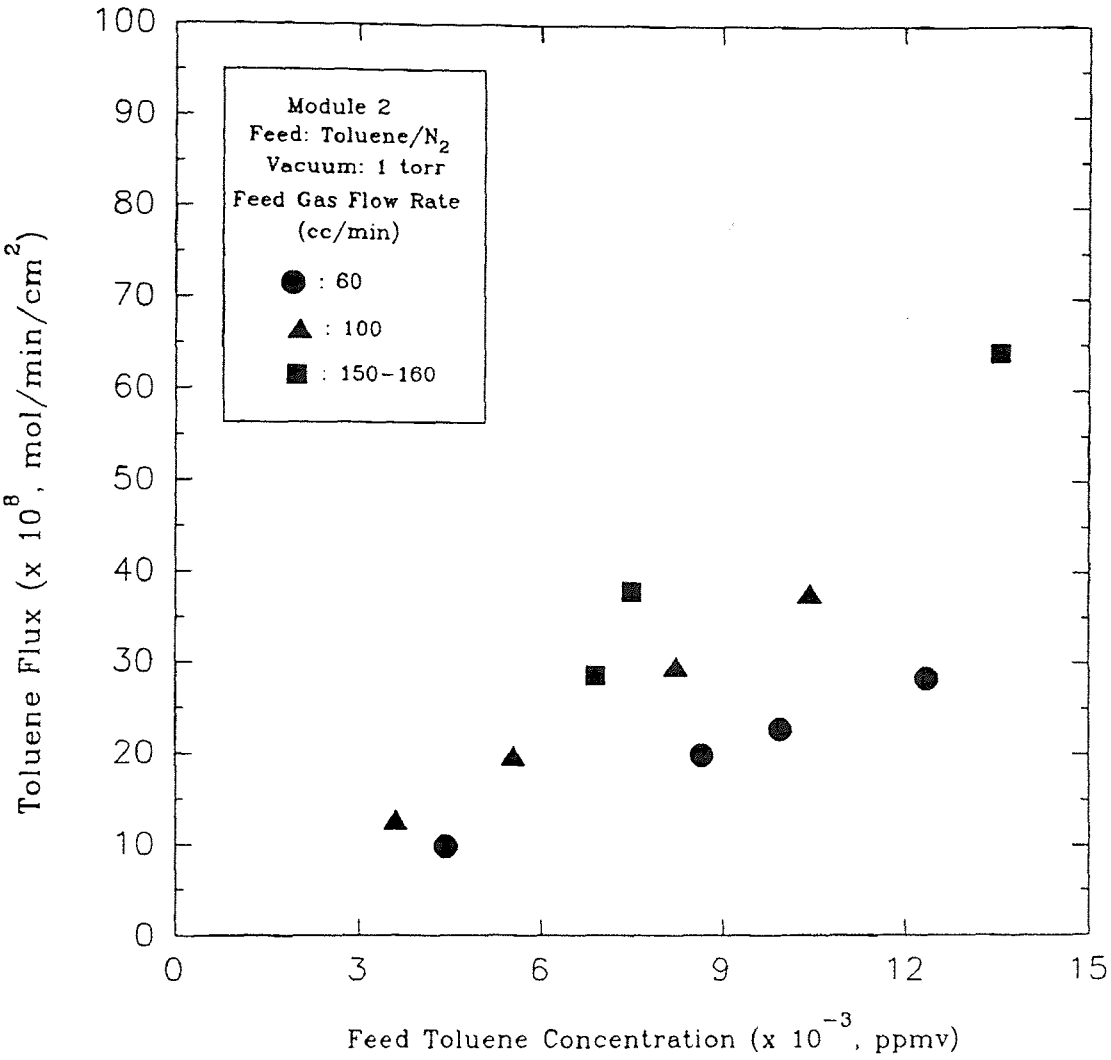

Figure A.15 Variation of Toluene Flux with Feed Inlet Toluene Vapor Concentration at Different Flow Rates

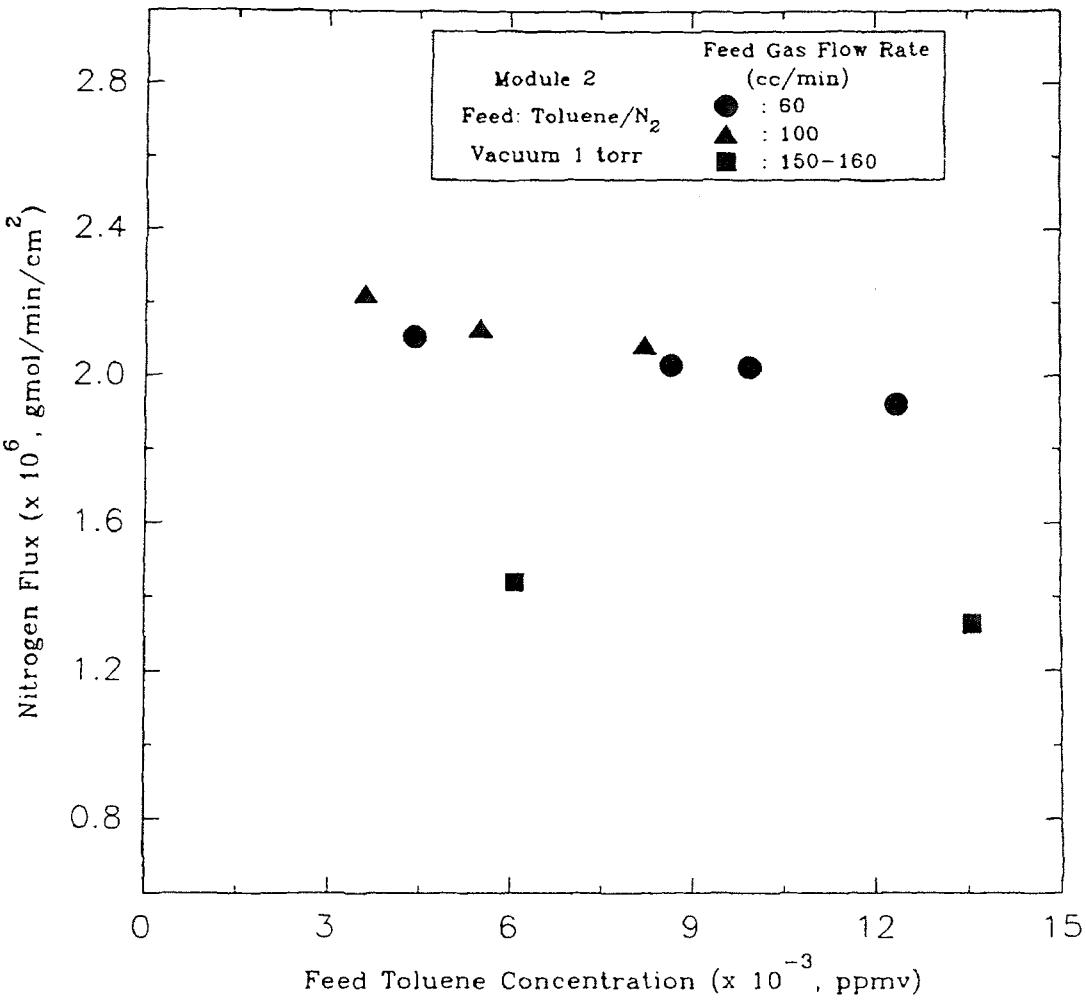

Figure A.16 Variation of Nitrogen Flux with Feed Inlet Toluene Vapor Concentration at Different Flow Rates

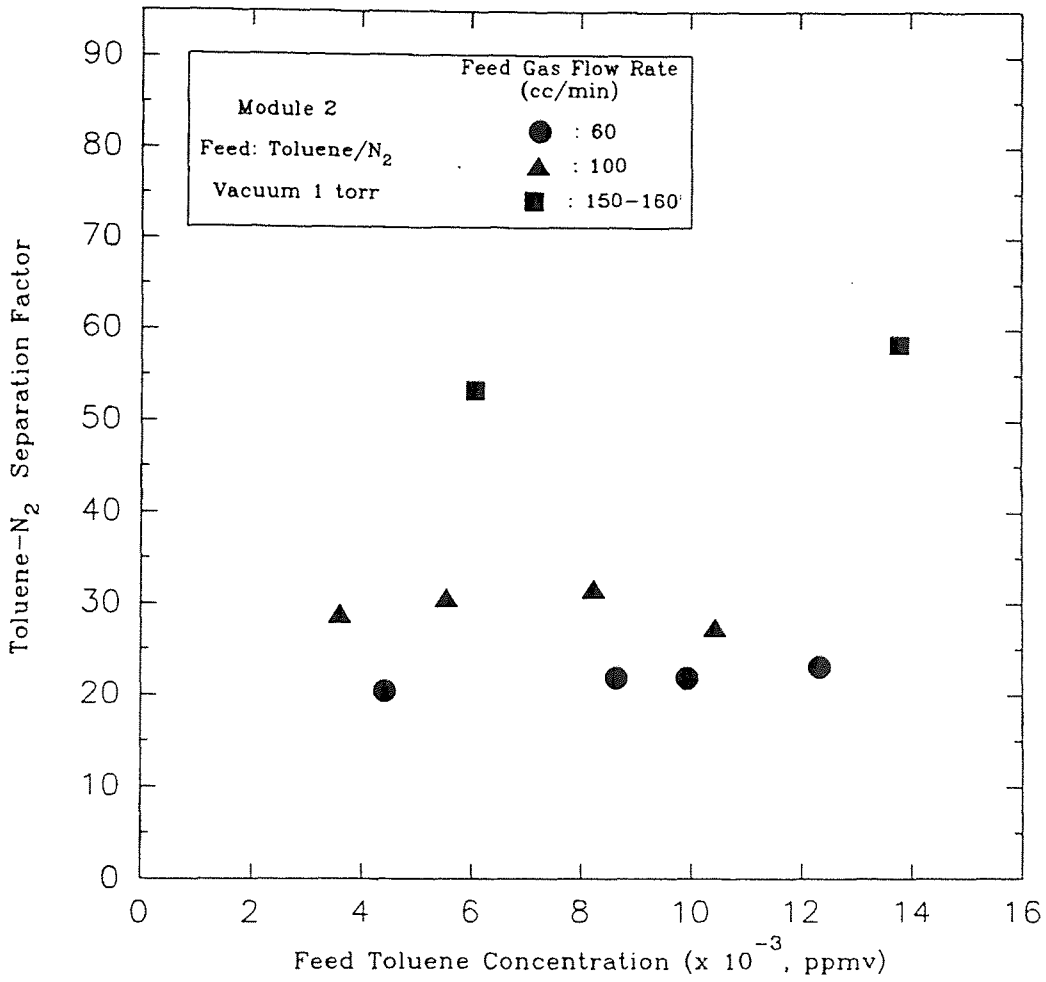

Figure A.17 Variation of Toluene-Nitrogen Separation Factor with Feed Inlet Toluene Vapor Concentration at Different Flow Rates

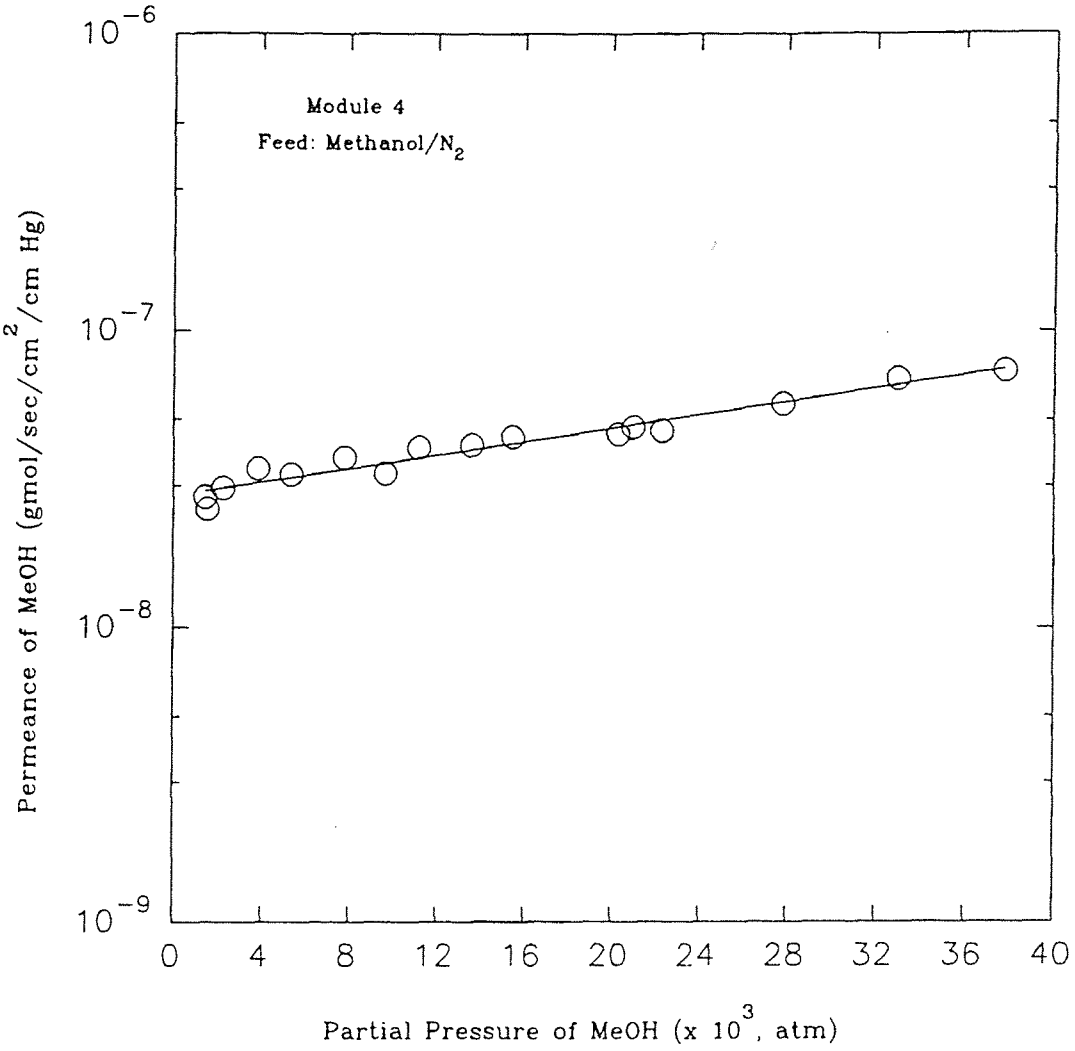

Figure A.18 Variation of Methanol Permeance with Methanol Concentration

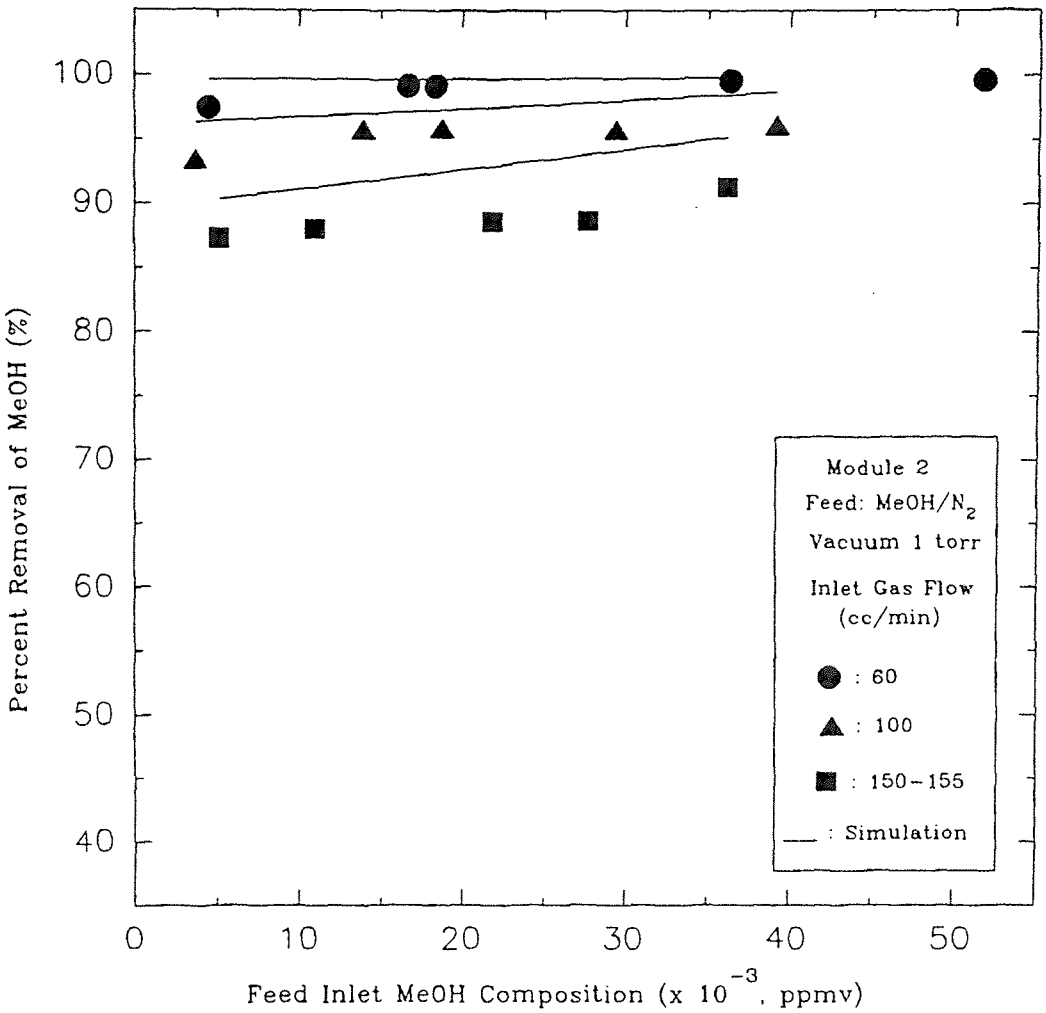

Figure A.19 Variation of Percent Removal of Methanol with Feed Inlet Methanol Vapor Concentration at Different Flow Rates

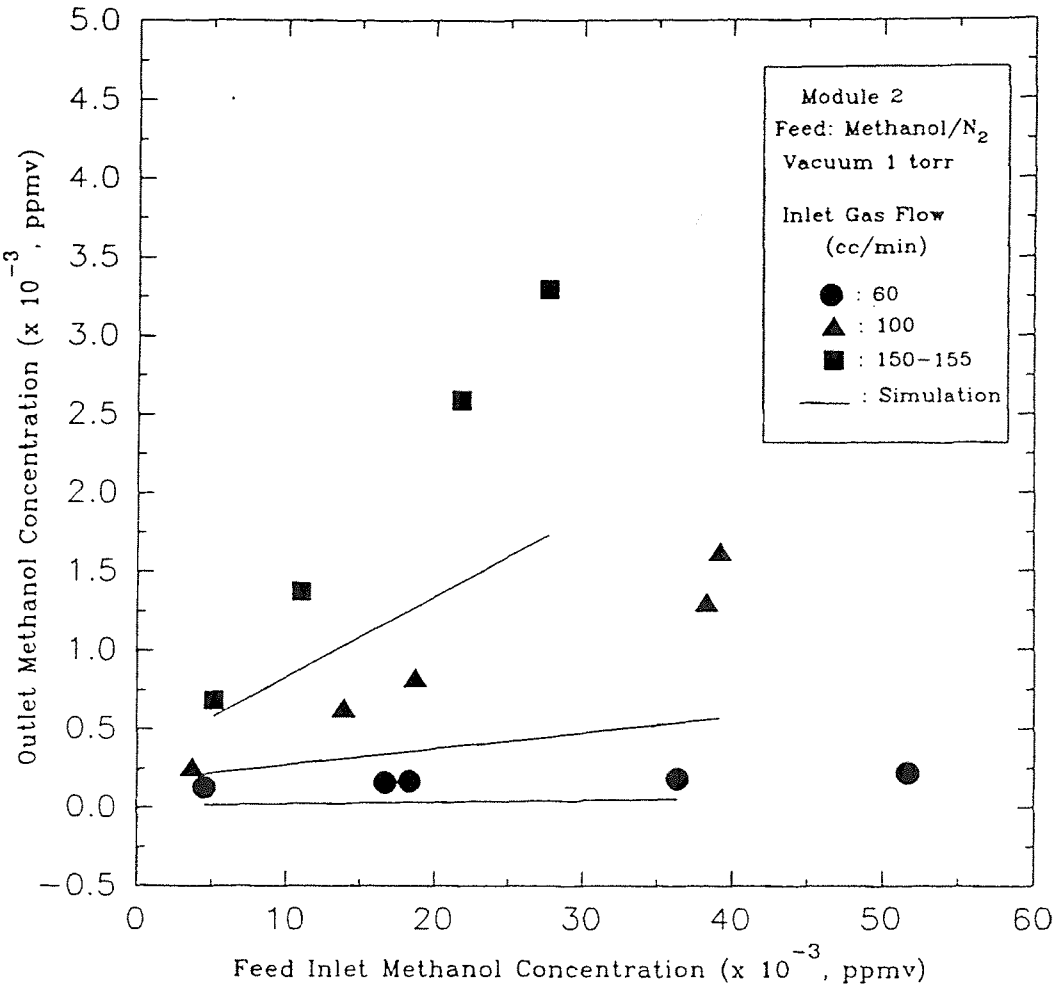

Figure A.20 Variation of Outlet Methanol Concentration with Feed Inlet Methanol Vapor Concentration at Different Flow Rates

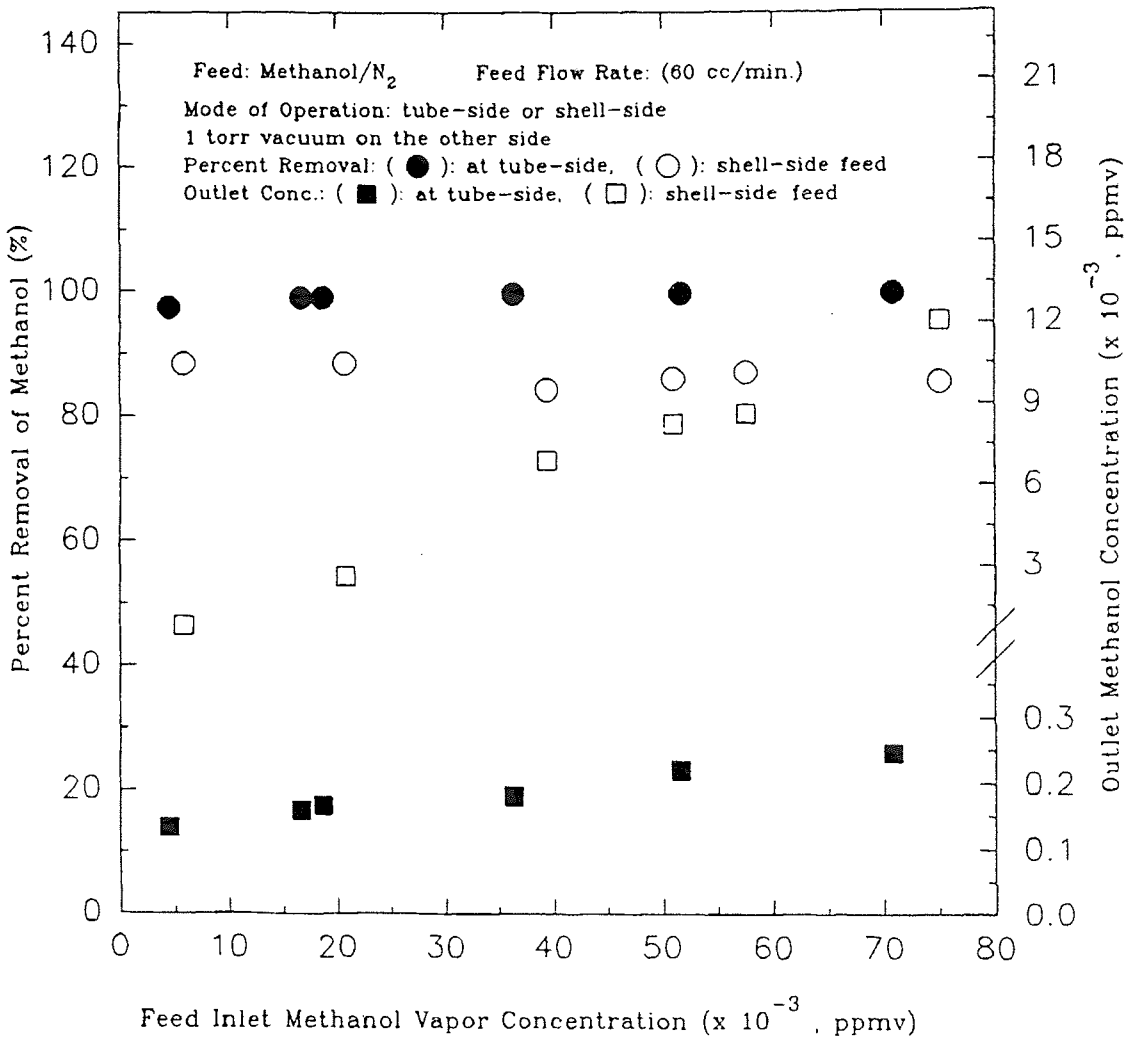

Figure A.21 Variation of Percent Removal and Outlet Concentration of Methanol with Feed Inlet Methanol Vapor Concentration for Shell-Side and Tube-Side Modes of Operation at 60 cc/min.

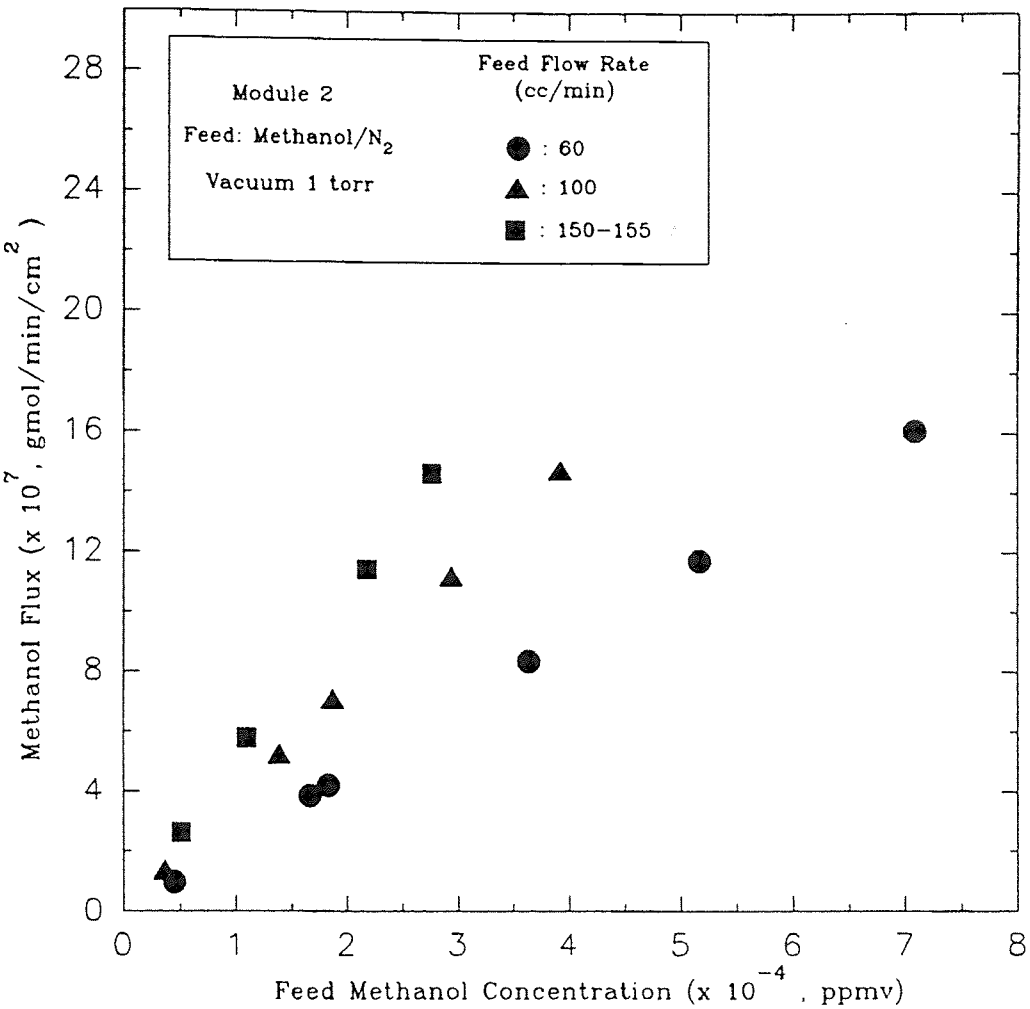

Figure A.22 Variation of Methanol Flux with Feed Inlet Methanol Vapor Concentration at Different Flow Rates

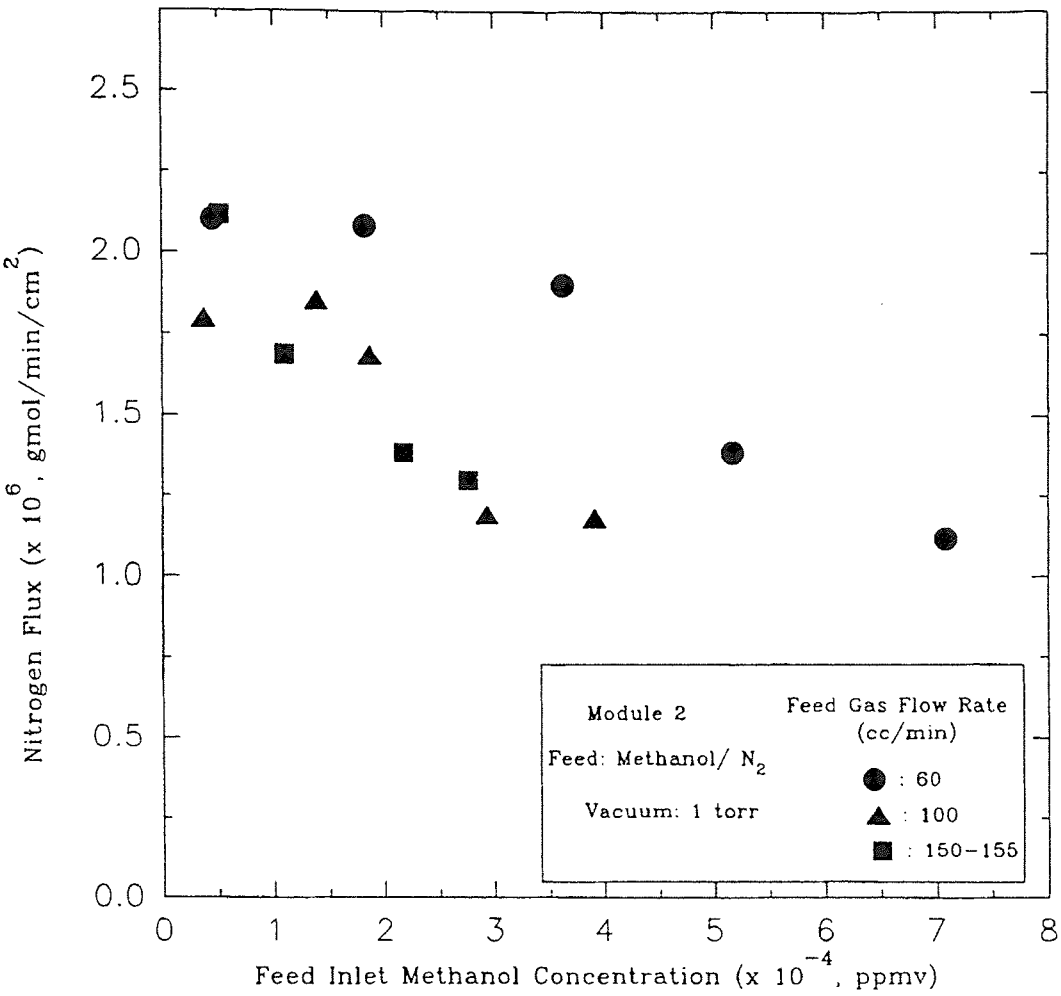

Figure A.23 Variation of Nitrogen Flux with Feed Inlet Methanol Vapor Concentration at Different Flow Rates

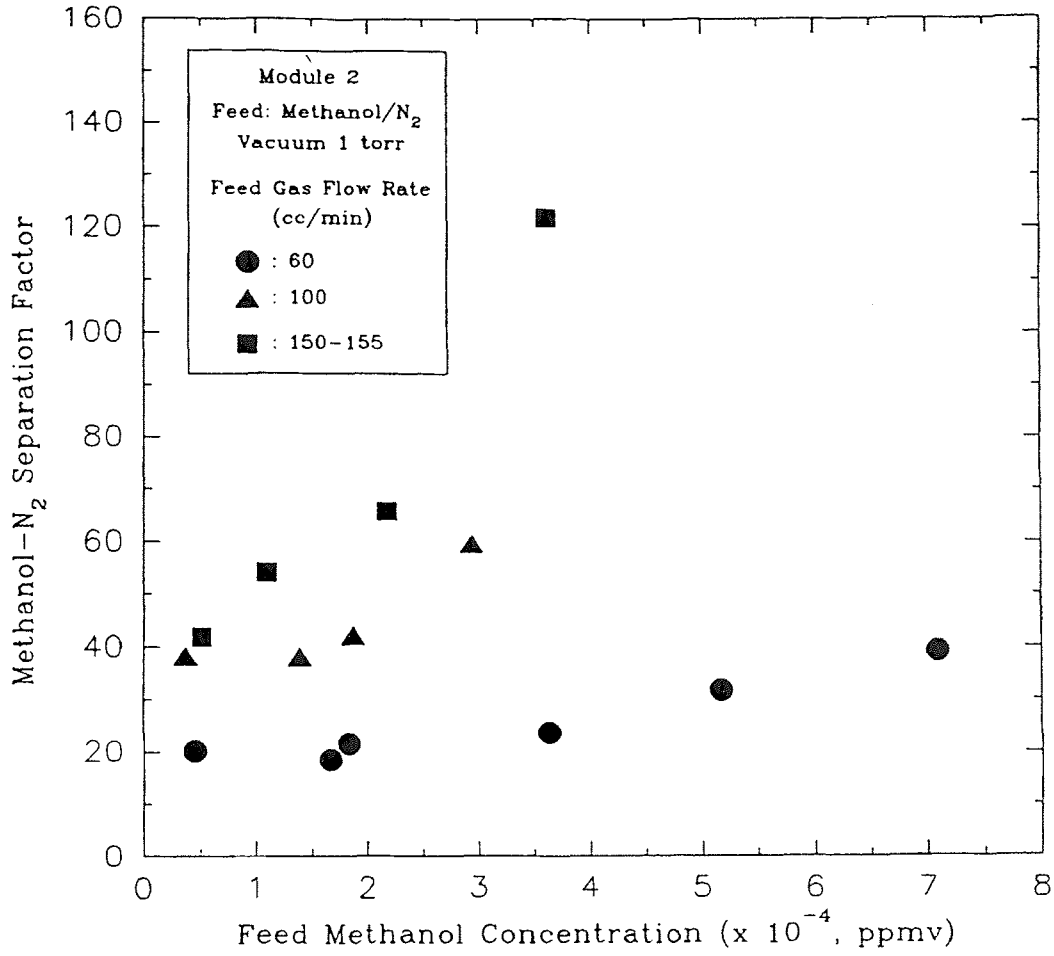

Figure A.24 Variation of Methanol-Nitrogen Separation Factor with Feed Inlet Methanol Vapor Concentration at Different Flow Rates

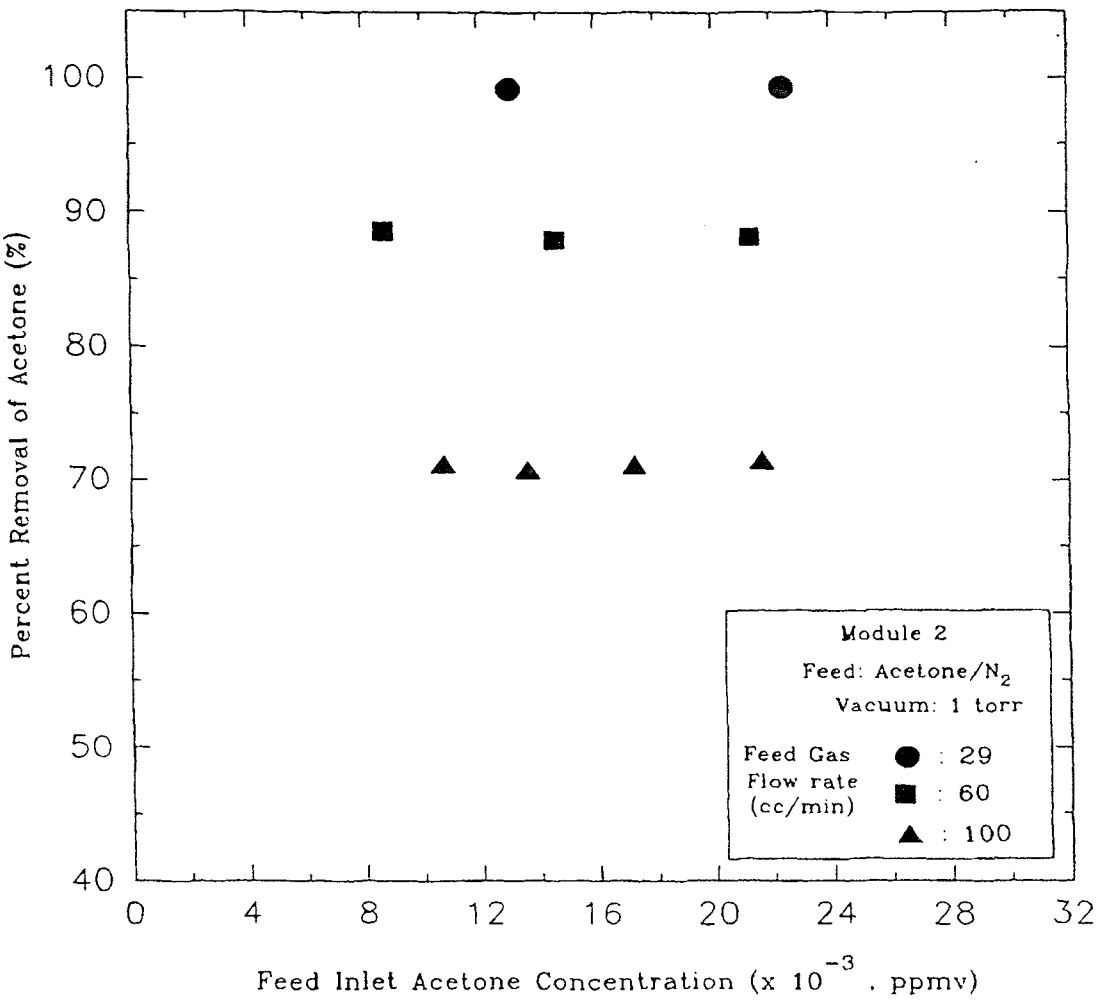

Figure A.25 Variation of Percent Removal of Acetone with Feed Inlet Acetone Vapor Concentration at Different Flow Rates

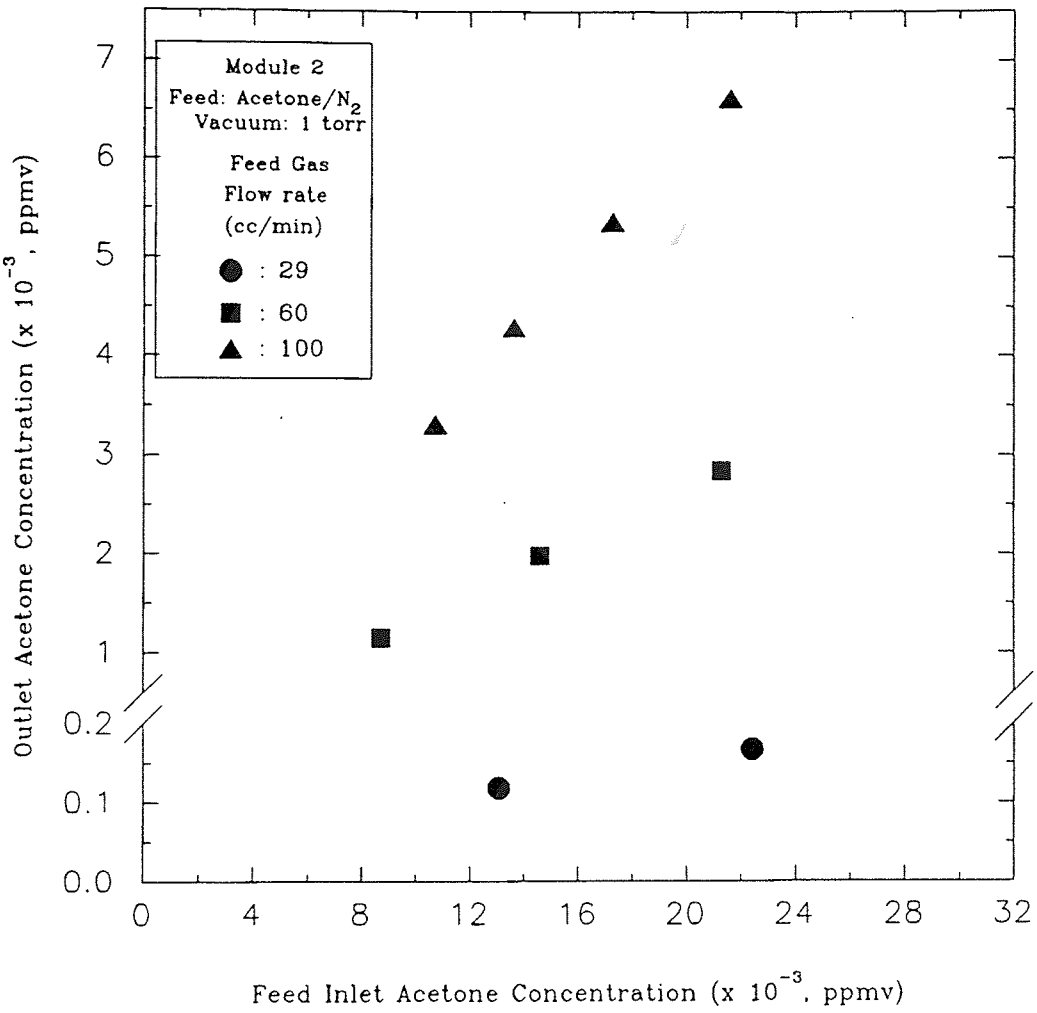

Figure A.26 Variation of Outlet Acetone Concentration with Feed Inlet Acetone Vapor Concentration at Different Flow Rates

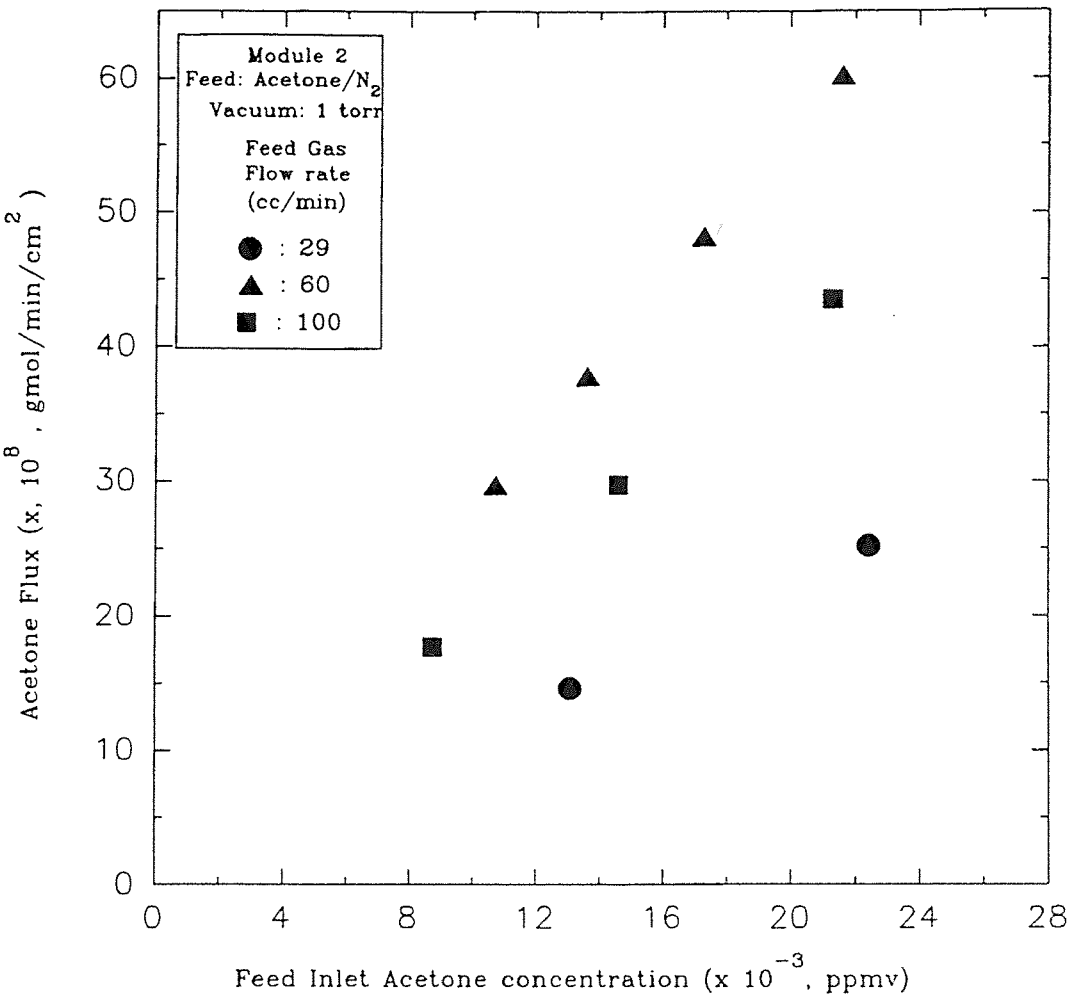

Figure A.27 Variation of Acetone Flux with Feed Inlet Acetone Vapor Concentration at Different Flow Rates

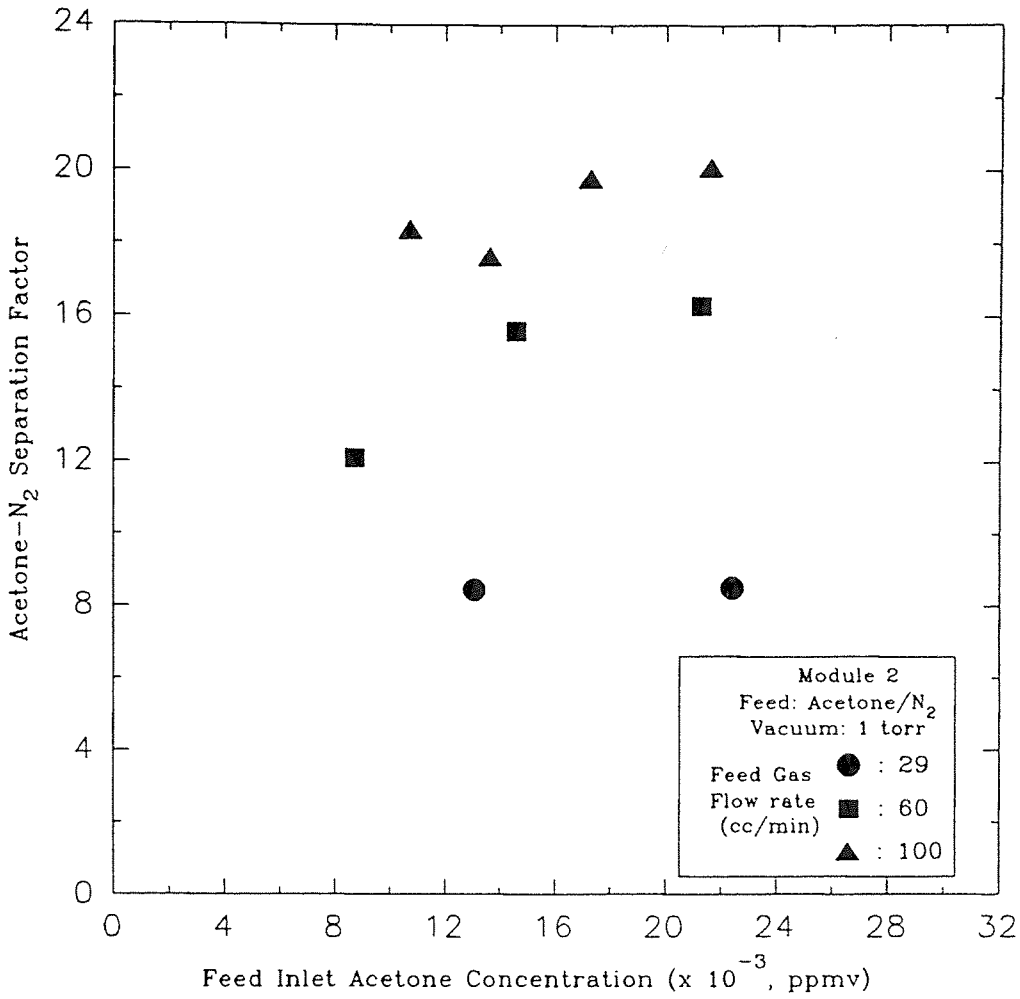

Figure A.28 Variation of Acetone-Nitrogen Separation Factor with Feed Inlet Acetone Vapor Concentration at Different Flow Rates

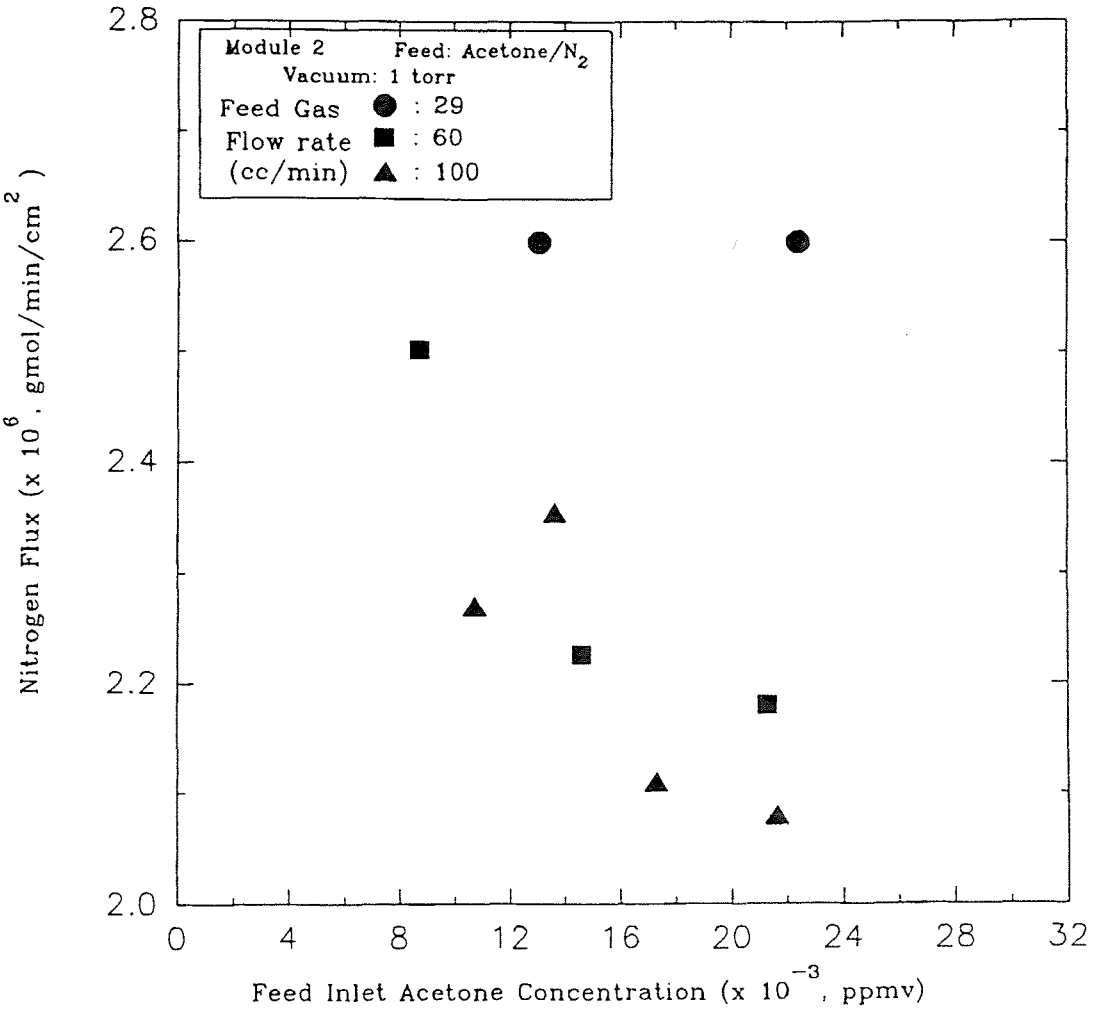

Figure A.29 Variation of Nitrogen Flux with Feed Inlet Acetone Vapor Concentration at Different Flow Rates

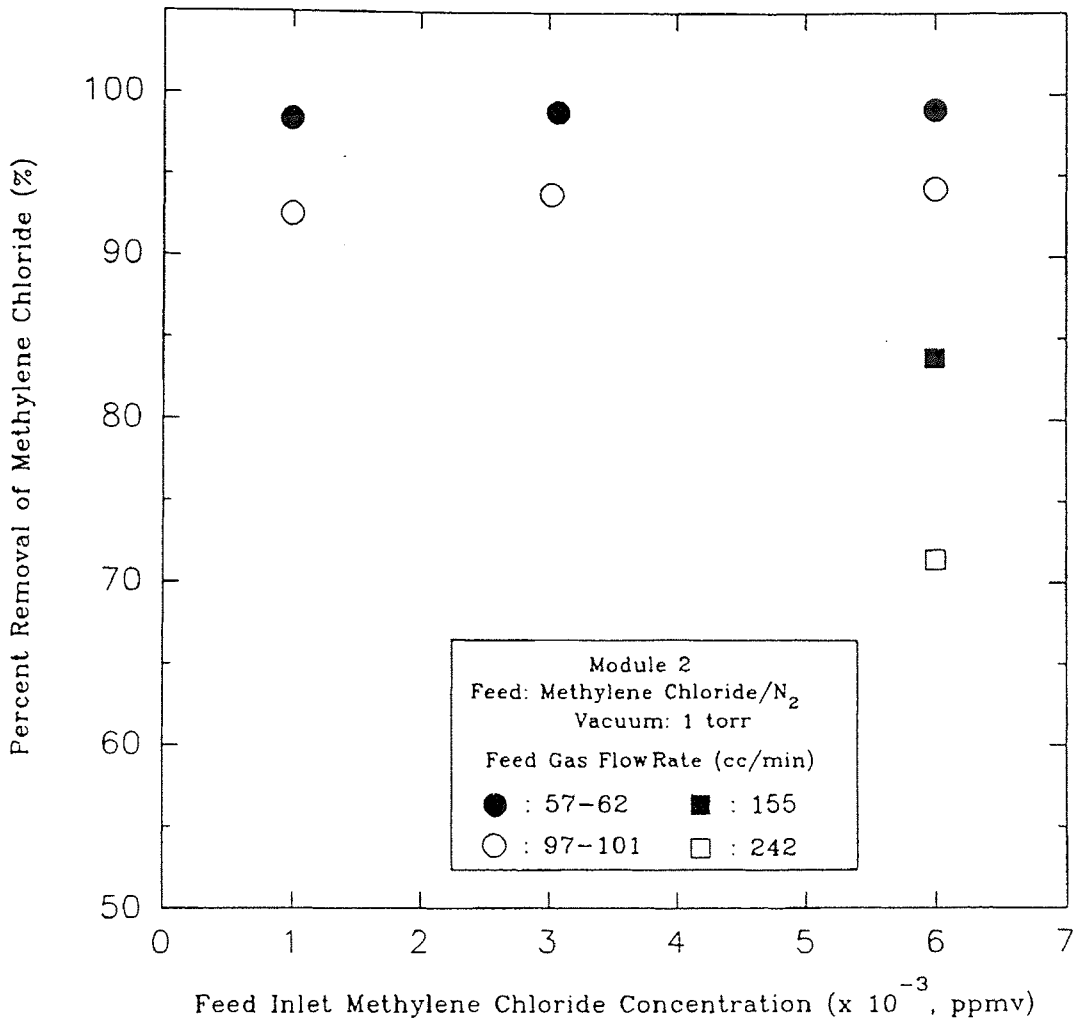

Figure A.30 Variation of Percent Removal of Methylene Chloride with Feed Inlet Methylene Chloride Vapor Concentration at Different Flow Rates

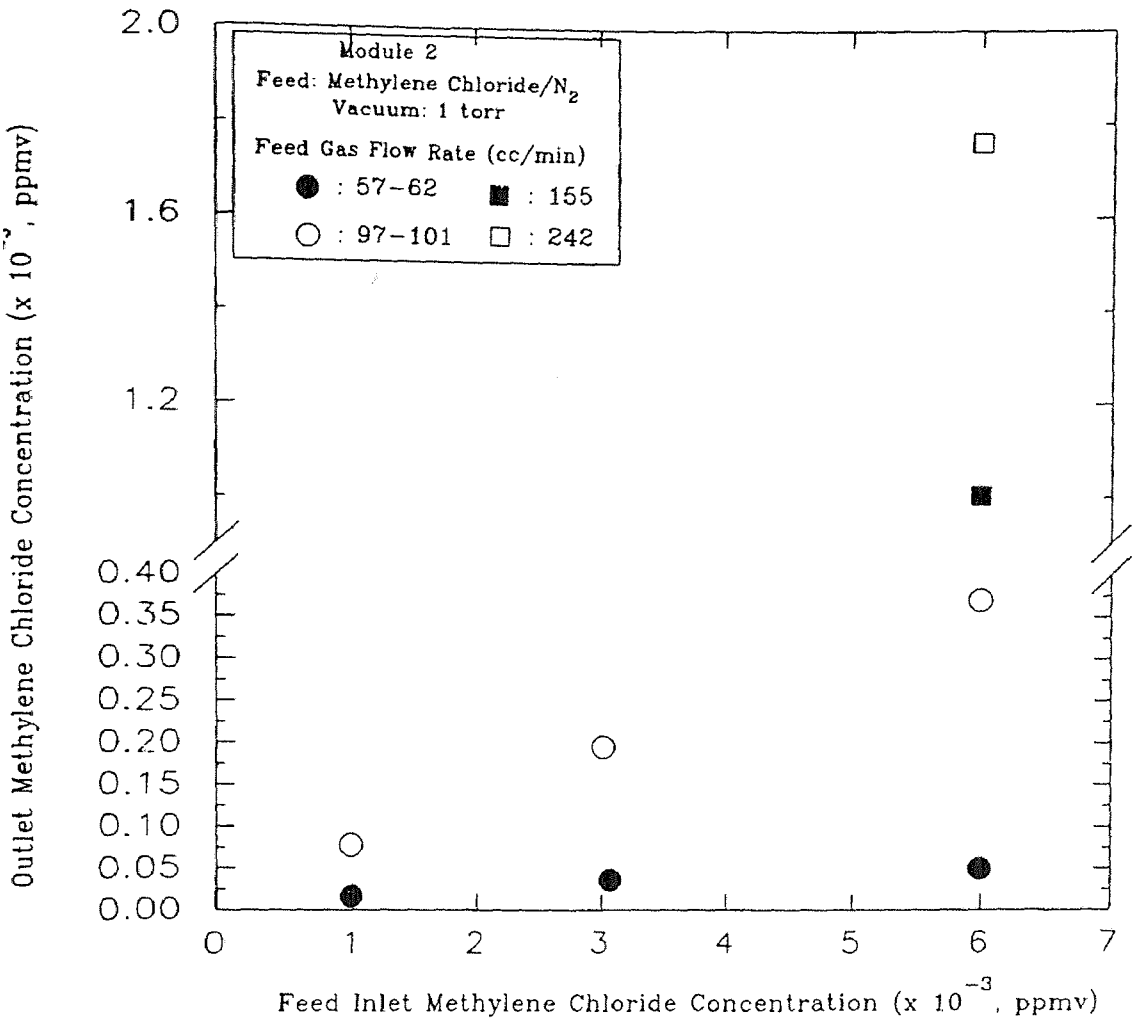

Figure A.31 Variation of Outlet Methylene Chloride Concentration with Feed Inlet Methylene Chloride Vapor Concentration at Different Flow Rates

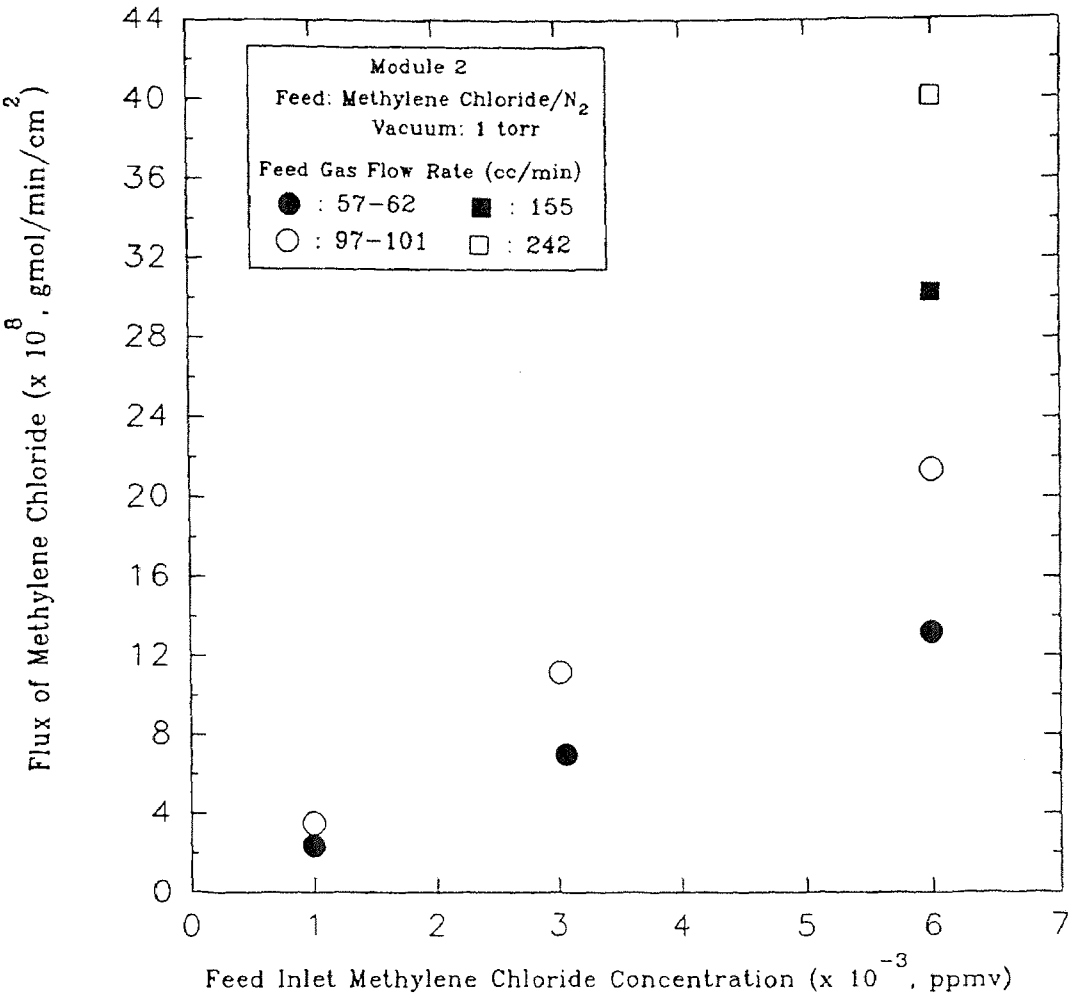

Figure A.32 Variation of Methylene Chloride Flux with Feed Inlet Methylene Chloride Vapor Concentration at Different Flow Rates

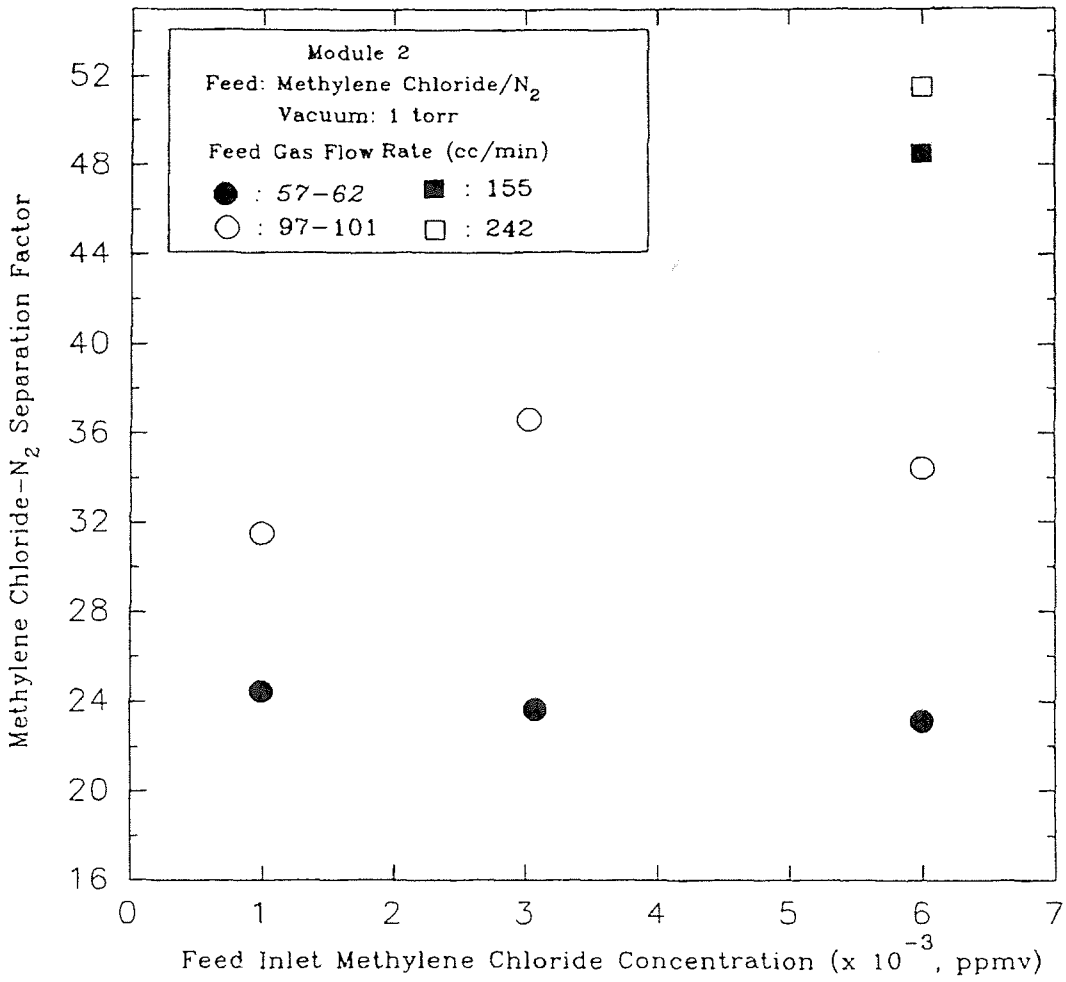

Figure A.33 Variation of Methylene Chloride-Nitrogen Separation Factor with Feed Inlet Methylene Chloride Vapor Concentration at Different Flow Rates

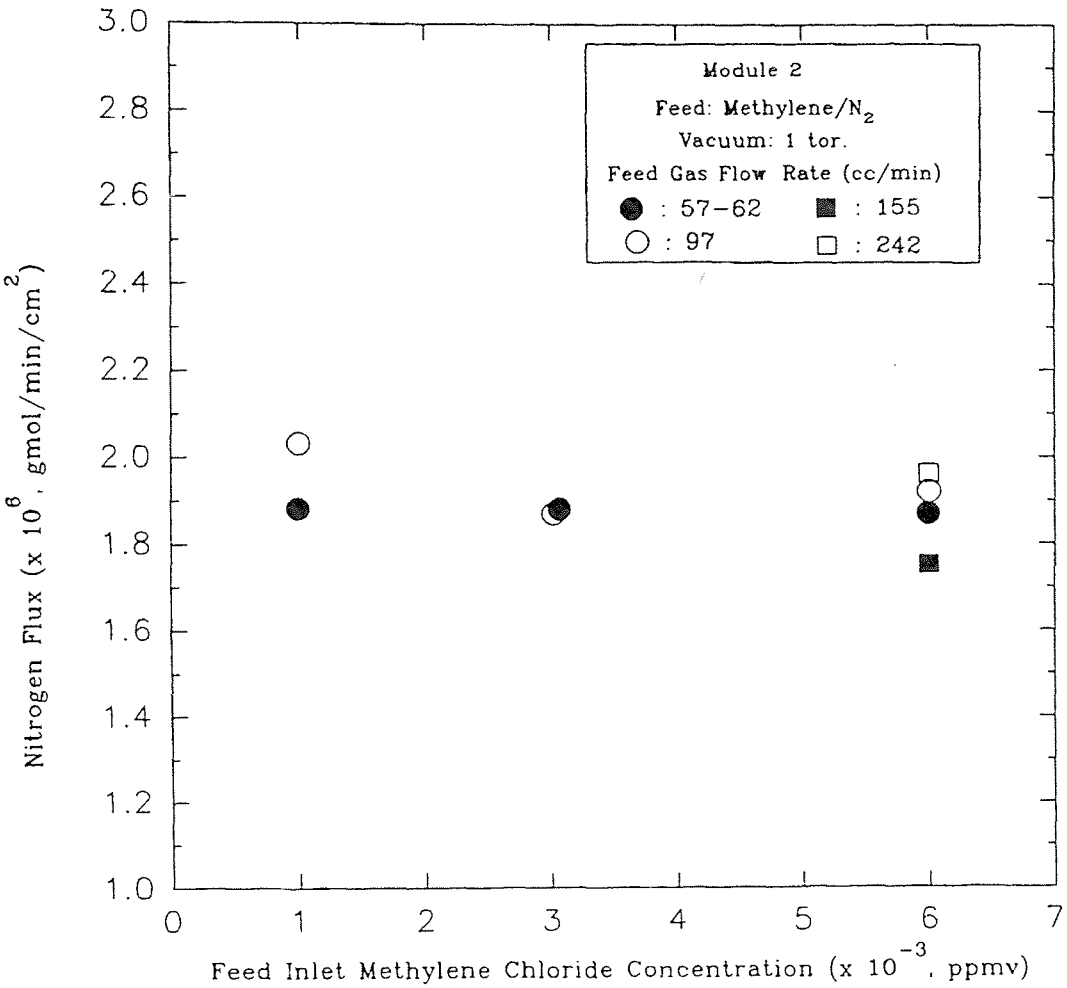

Figure A.34 Variation of Nitrogen Flux with Feed Inlet Methylene Chloride Vapor Concentration at Different Flow Rates

APPENDIX B

SAMPLE CALCULATIONS

Sample calculations for the performance of hollow fiber module in terms of permeate flux, percent removal, module-averaged permeance and separation factor are provided here.

Module Specifications (Module # 2)

# of Fibers, N: 50

Effective Fiber Length, l : 25 cm

I.D. of the Fiber : 240 μm

O.D. of the Fiber : 290 μm

Effective Surface Area (A) of the Module Based on Logarithmic Mean Diameter of the Fiber : $\pi.D_{lm}.l.N$, where $D_{lm} = (D_o-D_i) / \ln(D_o/D_i)$

$=3.14 \times \{[(290-240) / \ln (290/240)] \times 10^{-4} \}$ cm x 50 x 25 cm

$= 103.76$ cm^2

Experimental Data from table 2.3 for Toluene

Temperature : 30°C ; F/I : Feed Inlet ; F/O : Feed Outlet

F/I Flow Rate (Module), Q_i: 101.08 cm^3/min.

F/O Flow Rate (Module), Q_o : 93.92 cm^3/min.

Permeate Flow Rate, Q_p : $Q_i - Q_o$ = 101.08 - 93.92 = 7.16 cm^3/min.

ΔP (Through the Module) : 0.2 psig

F/I (Tube Side) Pressure : 76 cm Hg + [(76/14.69) x 0.2] cm Hg = 77.03 cm Hg

F/O (Tube Side) Pressure : 76 cm Hg

Permeate Pressure (Shell Side) : -29.88 inch Hg = [76 - (29.88 x 2.54)] cm Hg

= 0.10 cm Hg

Inlet Toluene Concentration (Module), $ppmv_{Tol,i}$: 10436 ppmv

Outlet Toluene Concentration (Module), $ppmv_{Tol,o}$: 888 ppmv

Calculations

To Calculate Molar Flow Rates of F/I, F/O and Permeate using : PV = nRT

For these calculations, the pressure is taken to be 76 cm Hg since all flow rate measurements were made at 1 atm.

F/I Molar Flow Rate, F_i : (76 cm. Hg) x (101.08 cm^3/min., Q_i) /

[(6.236 x 10^3 cm Hg.cm^3/gmol.°K) x 303.15°K]

= 4.06 x 10^{-3} gmol/min.

F/O Molar Flow Rate, F_o : (76 cm. Hg) x (93.92 cm^3/min., Q_o) /

[(6.236 x 10^3 cm Hg.cm^3/gmol.°K) x 303.15°K]

= 3.78 x 10^{-3} gmol/min.

Permeate Molar Flow Rate, F_p : (76 cm. Hg) x (7.16 cm^3/min., Q_p) /

[(6.236 x 10^3 cm Hg.cm^3/gmol.°K) x 303.15°K]

= 2.88 x 10^{-4} gmol/min.

Permeate Mole Fractions of Toluene and N_2

$x_{N2,i}$, $x_{N2,o}$: mole fraction of nitrogen in the feed side gas mixture at the feed inlet and at the feed outlet end of the permeator.

x_f, x_w : mole fraction of toluene in the feed side gas mixture at the feed inlet and at the feed outlet end of the permeator.

y_f, $y_{N2,p}$: mole fraction of toluene and nitrogen at the permeate outlet end of the permeator

$x_f = ppmv_{Tol,i} / 10^6$ $\quad x_f = 10436 / 10^6 = 0.010436$

$x_{N2,i} = 1 - x_f$ $\quad x_{N2,i} = 1 - 0.010436 = 0.989564$

$x_w = ppmv_{Tol,o} / 10^6$ $\quad x_w = 888 / 10^6 = 0.000888$

$x_{N2,o} = 1-x_w$ $\quad\quad$ $x_{N2,o} = 1- 0.000888 = 0.999112$

$y_f = (F_i \,.\, x_f - F_o \,.\, x_w)/ F_p$

$= [(4.06 \times 10^{-3}) \times 0.010436 - (3.78 \times 10^{-3}) \times 0.000888] / 2.88 \times 10^{-4}$

$= 0.135464$

$y_{N2,p} = 1 - y_f = 1-0.135464 = 0.864536$

Toluene and Nitrogen Permeate Flux

Toluene Permeate Flux

$= (F_p \,.\, y_f) / A = (2.88 \times 10^{-4}$ gmol/min.cm^2) x 0.135464 / (103.76 cm^2)

$= 37.60 \times 10^{-8}$ gmol / cm^2.min

Nitrogen Permeate Flux

$= (F_p \,.y_{N2,p}) / A = (2.88 \times 10^{-4}$ gmol/min.cm^2) x 0.864536 / (103.76 cm^2)

$= 24.0 \times 10^{-7}$ gmol / cm^2.min

Percent Removal of Toluene

$= (F_p.y_f / F_i.x_f) \times 100$

$= [(2.88 \times 10^{-4}) \times 0.135464 / (4.06 \times 10^{-3}) \times 0.010436] \times 100$

$= 92.08$

Module-Averaged Permeance of Toluene, Q_{tol} / δ_m

Q_{tol} / δ_m = Toluene Flux / $(P_{tol,f} - p_{tol,p})$

$P_{tol,f}$ = (F/I Pressure . x_f + F/O Pressure . x_w) / 2

$P_{tol,f} = (77.03 \times 0.010436 + 76.0 \times 0.000888) / 2$

$= 0.4357$ cm Hg

$p_{tol,f}$ = Permeate Pressure . y_f

$= 0.1 \times 0.135464 = 0.0135464$ cm Hg

Q_{tol} / δ_m = 37.60 x 10^{-8} gmol / cm^2.min / (0.4357 cm Hg - 0.0135464 cm Hg)

= 89.07 x 10^{-8} gmol / $cm.^2$ min. cm Hg

Module- Averaged Permeance of Nitrogen, Q_{N2} / δ_m

Q_{N2} / δ_m = Nitrogen Flux / ($P_{N2,f}$ - $p_{N2,p}$)

$P_{N2,f}$ = (F/I Pressure . $x_{N2,i}$ + F/O Pressure . $x_{N2,o}$) / 2

$P_{N2,f}$ = (77.03 x 0.989564 + 76.0 x 0.999112) / 2

= 76.0793 cm Hg

$p_{N2,p}$ = Permeate Pressure . $y_{N2,p}$

= 0.1 x 0.864536 = 0.086454 cm Hg

Q_{N2} / δ_m = 24.0 x 10^{-7} gmol / cm^2.min / (76.0793 cm Hg - 0.086454 cm Hg)

= 3.16 x 10^{-8} gmol / $cm.^2$ min. cm Hg

Separation Factor

= Q_{tol} / Q_{N2} = 89.07 x 10^{-8} / 3.16 x 10^{-8} = 28.19

APPENDIX C

PROGRAM FOR MODELING OF HOLLOW FIBER PERMEATOR FOR VOC REMOVAL

```
C INFORM.FOR
C This program is to collect the experimental data, convert
C the unit, and change those parameter into dimensionless form.
C The function of this program is to manage the data for IMSL program
C
      CHARACTER MOD*25,VOC*25
      READ *, MOD, VOC
      READ *, FIBLEN
C
C FIBLEN= length of fiber, cm
C
      READ *,TEMP
      TABS=TEMP+273.15
      READ *, AVOC
      READ *, BVOC
C     BVOC=BVOC/14.696
      READ *, AN2
      READ *, BN2
C     BN2=BN2/14.696
C
C TEMP= experimental temperature, oC
C QVOC= AVOC*exp(BVOC*PRVOC)
C QN2= AN2*exp(BN2*PRVOC) at constant temperature,
C where QVOC and QN2 are the permeability of VOC and N2
C
      READ *,DIN
      READ *,DOUT
C
C DIN, DOUT= inside and outside diameters of fiber, respectively, cm
C
      READ *,PREIN
      READ *,PREVAC
      READ *,VIN
      ATM=76.0
      PREF=76.0/ATM
      PFEED=PREIN/ATM/PREF
      PVAC=PREVAC/ATM/PREF
      VREF=VIN
      VFEED=VIN/VREF
C
C PREIN= pressure in the inlet of the feed, cm-Hg
C VIN= viscosity in the inlet of the feed, poise (g/cm/s)
C
      THICK=(DOUT-DIN)/2.0
C
C THICK= thickness of the fiber, cm
```

```
C
      READ *, FINLET
      READ *, FREFA
      FBOUND=FINLET/FREFA
      READ *, NFIBER
      RCONST=82.057
      FREF=1.0*FREFA/60.0/RCONST/(25.0+273.15)/NFIBER
C
C FINLET= feed inlet measured at R.T. and 1 atm, CC/min
C NFIBER= no. of fibers
C FREFA= reference flow rate, cc/min
C FREF= flow rate per fiber, mol/sec
C
      READ *, XINLET
C
C XINLET= mole fraction of VOC in the inlet of the pore
C
      PI=3.14159
      QREF1=FREF/PI/DOUT/PREF/FIBLEN
      QREF=QREF1/76.0
      PRINT *, 'ref permeability, (mol)/(s*cm2*cmHg) = ', QREF
C
C Dimensionless conversion to make XRIGHT=1 or S=1 in the derivation
C QREF= reference permeability coeff., (mol)/(s*cm2*cmHg)
C BETA= constant for dimesionless change, g/(cm*atm*sec**2)
C 1 atm = 1.0133E6 g/(cm*sec**2)
C
      BETA=128.0*RCONST*TABS*FREF**2*VREF/
     &     (PI**2*DIN**4*DOUT*(QREF1)*PREF**3)
      BETA=BETA/1.0133E6
      PRINT *, 'BETA, dimensionless, g/(cm*atm*s**2)= ',BETA
C
C Calculation of dimensionless constant
C
      Q0VOC=AVOC/QREF
      Q0N2=AN2/QREF
C
C Print and save the calculated data
C
      OPEN (5, FILE='INFORM.DAT',STATUS='NEW')
      WRITE (5,*) XINLET, PFEED, ' inlet X of VOC and pressure, atm'
      WRITE (5,*) FBOUND, '  boundary condition at feed inlet'
      WRITE (5,*) PVAC, '  pressure of the vacuum side, atm'
      WRITE (5,*) BETA, VFEED, ' dimensionless beta and feed viscosity'
      WRITE (5,*) Q0VOC, BVOC, '  exp data of
QVOC=Q0VOC*EXP(BVOC*PVOC)'
```

```
      WRITE (5,*) Q0N2, BN2, '  exp data of QN2=Q0N@*EXP(BN2*PVOC)'
      CLOSE (5,STATUS='KEEP')
      END

C YINIT.FOR
C This is a program to guess the initial value of YINIT in the AICHE-*.for.
C This program uses IMSL IVPRK/DIVPRK subroutine.
C

C
C Specifications for parameters
C NGRID is the number of grid
C
      INTEGER MXPARM, NEQ, NGRID
      PARAMETER (MXPARM=50, NEQ=5, NGRID=10)
C
      INTEGER IDO,ISTEP,NOUT
      REAL FCN, FLOAT, PARAM(MXPARM), T, TEND, TOL, Y(NEQ)
      INTRINSIC FLOAT
      EXTERNAL FCN, IVPRK, SSET, UMACH
      COMMON
XINLET,Q0VOC,BVOC,Q0N2,BN2,PFEED,PVAC,BETA,VFEED
C
C This portion is to collect the experimental data for calculations
C
      OPEN (1,FILE='INFORM.DAT',STATUS='OLD')
      READ (1,*) XINLET, PFEED
      READ (1,*) FBOUND
      READ (1,*) PVAC
      READ (1,*) BETA, VFEED
      READ (1,*) Q0VOC, BVOC
      READ (1,*) Q0N2, BN2
      CLOSE (1, STATUS='KEEP')
C
      CALL UMACH(2,NOUT)
C
C Set initial conditions
C
      T=0.0
      Y(1)=FBOUND
      Y(2)=1.0E-08
      Y(3)=XINLET
      Y(5)=PFEED
      ALA=FUNA(NEQ,X,Y)
      ALB=FUNB(NEQ,X,Y)
C     PRINT *, ALA,ALB
```

```
      Y4B1=ALB*Y(5)+(ALA-ALB)*(Y(5)*Y(3)+PVAC)
      Y4B2=4.0*ALA*Y(5)*PVAC*Y(3)*(ALA-ALB)
      Y4B3=2.0*PVAC*(ALA-ALB)
      Y(4)=(Y4B1-SQRT(Y4B1**2-Y4B2))/Y4B3

C
C Set error tolerance
C
      TOL=0.001
C
C Set PARAM to default
C
      CALL SSET (MXPARM, 0.0, PARAM,1)
C
C Select absolute error control
C
      PARAM(10)=1.0
C
C Print header
C
      WRITE (NOUT, 9999)
 9999  FORMAT(4X, 'ISTEP',5X, 'TIME')
      IDO=1
      XLEFT=0.0
      XRIGHT=1.0
      OPEN (2, FILE='YTEMP.DAT',STATUS='NEW')
      DO 10 ISTEP=1,NGRID
        TEND=XLEFT+(ISTEP-1)*(XRIGHT-XLEFT)/FLOAT(NGRID-1)
C       TEND=FLOAT(ISTEP)/FLOAT(NGRID)
C       TEND=FLOAT(ISTEP)
        CALL IVPRK(IDO, NEQ, FCN, T, TEND, TOL, PARAM, Y)
        WRITE (NOUT,'(I6,6F8.5)') ISTEP, T, Y
      WRITE (2,*) T, Y
  10  CONTINUE
      CLOSE (2, STATUS='KEEP')
C
C Final call to release workspace
C
      IDO=3
      CALL IVPRK(IDO, NEQ, FCN, T, TEND, TOL, PARAM, Y)
      CALL REVERSE(NEQ,NGRID)
      END
C
C Subroutine FCN
C
      SUBROUTINE FCN(NEQ,T,Y,YPRIME)
```

```
      INTEGER NEQ
      REAL T,Y(NEQ),YPRIME(NEQ),ALA,ALB,BETA,VREF
      COMMON
XINLET,Q0VOC,BVOC,Q0N2,BN2,PFEED,PVAC,BETA,VFEED
C
C Define differential equations
C
C     PRINT *, T,Y(3), Y(5),ALA
      ALA=FUNA(NEQ,X,Y)
      ALB=FUNB(NEQ,X,Y)
      Y1P1=ALA*(Y(5)*Y(3)-PVAC*Y(4))
      Y1P2=ALB*(Y(5)*(1.0-Y(3))-PVAC*(1.0-Y(4)))
      YPRIME(1)=(Y1P1+Y1P2)*(-1.0)
      Y2P1=Y1P1
      Y2P2=Y1P2
      YPRIME(2)=Y2P1+Y2P2
      Y3P1=ALA*(1.0-Y(3))*(Y(5)*Y(3)-PVAC*Y(4))
      Y3P2=ALB*Y(3)*(Y(5)*(1.0-Y(3))-PVAC*(1.0-Y(4)))
      YPRIME(3)=(Y3P1-Y3P2)*(-1.0)/Y(1)
      IF (T.EQ.0.0) THEN
        Y4AN1=ALA*(1.0-Y(4))*(Y(5)*YPRIME(3)+Y(3)*YPRIME(5))
        Y4AN2=ALB*Y(4)*(-Y(5)*YPRIME(3)+(1-Y(3))*YPRIME(5))
        Y4AN3=BVOC*(Y(3)*YPRIME(5)+YPRIME(3)*Y(5))*ALA*
     &        (1.0-Y(4))*(Y(5)*Y(3)-PVAC*Y(4))
        Y4AN4=BN2*(Y(3)*YPRIME(5)+YPRIME(3)*Y(5))*ALB*
     &        Y(4)*(Y(5)*(1.0-Y(3))-PVAC*(1.0-Y(4)))
       Y4AN=Y4AN1-Y4AN2+Y4AN3-Y4AN4
        Y4DN1=2.0*Y(3)*Y(5)*(ALA-ALB)
        Y4DN2=ALA*PVAC
        Y4DN3=3.0*(ALA-ALB)*PVAC*Y(4)
        Y4DN4=2.0*ALB*(Y(5)-PVAC)
       Y4DN=Y4DN1+Y4DN2-Y4DN3+Y4DN4
      YPRIME(4)=Y4AN/Y4DN
      ELSE
        Y4P1=ALA*(1.0-Y(4))*(Y(5)*Y(3)-PVAC*Y(4))
        Y4P2=ALB*Y(4)*(Y(5)*(1.0-Y(3))-PVAC*(1.0-Y(4)))
        YPRIME(4)=(Y4P1-Y4P2)/Y(2)
      ENDIF
      YPRIME(5)=BETA*VFEED*Y(1)*(-1.0)/Y(5)
      RETURN
      END
C
C Subroutine to reverse the order of Y value from IVPRK.  Since the
C calculation results derived from cocurrent configuration, it is
C necessary to reverse the value of L* and x, which were represented
C by Y(1) and Y(3) in the previous program
```

```
C
      SUBROUTINE REVERSE(NEQ,NGRID)
      INTEGER NEQ,NGRID
      REAL TT(20), YNEW(10,20)
      OPEN (3, FILE='YTEMP.DAT', STATUS='OLD')
      DO 100 I=1,NGRID
      READ (3,*) T, Y1, Y2, Y3, Y4, Y5
      TT(I)=T
      YNEW(1,NGRID+1-I)=Y1
      YNEW(2,I)=Y2
      YNEW(3,NGRID+1-I)=Y3
      YNEW(4,NGRID+1-I)=Y4
      YNEW(5,NGRID+1-I)=Y5
  100 CONTINUE
      CLOSE (3, STATUS='KEEP')
      OPEN (4, FILE='YINIT.DAT', STATUS='NEW')
      DO 200 J=1,NGRID
C     WRITE (4,*) TT(J),YNEW(1,J),YNEW(2,J),YNEW(3,J),YNEW(4,J)
      WRITE (4,*) YNEW(1,J),YNEW(2,J),YNEW(3,J),YNEW(4,J),YNEW(5,J)
  200 CONTINUE
      CLOSE (4, STATUS='KEEP')
      RETURN
      END

C
C Function to calculate the ALA value
C
      FUNCTION FUNA(NEQ,X,Y)
      REAL Y(NEQ)
      COMMON
XINLET,Q0VOC,BVOC,Q0N2,BN2,PFEED,PVAC,BETA,VFEED
      FUNA=Q0VOC*EXP(BVOC*Y(5)*Y(3))
      RETURN
      END
C
C Function to calculate the ALB values
C
      FUNCTION FUNB(NEQ,X,Y)
      REAL Y(NEQ)
      COMMON
XINLET,Q0VOC,BVOC,Q0N2,BN2,PFEED,PVAC,BETA,VFEED
      FUNB=Q0N2*EXP(BN2*Y(5)*Y(3))
      RETURN
      END
```

```
C AICHEXV.FOR
C This is a program tried to model the process of a hollow fiber
C module which has VOC flow in the tube and vacuum in the shell side
C using IMSL BVPFD/DBVFD.
C

C
C Specifications for Parameters
C
      INTEGER    LDYFIN,LDYINI,MXGRID,NEQNS,NINIT
      PARAMETER (MXGRID=100, NEQNS=5, NINIT=10,
LDYFIN=NEQNS,
   &         LDYINI=NEQNS)
      INTEGER I, J, NCUPBC, NFINAL, NLEFT, NOUT
      REAL        CONST, ERREST(NEQNS), FCNBC, FCNEQN, FCNJAC,
FLOAT
   &         PISTEP, TOL, XFINAL(MXGRID), XINIT(NINIT), XLEFT,
   &         XRIGHT, YFINAL(LDYFIN,MXGRID), YINIT(LDYINI,NINIT)
      LOGICAL LINEAR, PRINT
      INTRINSIC FLOAT
      EXTERNAL  BVPFD, CONST, FCNBC, FCNEQN, FCNJAC, SSET,
UMACH
      COMMON XINLET,Q0VOC,BVOC,Q0N2,BN2,PFEED,PVAC,
   &         BETA,VFEED,FBOUND
C
C ************************************************************
C
C This portion is to collect the experimental data. The converted
C data is derived from INFORM.FOR
C
      OPEN (1,FILE='INFORM.DAT',STATUS='OLD')
      READ (1,*) XINLET, PFEED
      READ (1,*) FBOUND
      READ (1,*) PVAC
      READ (1,*) BETA, VFEED
      READ (1,*) Q0VOC, BVOC
      READ (1,*) Q0N2, BN2
      CLOSE (1, STATUS='KEEP')
C     PRINT *, Q0VOC, BVOC, Q0N2, BN2
C
C QVOC= AVOC*exp(BVOC*PRVOC)
C QN2= AN2*exp(BN2*PRVOC) at constant temperature,
C where QVOC and QN2 are the permeability of VOC and N2
C
C ^^^^^^^^^^^^^^^^^^^^^^^^^^^^^^^^^^^^^^^^^^^^^^^^^^^^^^^^^^^^^^^^
C
```

```
C Set Parameters
C
      NLEFT=2
      NCUPBC=0
      TOL=0.0001
      XLEFT=0.0
      XRIGHT=1.0
      PISTEP=0.0
      PRINT= .FALSE.
      LINEAR= .FALSE.
C
C Define XINIT
C
      DO 10 I=1, NINIT
      XINIT(I)=XLEFT+(I-1)*(XRIGHT-XLEFT)/(FLOAT(NINIT-1))
C     PRINT *, XINIT(I)
 10   CONTINUE
C
C Get YINIT from YINIT.DAT which is calculated from YINIT.FOR by
C cocurrent assumptions
C
      OPEN (2,FILE='YINIT.DAT',STATUS='OLD')
      DO 20 I=1, NINIT
      READ (2,*) YINIT(1,I),YINIT(2,I),YINIT(3,I),
     &      YINIT(4,I),YINIT(5,I)
C     PRINT *, YINIT(1,I),YINIT(2,I),YINIT(3,I),YINIT(4,I),YINIT(5,I)
 20   CONTINUE
      CLOSE (2, STATUS='KEEP')
C
C Solve Problem
C
      CALL BVPFD(FCNEQN, FCNJAC, FCNBC, FCNEQN, FCNBC, NEQNS,
NLEFT,
     &      NCUPBC, NLEFT, XRIGHT, PISTEP, TOL, NINIT, XINIT,
     &      YINIT, LDYINI, LINEAR, PRINT, MXGRID, NFINAL,
     &      XFINAL, YFINAL, LDYFIN, ERREST)
C
C Print Results
C
      OPEN (3,FILE='AICHE-V.DAT',STATUS='NEW')
      CALL UMACH(2,NOUT)
      WRITE (NOUT, 9997)
      WRITE (NOUT, 9998) (I,XFINAL(I),(YFINAL(J,I), J=1,NEQNS),I=1,
     &      NFINAL)
      WRITE (NOUT, 9999) (ERREST(J), J=1,NEQNS)
      WRITE (3, *) ((YFINAL(J,I), J=1,NEQNS),I=1,
```

```
     &        NFINAL)
         WRITE (3,*) 'ERROR ESTIMATES'
         WRITE (3,*) (ERREST(J), J=1,NEQNS)
         CLOSE (3, STATUS='KEEP')
 9997    FORMAT (4X,'I',7X,'X',14X, 'Y1', 13X, 'Y2', 13X, 'Y3',
     &        13X,'Y4',13X,'Y5')
 9998    FORMAT (I5,1P6E15.6)
 9999    FORMAT (' ERROR ESTIMATES', 4X, 1P5E15.6)
         END
C
C Subroutines
C
C &&&&&&&&&&&&&&&&&&&&&&&&&&&&&&&&&&&&&&&&&&&&&&&&&&&&&&&&&&&&&&&&&&&&
C
         SUBROUTINE FCNEQN (NEQNS, X, Y, P, DYDX)
C
C  Y(1), Y(2), Y(3), Y(4), and Y(5) are L*, V*, x, y, and gamma1* in the
C  derivation, respectively.  DYDX(1), DYDX(2), DYDX(3), AND DYDX(4)
C  are dL*/ds, dV*/ds, dx/ds, dy/ds, dgamma1*/ds, respectively
C
         INTEGER NEQNS
         REAL X, Y(NEQNS), P, DYDX(NEQNS), ALA, ALB
         COMMON XINLET,Q0VOC,BVOC,Q0N2,BN2,PFEED,PVAC,
     &        BETA,VFEED,FBOUND
C
C  Define differential equations
C
C        PRINT *, Q0VOC, BVOC, Y(5), Y(3)
         ALA=FUNA(NEQNS,X,Y)
         ALB=FUNB(NEQNS,X,Y)
C        PRINT *,Y(1),Y(2),Y(3),Y(4)
         Y1P1=ALA*(Y(5)*Y(3)-PVAC*Y(4))
         Y1P2=ALB*(Y(5)*(1.0-Y(3))-PVAC*(1.0-Y(4)))
         DYDX(1)=Y1P1+Y1P2
         Y2P1=Y1P1
         Y2P2=Y1P2
         DYDX(2)=Y2P1+Y2P2
         Y3P1=ALA*(1.0-Y(3))*(Y(5)*Y(3)-PVAC*Y(4))
         Y3P2=ALB*Y(3)*(Y(5)*(1.0-Y(3))-PVAC*(1.0-Y(4)))
         DYDX(3)=(Y3P1-Y3P2)/Y(1)
         IF (X.EQ.0.0) THEN
           Y4AN1=ALA*(1.0-Y(4))*(Y(5)*DYDX(3)+Y(3)*DYDX(5))
           Y4AN2=ALB*Y(4)*(-Y(5)*DYDX(3)+(1.0-Y(3))*DYDX(5))
           Y4AN3=BVOC*(Y(3)*DYDX(5)+DYDX(3)*Y(5))*ALA*
     &          (1.0-Y(4))*(Y(5)*Y(3)-PVAC*Y(4))
```

```
          Y4AN4=BN2*(Y(3)*DYDX(5)+DYDX(3)*Y(5))*ALB*
     &         Y(4)*(Y(5)*(1.0-Y(3))-PVAC*(1.0-Y(4)))
          Y4AN=Y4AN1-Y4AN2+Y4AN3-Y4AN4
          Y4DN1=2.0*Y(3)*Y(5)*(ALA-ALB)
          Y4DN2=ALA*PVAC
          Y4DN3=3.0*(ALA-ALB)*PVAC*Y(4)
          Y4DN4=2.0*ALB*(Y(5)-PVAC)
          Y4DN=Y4DN1+Y4DN2-Y4DN3+Y4DN4
          DYDX(4)=Y4AN/Y4DN
          ELSE
          Y4P1=ALA*(1.0-Y(4))*(Y(5)*Y(3)-PVAC*Y(4))
          Y4P2=ALB*Y(4)*(Y(5)*(1.0-Y(3))-PVAC*(1.0-Y(4)))
          DYDX(4)=(Y4P1-Y4P2)/Y(2)
          ENDIF
          DYDX(5)=BETA*VFEED*Y(1)/Y(5)
          RETURN
          END
C
C &&&&&&&&&&&&&&&&&&&&&&&&&&&&&&&&&&&&&&&&&&&&&&&&&&&&&&&&&&&&&&&&&&&&&&&&
C
C  Subroutine to evaluate Jacobian
C
          SUBROUTINE FCNJAC (NEQNS, X, Y, P,DYPDY)
          INTEGER NEQNS
          REAL X,Y(NEQNS),P,DYPDY(NEQNS,NEQNS),YPRIME(6)
          COMMON XINLET,Q0VOC,BVOC,Q0N2,BN2,PFEED,PVAC,
     &         BETA,VFEED,FBOUND
C
          ALA=FUNA(NEQNS,X,Y)
          ALB=FUNB(NEQNS,X,Y)
          DELTA=1.0E-5
C
C         Evaluate deratives
C
          DO 10 I=1,NEQNS
          K=I
          YPRIME(I)=FUNC(NEQNS,X,Y,I)
   10     CONTINUE
C
C         Estimate partial derative numerically
C
          DO 30 J=1,NEQNS
          Y(J)=Y(J)+DELTA
          DO 20 I=1,NEQNS
          K=I
```

```
      DYPDY(I,J)=(FUNC(NEQNS,X,Y,K)-YPRIME(I))/DELTA
 20   CONTINUE
      Y(J)=Y(J)-DELTA
 30   CONTINUE
      RETURN
      END
C
C Function to calculate the Jacobian values
C
      FUNCTION FUNC(NEQNS,X,Y,I)
      REAL Y(NEQNS)
      COMMON XINLET,Q0VOC,BVOC,Q0N2,BN2,PFEED,PVAC,
     &       BETA,VFEED,FBOUND
      ALA=FUNA(NEQNS,X,Y)
      ALB=FUNB(NEQNS,X,Y)
      GO TO (1,2,3,4,5),I
 1    Y1P1=ALA*(Y(5)*Y(3)-PVAC*Y(4))
      Y1P2=ALB*(Y(5)*(1.0-Y(3))-PVAC*(1.0-Y(4)))
      FUNC=Y1P1+Y1P2
      RETURN
 2    Y2P1=ALA*(Y(5)*Y(3)-PVAC*Y(4))
      Y2P2=ALB*(Y(5)*(1.0-Y(3))-PVAC*(1.0-Y(4)))
      FUNC=Y2P1+Y2P2
      RETURN
 3    Y3P1=ALA*(1.0-Y(3))*(Y(5)*Y(3)-PVAC*Y(4))
      Y3P2=ALB*Y(3)*(Y(5)*(1.0-Y(3))-PVAC*(1.0-Y(4)))
      FUNC=(Y3P1-Y3P2)/Y(1)
      RETURN
 4    IF (X.EQ.0.0) THEN
      Y3P1=ALA*(1.0-Y(3))*(Y(5)*Y(3)-PVAC*Y(4))
      Y3P2=ALB*Y(3)*(Y(5)*(1.0-Y(3))-PVAC*(1.0-Y(4)))
      DYDX3=(Y3P1-Y3P2)/Y(1)
      DYDX5=BETA*VFEED*Y(1)/Y(5)
        Y4AN1=ALA*(1.0-Y(4))*(Y(5)*DYDX3+Y(3)*DYDX5)
        Y4AN2=ALB*Y(4)*(-Y(5)*DYDX3+(1.0-Y(3))*DYDX5)
        Y4AN3=BVOC*(Y(3)*DYDX5+DYDX3*Y(5))*ALA*
     &       (1.0-Y(4))*(Y(5)*Y(3)-PVAC*Y(4))
        Y4AN4=BN2*(Y(3)*DYDX5+DYDX3*Y(5))*ALB*
     &       Y(4)*(Y(5)*(1.0-Y(3))-PVAC*(1.0-Y(4)))
       Y4AN=Y4AN1-Y4AN2+Y4AN3-Y4AN4
        Y4DN1=2.0*Y(3)*Y(5)*(ALA-ALB)
        Y4DN2=ALA*PVAC
        Y4DN3=3.0*(ALA-ALB)*PVAC*Y(4)
        Y4DN4=2.0*ALB*(Y(5)-PVAC)
       Y4DN=Y4DN1+Y4DN2-Y4DN3+Y4DN4
      FUNC=Y4AN/Y4DN
```

```
      ELSE
        Y4P1=ALA*(1.0-Y(4))*(Y(5)*Y(3)-PVAC*Y(4))
        Y4P2=ALB*Y(4)*(Y(5)*(1.0-Y(3))-PVAC*(1.0-Y(4)))
      FUNC=(Y4P1-Y4P2)/Y(2)
      ENDIF
      RETURN
 5    FUNC=BETA*VFEED*Y(1)/Y(5)
      RETURN
      END
C
C &&&&&&&&&&&&&&&&&&&&&&&&&&&&&&&&&&&&&&&&&&&&&&&&&&&&&&&&&&&&&&&&&&&&&&&&
C
C  Subroutine to set boundary conditions
C
      SUBROUTINE FCNBC (NEQNS, YLEFT, YRIGHT, P, F)
      INTEGER NEQNS
      REAL YLEFT(NEQNS), YRIGHT(NEQNS), P, F(NEQNS)
      COMMON XINLET,Q0VOC,BVOC,Q0N2,BN2,PFEED,PVAC,
     &       BETA,VFEED,FBOUND
C
C  Define boundary conditions
C
      ALA=FUNA(NEQNS,X,YLEFT)
      ALB=FUNB(NEQNS,X,YLEFT)
C     PRINT *,ALA,ALB,Q0VOC,Q0N2
      F(1)=YLEFT(2)-0.0
      Y4B1=ALB*YLEFT(5)+(ALA-ALB)*(YLEFT(5)*YLEFT(3)+PVAC)
      Y4B2=4.0*ALA*YLEFT(5)*PVAC*YLEFT(3)*(ALA-ALB)
      Y4B3=2.0*PVAC*(ALA-ALB)
      ZZZ=(Y4B1-SQRT(Y4B1**2-Y4B2))/Y4B3
C     PRINT *,ZZZ,ALA,ALB
      F(2)=YLEFT(4)-ZZZ
C
C  BCL and XINLET are boundary conditions of L* and x at S=1, respectively
C
      F(3)=YRIGHT(1)-FBOUND
      F(4)=YRIGHT(3)-XINLET
      F(5)=YRIGHT(5)-PFEED
      RETURN
      END
C
C Function to calculate the ALA value
C
      FUNCTION FUNA(NEQNS,X,Y)
      REAL Y(NEQNS)
```

```
      COMMON XINLET,Q0VOC,BVOC,Q0N2,BN2,PFEED,PVAC,
     &       BETA,VFEED,FBOUND
      FUNA=Q0VOC*EXP(BVOC*Y(5)*Y(3))
      RETURN
      END
C
C Function to calculate the ALB values
C
      FUNCTION FUNB(NEQNS,X,Y)
      REAL Y(NEQNS)
      COMMON XINLET,Q0VOC,BVOC,Q0N2,BN2,PFEED,PVAC,
     &       BETA,VFEED,FBOUND
      FUNB=Q0N2*EXP(BN2*Y(5)*Y(3))
      RETURN
      END
```

REFERENCES

Armand, B.L., H.B. Uddholm, and P.T. Vikstrom, "Absorption Method to Clean Solvent-Contaminated Process Air," *Ind. Eng. Chem. Res.*, **29**, 436 (1990).

Baker, R.W., "Process for Recovering Organic Vapors from Air," *United States Patent*, 4,553,983, (Nov. 18, 1988).

Baker, R.W., N. Yoshioka, J.M. Mohr, and A.J. Khan, "Separation of Organic Vapors from Air," *J. Membrane Sci.*, **31**, 259-272 (1987).

Behling, R.O., K. Ohlrogge, and K.V. Peinemann, "The Separation of Hydrocarbon from Waste Vapor Stream", *AIChE Symp. Ser.*, **85**(272), 68-73 (1989).

Cha, J., "Removal of Vapors from Air by Selective Membrane Processes," Ph.D.Dissertation, New Jersey Institute of Technology, Newark, NJ (1994).

EPA, "Control of Volatile Organic Emissions from Existing Stationary Sources, Vol. I, Control Methods for Surface Coating Operations," Environmental Protection Agency, Office of Air Quality Planning and Standards, EPA-450/2-76-028 (November, 1976).

Feng, X., S. Sourirajan, F.H. Tezel, and T. Matsuura, "Separation of Organic Vapor from Air by Aromatic Polyamide Membranes," *J. Appl. Pol. Sci.*, **43**, 1071-1079 (1991).

Feng, X., S., Sourirajan, F.H. Tezel, and T. Matsuura, "Separation of Volatile Organic Compound/ Nitrogen Mixtures by Polymeric Membranes," *Ind. Eng.Chem. Res.*, **32**, 533-539 (1993).

Guha, A.K., S. Majumdar, and K.K. Sirkar, "Gas Separation Modes in a Hollow Fiber Contained Liquid Membrane Permeator," *Ind. Eng. Chem. Res.*, **31**, 593 (1992).

Guha, A.K., "Studies on Different Gas Separation Modes with Hollow Fiber Contained Liquid Membrane," Ph.D. Diss., Stevens Institute of Technology, Hoboken, NJ (1989).

Kimmerle, K., C.M. Bell, and W. Gudernatsch, "Solvent Recovery from Air," *J. Memb. Sci.*, **36**, 477-488 (1988).

Majumdar, S., "New Liquid Membrane Techniques for Gas Separation," Ph.D. Diss., Stevens Institute of Technology, Hoboken, NJ (1986).

Matson, S.L., J. Lopez, and J.A., Quinn, "Separation of Gases with Synthetic Membranes,"*Chem. Eng. Sci.*, **38**(4), 503-524 (1983).

REFERENCES
(Continued)

Mukhopadhyay, N., and E.C. Moretti, "Current and Potential Future Industrial Practices for Reducing and Controlling Volatile Organic Compounds," A Publication by Center for Waste Reduction Technologies: AIChE (1993).

Pan, C.Y., and H.W. Habgood, "Gas Separation by Permeation. Part II," *Can. J. Chem. Eng.*, **56**, 210 (1978b).

Papadopoulos, H., "Further Studies on Hollow Fiber Contained Liquid Membrane Separation of Gas and Liquid Mixtures," Ph.D. Diss., Stevens Institute of Technology, Hoboken, NJ (1992).

Peinemann, K.V., J.M. Mohr, and R.W. Baker, "The Separation of Organic Vapors from Air," *AIChE. Symp. Series*, **82**(250), 19-26 (1986).

Pinnau, I., J.G. Wijmans, I. Blume, T. Kuroda and K.V., Peinemann, "Gas Permeation through Composite Membranes," *J.Membrane Sci.*, **37**(81), 8 (1988).

Ruddy, E.N., and L.A. Carroll, "Select the Best VOC Control Strategy," *Chem. Eng. Prog.*, 28-35, (July, 1993).

Sengupta, A., and K.K. Sirkar, "Membrane Gas Separation," in *Progress in Separation and Filtration*, R.J. Wakeman, eds., Elsevier Science Publishers, Amsterdam, 289-415 (1986).

Sirkar, K.K., "Removal and Recovery of VOCs from Waste Gas Streams by a Hollow Fiber Permeator," Annual Report submitted to CWRT, AIChE by New Jersey Institute of Technology, (November 9, 1994).

Stern, S.A., and H.L. Frisch, "The Selective Permeation of Gases through Polymers," *Ann. Rev. Mater. Sci.*, **11**, 523 (1981).

Strathmann, H., C.M. Bell, and K. Kimmerle, "Development of Synthetic Membranes for Gas and Vapor Separation," *Pure & Appl. Chem.*, **58**(12), 1663-1668 (1986).

Wijmans, J.G., and V.D. Helm, "A Membrane System for the Separation and Recovery of Organic Vapors from Gas Streams," *AIChE Symp. Ser.*, **272**(85), 74-79 (1989).

Zolandz, R.R., and G.K., Fleming, "Gas Separation," in *Membrane Handbook*, W.S.W. Ho, and K.K. Sirkar, eds., Chapman and Hall, New York (1992).